The ICORASS Feasibility Study

Final report

B.H. Bulder (ECN)
H.B. Hendriks (ECN)
P.J. van Langen (ECN)
C. Lindenburg (ECN)
H. Snel (ECN)
P. Bauer (TU-D)
H. Polinder (TU-D)
R.P.J.O.M. van Rooij (TU-D)
H. Subroto (TU-D)
M.B. Zaayer (TU-D)

ECN-E--07-010

Abstract

This is the final report of the joint TU-D/ECN project ICORASS (*Integral Composite Offshore Rotor Active Speed Stall control*)[1]. This project was performed to investigate the feasibility of a very large offshore wind turbine consisting of integrated components to offer a major improvement in the levelized production costs and reliability of offshore wind energy.

The ICORASS concept was originally described as a (very) large robust wind turbine with integrated components. To create a robust wind turbine the idea was to reduce the number of components and integrate functions as far as possible into single components. By increasing the size of the wind turbine the number of wind turbines in the wind farm, of a specific nominal power, will reduce and hence reduce the chance of failure. Another reason for increasing the size of the wind turbine is the lower specific maintenance cost.

The project focus was on the wind turbine concept taking into account the interaction with the wind farm design. The technological aspects of the wind turbine that have been investigated are:

1) the aerodynamic rotor design regarding performance, active speed stall controllability and preliminary aeroelastic stability;
2) the generator design and rotor speed control concept;
3) the support structure and nacelle layout including both installation and operation and maintenance concepts.

The low speed active stall control option was preferred over the high speed option. No technological barriers were found, although quite a lot of fields were identified for further research. Especially on the aerodynamic stall properties, structural blade layout and controllability should be elaborated before a final decision is made on the viability of the ICORASS concept.

From the economical evaluation of the concept it appears that the up scaling from current large scale turbines (3-6MW) towards the intended 10MW for the ICORASS turbine introduces a levelized production cost increase. Although, the active speed stall regulated concept seems to provide a cost reduction with respect to pitch regulated wind turbines due to a decrease in both hardware and maintenance costs. However, the increased fatigue loads may cancel out these beneficial effects.

Acknowledgement/Preface

This project is supported with a grant of the Dutch Programme EET (Economy, Ecology, Technology) a joint initiative of the Ministries of Economic Affairs, Education, Culture and Sciences and of Housing, Spatial Planning and the Environment. The programme is run by the EET Programme Office, SenterNovem.

SenterNovem KIEM projectnummer: KIEM03028.
ECN projectnummer: 7.4360.

Keywords

ICORASS, wind turbine, integral composite rotor, active speed stall control, offshore, deep water, direct drive, down wind, two-bladed.

[1] Initially Polymarin Composites was the project coordinator but due to bankruptcy of that company TU-D and ECN performed the project without an industrial partner.

Contents

List of tables 5

List of figures 5

Nomenclature 7

1. Introduction 9

2. Terms of reference 11
   - 2.1 Reference wind farm design 11
   - 2.2 General wind turbine parameters 14
   - 2.3 Operation and maintenance data 15
   - 2.4 Requirements 16
   - 2.5 Assessment criteria 16
   - 2.6 References 17

3. Rotor design 19
   - 3.1 High lambda or low lambda design 19
   - 3.2 Aerodynamic design 20
     - 3.2.1 Initial aerodynamic design 20
     - 3.2.2 Turbine parameters 20
     - 3.2.3 Optimisation criterion 21
     - 3.2.4 Optimum aerodynamic design 21
       - 3.2.4.1 Performance curves 23
       - 3.2.4.2 Blade distributions 24
   - 3.3 Structural design 25
   - 3.4 Aeroelastic analysis 27
     - 3.4.1 Analysed modes 27
     - 3.4.2 Natural frequencies 29
     - 3.4.3 Aerodynamic damping 30
   - 3.5 Conclusions 31
   - 3.6 References 31

4. Consequences for the generator system and generator design 33
   - 4.1 Control strategies 33
   - 4.2 Pitch control 36
   - 4.3 ICORASS with heavily overrated generator system 36
   - 4.4 ICORASS control with speed limit 37
   - 4.5 ICORASS control with power limited to 10 MW. 38
   - 4.6 ICORASS control with torque limited to 14 MNm. 39
   - 4.7 Additional power and torque necessary for decreasing the rotor speed. 40
   - 4.8 Conclusions 41
     - 4.8.1 Preliminary generator system choice 42

5. Control and safety design 45
   - 5.1 Control system 45
   - 5.2 Protection system 45
   - 5.3 Conclusion 46
   - 5.4 References 46

6. Wind farm design 47
   - 6.1 Introduction 47
   - 6.2 Lay-out of wind farms with ICORASS wind turbines 47
   - 6.3 Electrical concepts for offshore wind farms with ICORASS wind turbines 47
     - 6.3.1 Inventory of electrical concepts 48

6.3.2 Economical evaluation: case study 49
6.4 References 49

7. Support structure, installation and O&M design 51
7.1 Nacelle and drive train 51
7.1.1 Main concept 51
7.1.1.1 Reference concepts 51
7.1.1.2 Concept selections for ICORASS 52
7.1.2 Design and analysis of principal dimensions 54
7.1.2.1 Brakes 54
7.1.2.2 Main bearing 57
7.1.2.3 Yaw system 59
7.2 Support structure 60
7.2.1 Three or four legs 60
7.2.2 Pile design and stiffness 62
7.2.3 Truss design 63
7.3 Installation 64
7.3.1 Focal point 64
7.3.2 Lifting of the tower 65
7.3.3 Installation of rotor and nacelle 66
7.4 Maintenance 68
7.5 References 70

8. Economical evaluation 73
8.1 Calculation of levelized production cost 73
8.2 Cost breakdown 73
8.3 Concept variation effects on *LPC* 74
8.3.1 Energy yield 75
8.3.2 Costs 75
8.3.2.1 Operation &Maintenance costs 75
8.3.2.2 Hardware costs 76
8.3.2.3 Overhaul costs 76
8.3.2.4 Transport & Installation costs 77
8.4 Conclusions 77
8.5 References 78

Conclusions and recommendations 79

Appendix A Airfoil characteristics 81

Appendix B Economical evaluation of the offshore wind farm layout 85
B.1 Electrical wind farm layout 1 87
B.2 Electrical wind farm layout 2 88
B.3 Electrical wind farm layout 3 89
B.4 Electrical wind farm layout 4 90

List of tables

Table 2.1: *Data for the reference wind farm design.* 11
Table 2.2: *Distribution of the wind speed direction: Hoek van Holland, [2.2].* 11
Table 2.3: *General wind turbine parameters.* 14
Table 2.4: *Yearly failure frequencies [2.4].* 15
Table 3.1: *Optimum aerodynamic blade design.* 21
Table 3.2: *Power curve for the optimum blade.* 23
Table 3.3: *Scaling factors* 26
Table 4.1: *Wind turbine and generator material characteristics.* 33
Table 4.2: *Generator dimensions and weights.* 41
Table 4.3: *Generator system cost and energy yield for different control strategies.* 42
Table 7.1: *Qualifications of nacelle concepts presented in Figure 7.2.* 53
Table 7.2: *Options, functions and system qualities for yaw brakes.* 54
Table 7.3: *Estimated contributions to loads on main bearing and yaw system.* 58
Table 7.4: *Pile dimensions and elements of the pile stiffness matrix.* 63
Table 7.5: *Some heavy lift vessels with high hoisting heights.* 65
Table 7.6: *Definition of concepts for comparison of reliability.* 68
Table 7.7: *Positioning the ICORASS concept in the DOWEC Concept reliability study (Data of other concepts from [7.30]).* 68
Table 7.8: *Assumptions relating to the potential maintenance costs and downtime reductions of ICORASS.* 69
Table 8.1: *Preliminary breakdown of the levelized production costs based on DOWEC.* 73
Table 8.2: *DOWEC wind farm costs.* 74
Table 8.3: *Energy yield per wind turbine.* 75
Table 8.4: *Hardware investment costs.* 76
Table 8.5: *Energy yield and cost of the ICORASS concept compared tot the DOWEC Concept.* 77
Table A.1: *Spanwise airfoil distribution.* 81
Table A.2: *Hardware cost calculation for electrical wind farm layout 1.* 87
Table A.3: *Hardware cost calculation for electrical wind farm layout 2.* 88
Table A.4: *Hardware cost calculation for electrical wind farm layout 3.* 89
Table A.5: *Hardware cost calculation for electrical wind farm layout 4.* 90

List of figures

Figure 2.1: *Zones with similar wind characteristics at the Dutch part of the North Sea copied from [2.3].* 12
Figure 2.2: *Bathymetry chart of the North Sea.* 13
Figure 2.3: *Relative losses in the drive train (P_{loss}/P_{aero} vs. P_{aero}/P_{rated}).* 14
Figure 3.1: *Sketch of active speed stall control concepts.* 19
Figure 3.2: *Chord distributions.* 22
Figure 3.3: *Thickness distributions.* 22
Figure 3.4: *Twist distributions.* 22
Figure 3.5: *Electric power for the optimum blade as a function of wind speed.* 24
Figure 3.6: *Stationary axial force for the optimum blade as a function of wind speed.* 24
Figure 3.7: *Rotational speed for the optimum blade as a function of wind speed.* 24
Figure 3.8: *Shaft/generator torque for the optimum blade as a function of wind speed.* 24
Figure 3.9: *Circulation distribution along the blade for wind speeds below rated power.* 24

Figure 3.10: *Angle of attack distribution along the blade for all wind speeds.* 25
Figure 3.11: *Blade mass density.* 26
Figure 3.12: *Flat- and edgewise stiffness.* 26
Figure 3.13: *Torsion and tension stiffness.* 26
Figure 3.14: *Mass moments of inertia.* 26
Figure 3.15: *1P Gravity loading mode.* 27
Figure 3.16: *First flatwise mode.* 28
Figure 3.17: *First edgewise mode.* 28
Figure 3.18: *Frequencies of the first two eigenmodes.* 29
Figure 3.19: *Aerodynamic damping of the first flatwise mode.* 30
Figure 3.20: *Aerodynamic damping of the 1P gravity loading mode and first edgewise mode.* 30
Figure 4.1: *Power curves of the ICORASS blades at constant speeds of 6.5-11 rpm.* 34
Figure 4.2: *Torque curves of the ICORASS blades at constant speeds of 6.5-11 rpm.* 34
Figure 4.3: *Characteristics of a turbine with pitch control, a rated speed of 10 rpm and a rated torque of 10 MNm.* 36
Figure 4.4: *Characteristics of an ICORASS turbine with a heavily overrated generator system that can take a power of 18 MW.* 37
Figure 4.5: *Characteristics of an ICORASS turbine in which the speed is limited to 7.2 rpm so that the power never exceeds 10 MW. The rated torque is 14 MNm.* 38
Figure 4.6: *Characteristics of an ICORASS turbine in which the power is limited to 10 MW. The rated torque is 14 MNm.* 39
Figure 4.7: *Characteristics of an ICORASS turbine in which the torque is limited to 14 MNm. The rated power is 14 MW.* 40
Figure 4.8: *Rotor speed as a function of wind speed for the control concept where the power is limited to 10 MW.* 41
Figure 6.1: *Individual variable speed systems with back-to-back converters [6.1].* 48
Figure 6.2: *Individual variable speed systems with multi-terminal DC [6.1].* 49
Figure 7.1: *Schematic representation of direct drive concepts with characteristics and manufacturers [7.1] – [7.7].* 51
Figure 7.2: *Schematic representation of two options for the nacelle concept of the ICORASS turbine.* 53
Figure 7.3: *Power curve of the ICORASS rotor for various rotational speeds.* 55
Figure 7.4: *Relation between braking torque and time till stand still after overspeed at cut-out wind speed.* 57
Figure 7.5: *Equivalent radial load on main bearing as a function of its diameter.* 59
Figure 7.6: *Hub moment about vertical axis for half the rotor cycle. Azimuth equals zero for a vertical rotor.* 59
Figure 7.7: *Cross sections of truss tower configurations with 3 and 4 legs with two load cases A and B each.* 61
Figure 7.8: *Simplified model of pile deformation by a cantilever beam.* 62
Figure 7.9: *Displacement method in a finite element analysis to get stiffness.* 63
Figure 7.10: *Conceptual truss design.* 64
Figure 7.11: *Modes of rotation and lifting of the tower.* 65
Figure 7.12: *Hoisting the rotor and generator with the same internal crane.* 67
Figure 7.13: *Schematic overview of the nacelle layout, showing accessibility and the yaw system.* 70
Figure 8.1: *Total levelized wind farm costs.* 77
Figure A.1: *Airfoil characteristics DU40_X60.* 82
Figure A.2: *Airfoil characteristics DU35_X60.* 82
Figure A.3: *Airfoil characteristics DU30_X60.* 83
Figure A.4: *Airfoil characteristics DU25_X60.* 83
Figure A.5: *Airfoil characteristics FFA-W3-221_107.* 84
Figure A.6: *Airfoil characteristics NACA-63618.* 84

Nomenclature

Latin Symbols

Symbol	*Units*	*Explanation*	*Formula*
a	[m/s]	Weibull mean/scale factor	
a	[-]	Annuity factor (dep. on discount rate and economic lifetime)	
A	[m^2]	Area	
B	[-]	Number of blades	
c	[-]	Capacity factor	$c = E/\left(365 \cdot 24 \cdot P_{rated} \cdot 1000\right)$
C_P	[-]	Power coefficient	
C_T	[-]	Thrust coefficient	
D	[m]	Rotor diameter	
E	[Gh]	Yearly energy yield	
E	[N/m^2]	Young's elasticity modulus	
F_{ax}	[kN]	Axial or Thrust Force	
I	[€]	Initial investment	
I	[m^4]	Cross sectional moment of inertia	
I, J	[$kg\ m^2$]	Rotor rotational inertia	
k	[-]	Weibull shape factor	
k_v	[-]	Variable drive train losses	
l, L	[m]	Length	
m	[kg]	Mass	
m	[kg/m]	Blade mass per unit length	
M	[-]	Mach number	
$M_{bl.root}$	[kNm]	Blade root bending moment	
n	[-]	Number of turbines in the wind farm	
P	[MW]	Power	
r	[m]	Radial position	
r	[-]	Interest rate	
R	[m]	(Rotor) radius	
Re	[-]	Reynolds number	
Q, T, M	[kNm]	(Rotor) torque	
SF	[-]	Scaling factor	
U, V	[m/s]	Wind speed	
w_k	[-]	Weibull shape factor	
z	[m]	Height or roughness	

Greek Symbols

Symbol	*Units*	*Explanation*	*Formula*
α	[º]	Angle of attack	
Γ	[m^2/s]	Circulation	
η_{park}	[-]	Array efficiency	$\eta_{park} = E_{farm} / nE_{turbine,sol}$
λ	[-]	Tip speed ratio	$\lambda = \omega R / V_w$
θ	[º]	Twist angle	
ω, Ω	[rpm]	Rotor rotational speed	
ω	[Hz]	Natural frequency	

Subscripts	
Symbol	*Explanation*
0	At ground level
∞	Undisturbed
aero	Aerodynamic
ave	Average
c	Chordwise
crit	Critical
edge	Edgewise
elec	Electrical
f	Fixed
flat	Flatwise
h	At hub height
park	Wind farm or array
r	Reference
R	Radial
rated	At nominal power
rel	Relative
sol	Solitaire or stand alone
t	Edgewise, blade thickness direction
turbine	Wind turbine
w	Wind

Abbreviations	
Name	*Explanation*
AUE	Annual utilised energy.
CG, COG	Centre of gravity
LPC	Levelized Production Costs.
O&M	Operation and maintenance
T&I	Transport and installation
TOM	Total levelized annual “downline cost” (i.e. O&M, insurance, retrofit and salvage cost).

Terminology	
Name	*Explanation*
Weibull distribution	Probability distribution used for wind speed.
Wind shear	Vertical shear of the average wind speed using log-law.

1. Introduction

Technical, economical and ecological uncertainties hamper the large scale implementation of offshore wind energy. The current generation of offshore wind turbines consists of adjusted on-shore turbines. Because of the highly sophisticated control mechanisms these turbines are very maintenance demanding, therefore the cost level is too high and the reliability not high enough.

Within the ICORASS project a feasibility study has been performed for a dedicated large off-shore wind turbine concept. Maximum robustness, high reliability and minimum maintenance are pursued. Therefore, the wind turbine concept, wind turbine size, installation technology and operation and maintenance strategy are (re)considered. With the minimization of the number of -rotating- components and the maximization of the component integration in mind, a 10MW, two-bladed, integrated rotor, direct drive turbine is studied.

The long-term goal of this project is twofold:
- realization of a considerable part of both Dutch and world wide offshore wind energy;
- demonstration of the important role of Dutch offshore wind energy industry and R&D.

The technological concepts concerning this study are:
- aerodynamics and aero-elastics of a very large two-bladed stall regulated turbine;
- conceptual design of the support structure;
- wind farm design and quality of electrical energy;
- installation and maintenance strategies.

Based on these technological subjects an assessment of the total levelized production cost of the produced energy is made.

In the original project plan and initial phase of the ICORASS project Polymarin Composites (PMC) participated as third project partner. PMC holds Dutch and European patents at the integrated rotor concept and its manufacturing methods. With their withdrawal from the project, the manufacturability of an integrated rotor and direct drive generator as well as the composite manufacturing techniques lie outside the scope of this project.

Chapter 2 is used to define the reference conditions for the ICORASS turbine. The technological aspects are dealt with in chapter 3-7. This knowledge is used in chapter 8 to calculate the economical effects. Finally both technological and economical conclusions are drawn.

Not all design parameters will be consistent in this report, i.e. due to the fact that during performance of the project these parameters changed.

2. Terms of reference

This chapter is used to define the reference conditions used in the feasibility study. To estimate the possible improvements of the ICORASS concept with current state of the art wind turbines it is necessary to agree on external conditions and reference size of the wind turbine and wind farm.

2.1 Reference wind farm design

The reference design will be a large, approximately 500-1000MW, offshore wind power plant.

Table 2.1: *Data for the reference wind farm design.*

Location		North Sea.	
Water depth		Less than 40m	See Figure 2.2.
Distance to shore		More than 40km.	
Weibull wind speed parameters @ 80 m height		V_{ave} = 10m/s k = 2.25	See Figure 2.1.
Wind shear profile		Determined from a roughness height of 0.0001m.	
Turbulence (IEC description)	I_{15} a	0.12 3	See ref. [2.2].
Wind rose		See Table 2.2.	
Wind farm turbine spacing		Approx. 8D.	
Wind farm array efficiency		~ 95%	
Water conditions		Unknown.	
Soil conditions		Sand.	
Economic parameters		Interest rate	7%
		Inflation rate	2%
		Economic lifetime	12 year

Table 2.2: *Distribution of the wind speed and direction: Hoek van Holland, [2.2].*

Sector	% of time
N	7.4
NNE	7.2
NEE	6.2
E	7.2
SEE	5.0
SSE	4.8
S	9.1
SSW	13.3
SWW	15.4
W	9.7
NWW	7.6
NNW	6.6

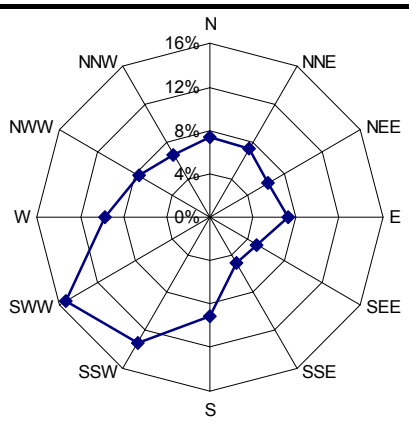

Zone	U_{ave} from derived Weibull [*m/s*]	Weibull mean factor *a* [*m/s*]	Weibull scale factor *k* [-]	Mean power density from derived Weibull [W/m^2]
1	9.3	10.5	2.04	924.4
2	9.8	11.0	2.16	1010.4
3	9.7	10.9	2.21	956.7
4	10.0	11.2	2.25	1036.6

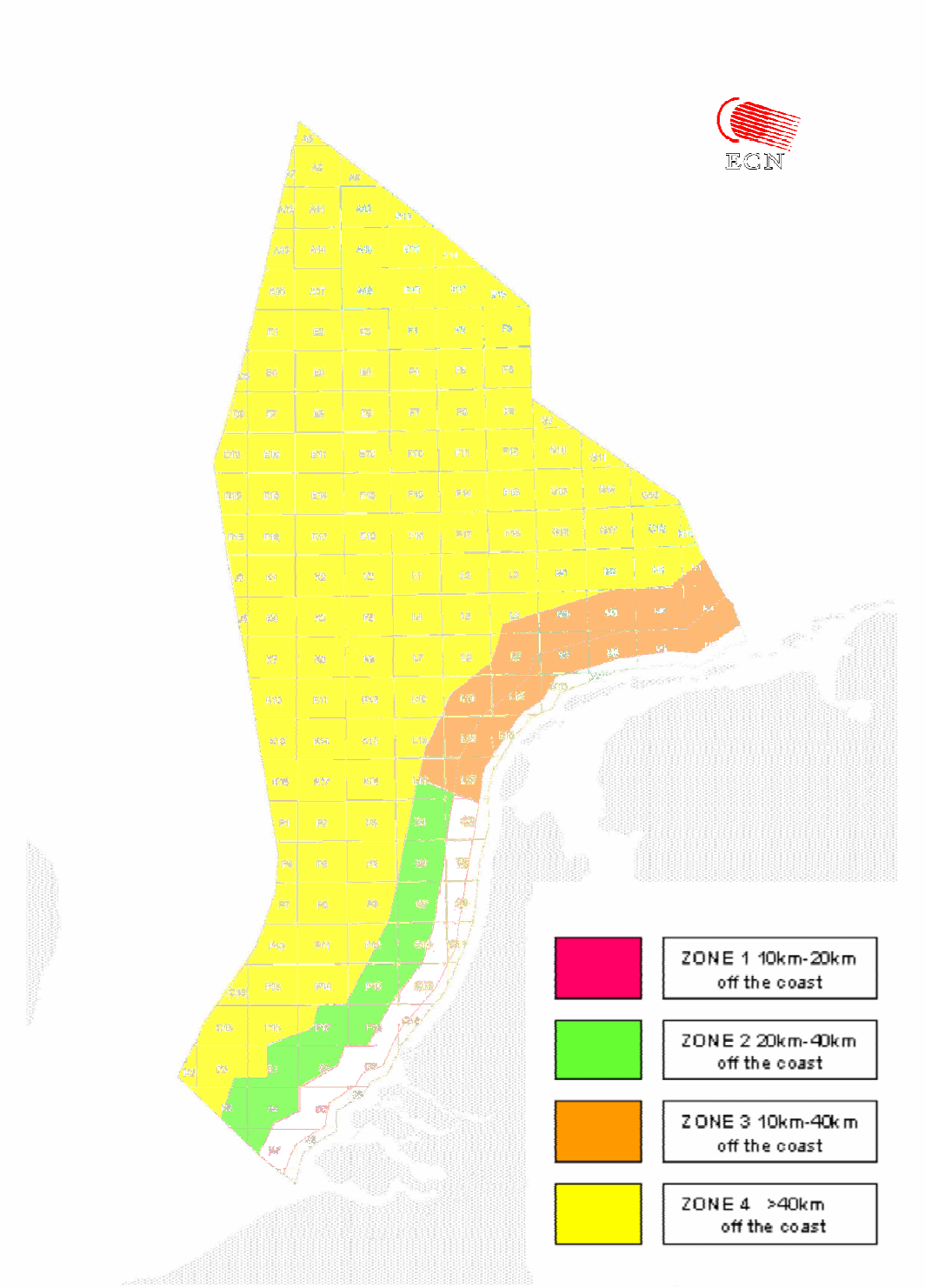

Figure 2.1: *Zones with similar wind characteristics at the Dutch part of the North Sea copied from [2.3].*

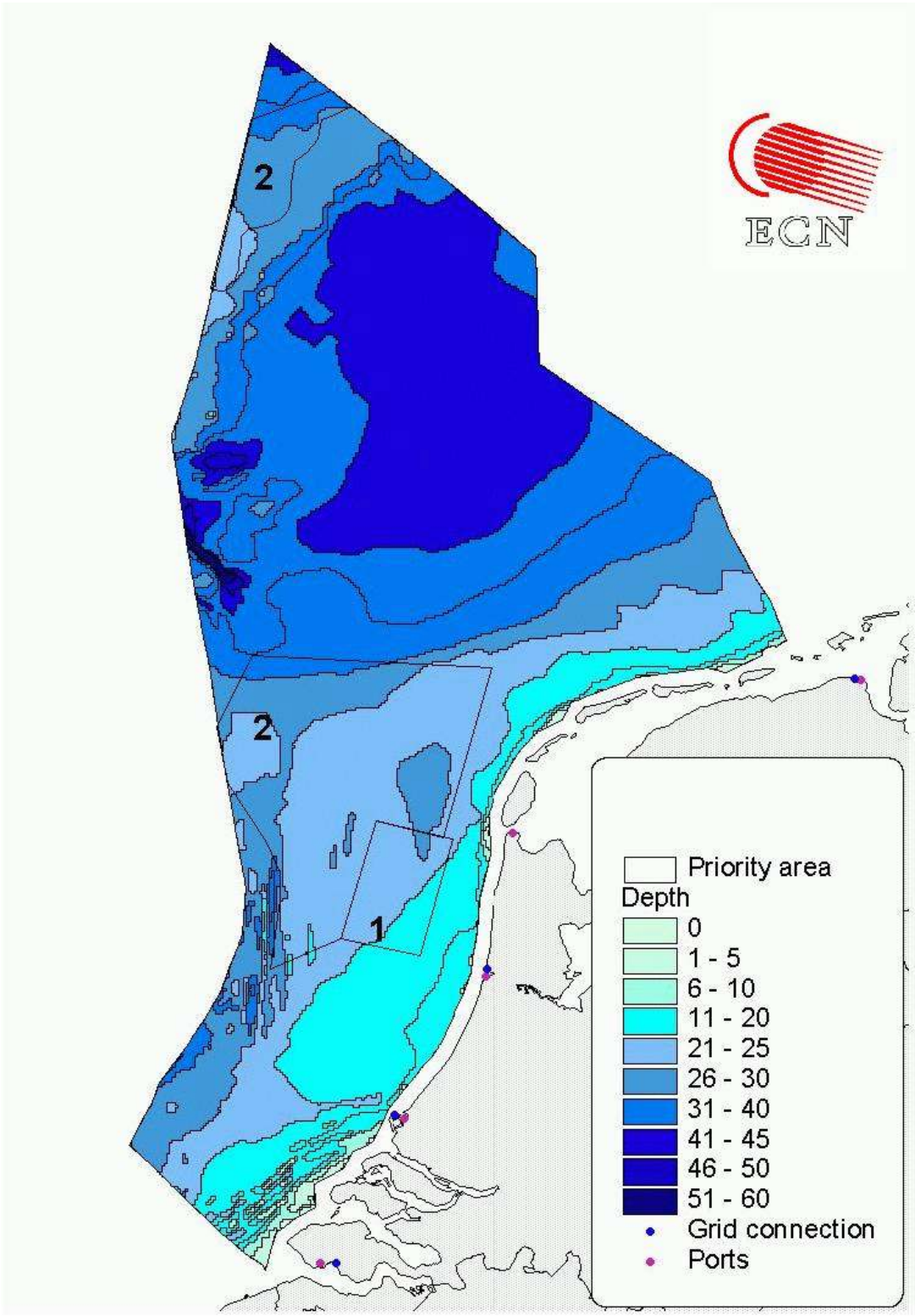

Figure 2.2: *Bathymetry chart of the North Sea.*

2.2 General wind turbine parameters

The initial wind turbine model is designed using the BladOpt code, the code description, theory and user's manual can be obtained from the ECN website [2.8].

Table 2.3: *General wind turbine parameters.*

Turbine data	General	Rated power:	10 MW
		Rotor diameter:	170 m
		Hub height:	>110 m[2]
		Number of blades:	2
		Down wind rotor.	
	Electrical system	Direct drive generator.	
		Active stall speed control.	
		Variable speed (λ_0=9.0).	

Losses in the drive train are assumed to be 3% of the nominal power plus 7% of the actual aerodynamic power. The relative losses are shown in Figure 2.3.

(2.1) $$P_{elec} = (1 - 0.07)P_{aero} - 0.03P_{rated}$$

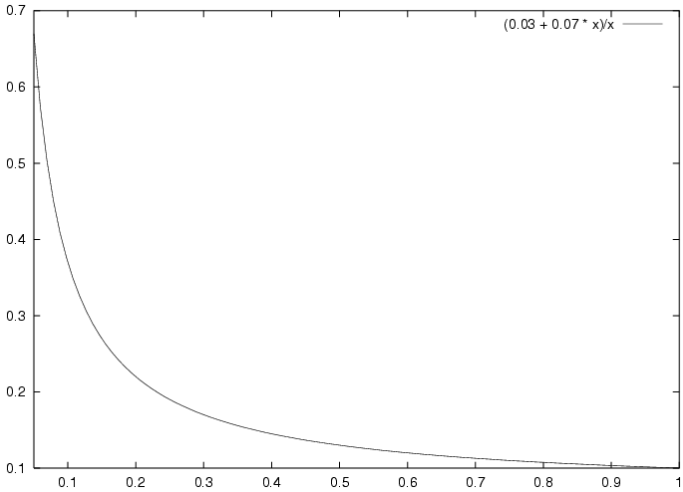

Figure 2.3: *Relative losses in the drive train (P_{loss}/P_{aero} vs. P_{aero}/P_{rated}).*

The remaining wind turbine parameters, which identify the turbine model, are the aerodynamic profile distribution. For root to tip: DU40, DU35, DU30, DU25, FFA-W3-211_107, NACA-63618. The overall aerodynamic rotor blade design is created with the ECN BOT code taking only the aerodynamic performance into account, see chapter 3.

The resulting energy yield for the given wind speed distribution will be approximately 46 GWh/yr assuming 100% availability and no array wake losses. The capacity factor is then approximately 53% which is realistic for an offshore wind turbine for the given wind conditions.
The power density of the rotor is P_{rated}/A_{rotor} = 440.6 W/m^2 (based on the un-coned rotor radius).

[2] Minimum height determined by rotor radius, maximum wave height and splash

2.3 Operation and maintenance data

The O&M cost include all costs related to the operation of the wind power plant, i.e. operating costs, maintenance costs, insurance costs, etc. For the determination of the O&M cost it will be necessary to use some (assumed) failure data. To prevent too much detail it is assumed that each wind turbine will have e.g. four kinds of failures:

1) insignificant failure:
   - wind turbine will remain working;
   - maintenance has to be applied within 1 week.
2) minor failure:
   - wind turbine is not operational;
   - maintenance effort is less than 6 hr;
   - no additional equipment.
3) significant failure:
   - wind turbine is not operational;
   - maintenance effort is more than 6 hr however;
   - no additional equipment necessary.
4) failure of component:
   - wind turbine is not operational;
   - maintenance effort big;
   - additional equipment, i.e. crane is necessary.

For each of these failure categories the probability of occurrence has to be determined together with the cost, including loss of energy yield, related to the repair. For multi rotor platforms the implications related to the other machines on the platform has to be taken into account.

Table 2.4: *Yearly failure frequencies [2.4].*

	LWK	WMEP	WindStats	
			DK	GE
Blades + Rotor + Rotorbrake	0.31	0.26	0.06	0.25
Pitch mechanism	0.11	0.01	0.00	0.13
Gearbox	0.08	0.09	0.05	0.10
Generator	0.21	0.08	0.05	0.16
Yaw system	0.12	0.15	0.06	0.16
Electrics + inverter	0.37	0.58	0.00	0.41
Hydraulics	0.14	0.21	0.04	0.12
Electronics	0.27	0.40	0.00	0.26
Control system + instrumentation	0.16	0.18	0.13	0.16
Shaft + Bearings + Brake	0.09	0.18	0.04	0.08
Others	0.29	0.08	0.27	2.25
Total	2.13	2.23	0.70	4.07

Failure data generated for the DOWEC project is used see Table 2.4, in which the following public sources are used:

- Eggersglüß, W. *Windenergie Praxisergebnisse 1995-2000.* LandwirtschaftskammerSchleswig-Holstein, Rendsburg, Germany, 1995-2000. [*LWK*]
- *Wissenschaftliches Meß- und EvaluierungsProgramm Jahresauswertung 1998-2000*. Institut für Solare EnergieversorgungsTechnik, Universität Gesamthochschule Kassel, Germany, 1998-2000. [*WMEP*].
- *WindStats Newsletter*, Volume 12 No 4 (Autumn 1999) - Volume 14 No 4 (Autumn 2001), Denmark. [*DK* and *GE*].

2.4 Requirements

The requirements are imposed by design codes and standards that are applicable for an (offshore) wind energy station. These requirements will change when the design codes and standards are updated.

The standards will deal with the:
- integrity of the structure [2.5]-[2.6],
- grid requirements, [2.10]-[2.11] .

The wind turbine design will have to comply with the standard [2.6]. The Dutch requirements for electricity producing plants are in grid code and system code [2.10]-[2.11].

Offshore codes and regulations (Lloyd's Register):
1) Rules and Regulations for the Construction and Classification of a Floating Offshore Unit at a Fixed Location.
2) Rules and Regulations for the Classification of Mobile Offshore Units.
3) Rules and Regulations for the Classification of Fixed Offshore Installations.
4) Rules and Regulations for the Construction and Classification of Submersibles and Underwater Systems.

2.5 Assessment criteria

Assessment of the design will be based on cost and potential of reducing the cost. Therefore the cost will be determined according to the levelized production cost method [2.9]. Levelized means that no variations in cost or energy yield are assumed during the lifetime of the project.

The simplified method will be used, which means that the following equation has to be evaluated:

$$LPC = \frac{I/a}{AUE} + \frac{TOM}{AUE},$$

in which I is the initial investment, a the annuity factor, AUE the annual utilised energy and TOM the total levelized annual "downline cost" (i.e. O&M, insurance, retrofit and salvage costs).

This results in a yearly capital cost and operating and maintenance cost divided by the net energy production minus electrical an aerodynamic losses within the wind farm. To determine the cost of energy it is necessary to determine the following quantities:
- Energy yield, determined on the basis of the power curve, wind conditions, wind turbine availability, wind farm losses, electricity losses in the wind farm and between wind farm and grid connection;
- Total investment cost, i.e. cost of the wind turbines , floaters, installation, electrical infrastructure in the wind farm and between wind farm and grid;
- Operating and maintenance cost, including insurance cost;
- Economic parameters like interest and depreciation period.

2.6 References

[2.1] Haskoning. *Near-shore study wind energy, Voorstudie locatieselectie.*

[2.2] Stork. *Near-shore wind energy, Technische realisatie.*

[2.3] Eecen, P.J. & Niño, R.R. *Zones with similar wind regimes at the North Sea*. ECN-Wind Memo-02-011. Petten, March 2002.

[2.4] Vallinga, R. *Estimation of Turbine Reliability figures within the DOWEC project.* (http://www.ecn.nl/en/wind/additional/special-projects/dowec/). DOWEC-086. Bunnik, May 2002.

[2.5] International standard IEC 61400-1. *Wind Turbine Generator Systems, Part1 – Safety requirements*, 2nd edition. 1999-02.

[2.6] International standard IEC 61400-3. *Safety requirements for offshore wind turbines.* In preparation.

[2.7] Germanischer Lloyd. *IV - Non-marine technology, part 2, Offshore Wind Energy*, 1998.

[2.8] Bulder, B.H., Barhorst, S.A.M., Schepers, J.G. & Hagg, F. *Theory and user Manual BLADOPT.* ECN--C-01-011, Petten, August 2001.

[2.9] Hunter, R. & Tande, J.O. *Recommended practices for wind turbine testing and evaluation" # 2. Estimation of cost of energy from wind energy conversion systems.* International Energy Agency, 2nd edition, 1994.

[2.10] Dienst uitvoering en Toezicht Electriciteitswet, *NetCode*, 99-121, 1999-12-15.

[2.11] Dienst uitvoering en Toezicht Electriciteitswet, *SysteemCode*, 99-122, 1999-12-15.

3. Rotor design

This chapter is used to present the aerodynamic rotor design. A detailed structural design lies beyond the scope of the conceptual design in this project; the same holds for the structural integration of the generator rotor in the wind turbine rotor. By estimating the structural properties of the composite blade from the data of another multi-megawatt rotor, a preliminary aero-elastic stability analysis of the design has been conducted with an aero-elastic code.

3.1 High lambda or low lambda design

As was stated before, the aerodynamic power is controlled by active stall (rotor) speed control. With increasing wind speed the aerodynamic power coefficient should be decreased to ensure continuous (rated) electrical power. The idea behind active stall speed control is that a large, deliberate deviation (decrease) of the tip-speed ratio from the optimum tip-speed-ratio can be used to decrease the power coefficient robustly without using a sophisticated pitch control mechanism. Another idea which has been investigated is to use a passive speed power control, where the rotor speed is free and the power coefficient will decrease while the rotor speed deviates (increases) from the optimum tip speed ratio and the power coefficient reduces till equilibrium is found with the generator torque.

These two ways of speed control are identified as:

1) High lambda: If the aerodynamic power increases above rated power, the generator only consumes rated power and therefore the turbine rotor is let free to accelerate. Then the aerodynamic efficiency decreases, drag forces increase and equilibrium is obtained again at a higher tip-speed ratio than the optimum tip-speed ratio.
2) Low lambda: If the aerodynamic power increases above rated power, the rotor speed is decreased by increasing the generator torque so that the tip-speed ratio is below its optimum and the aerodynamic efficiency is decreased.

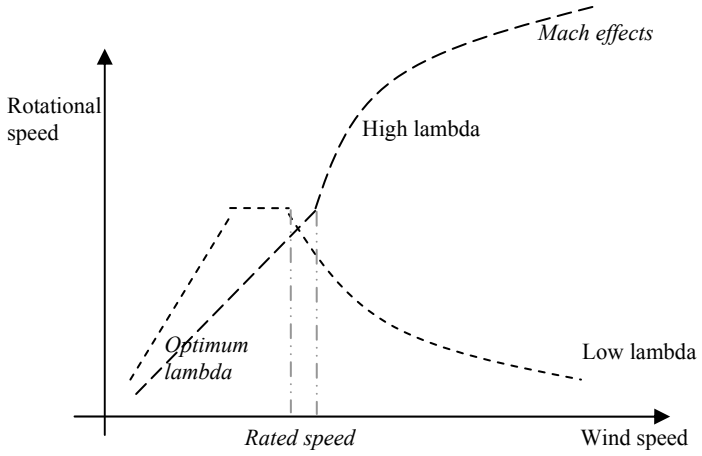

Figure 3.1: *Sketch of active speed stall control concepts.*

The high-lambda concept has the big benefit over the low-lambda concept that neither control nor an over-dimensioned generator is needed because the rotor itself will find equilibrium at a higher rotational speed. Another advantage is that it is not necessary to shut down the wind turbine at high wind speeds, that increases the value of the electricity produced with it.

However, at too many points the high-lambda concept is unfavourable. Firstly the optimum tip-speed ratio should be very low (around 5) so that there is sufficient margin for the rotor to speed up and decrease the aerodynamic efficiency. Such a low value for the optimum lambda is in contradiction with the option of a two bladed rotor introducing very large chord lengths (and thus high blade mass, high axial forces, etc) that is unfavourable for the cost of the rotor and other components of the wind turbine.
Secondly, for very high wind speeds the rotational speed will get so high (e.g. at $\lambda = 11$ for $U_\infty =$ 20 m/s $\Omega = 25$ rpm and the tip speed $\Omega R = 220$m/s ≈ 0.65 Mach) that compressibility effects will play a very important role. According to Hoerner [3.1],[3.2] at these speeds the slope of the lift curve will increase (the influence on maximum lift is not described there but it is assumed that the maximum lift coefficient will not increase), but more important the drag coefficient increases very sharply (which was desired) above a certain angle of attack and the critical Mach number ($M_{crit} \approx 0.65$ for t/c=0.18). Thus the rotor will be decelerated very fast at this speed. Besides problem of the ignorance of these effects in wind turbine aerodynamics (with the present models it is impossible to predict the loads accurately), the loads on the rotor and other components will most probably be higher than for the low-lambda design.

Therefore it is decided to use low-lambda aerodynamic power control in this study. The consequences for the conceptual generator design are described in chapter 1, where four different options for low-lambda control are discussed.

3.2 Aerodynamic design

For the aerodynamic design the ECN tool Blade Optimisation Tool (BOT) is used. The Blade Optimisation Tool is based on the stationary blade element momentum method including rotational effects on the lift coefficient and the correction for the finite number of blades (the Prandtl tip loss factor) [3.3].

3.2.1 Initial aerodynamic design

BOT needs an airfoil distribution (including the airfoils' aerodynamic coefficients; shown in Appendix A) as well as an initial aerodynamic design in terms of chord and twist distribution. The initial design is shown in Figure 3.2.

3.2.2 Turbine parameters

The parameters used in the optimisation are shown below. Note that the optimum tip-speed ratio at wind speeds below rated is higher than for a three-bladed turbine to ensure high rotational speeds (therefore low generator torques and enough space for active speed stall control) and small chord lengths.

Turbine parameters

Preferred TSR for low wind speeds:	$\lambda_0 = 9.0$.
Maximum rotational speed:	$\Omega_{max} = 8.0$ rpm.
Maximum electric power	$P_{rated} = 10$MW.
Fixed drive train losses:	$P_f = 300$kW (3% of P_{rated}).
Variable drive train losses:	$k_v = 7\%$ (775kW at P_{rated}).

Wind climate parameters

Using $U_{average}$=8.0m/s op H=10m and $U_{average}$=9.7m/s at H=100m;
According to the log-law wind-shear model: $U_{average}$=9.78 at H=H_{hub}=110m.
A Weibull wind speed distribution is assumed, with:

Air density:	$\rho_{air} = 1.225$ kg/m^3.
Weibull shape factor:	$k = 2.2$.
Weibull scale factor (from $U_{average}$):	$a = 11.05$ m/s

Regulation
The aerodynamic power for wind speeds above rated is regulated using active rotor speed stall control. This means that for increasing wind speed, the rotational speed is decreased such that the angle of attack at the blade increases, the flow stalls and the power is kept constant.

3.2.3 Optimisation criterion

In BOT the chord and twist distribution is optimised for maximum annual yield. Since for all wind speeds above rated wind speed ($U > U_{rated} = 12m/s$), the maximum power is obtained using this stationary method, the blade can be optimised for $U < U_{rated}$. Afterwards the rotational speed for $U > U_{rated}$ is determined such that $P = P_{rated}$ using active rotor speed stall control.

3.2.4 Optimum aerodynamic design

After the initial design based on maximum annual yield, some adjustments were made to reduce the design loads and to preserve stable blade vibrations in stalled operation:

- The chord length is reduced (to ±85%) to reduce aerodynamic loads.
- The tip chord is reduced to ensure a smooth circulation decrease (noise reduction).
- The twist is optimised for maximum annual yield after chord reduction.
- The root chord is reduced and the twist in the root region is highly lowered to enforce that stall starts at the blade root (to enhance aerodynamic damping).
- Back twist at the tip is added to introduce lower angles of attack (noise reduction and addition of positive aerodynamic damping).

These adjustments lead to the optimum, in the sense as describe above, aerodynamic design shown in Table 3.1 and Figure 3.2-Figure 3.4.

Table 3.1: "*Optimum" aerodynamic blade design.*

Radius [m]	Chord [m]	Twist [°]	Thickness [%]	Thickness [m]	Airfoil [-]
6.00	10.00	6.50	40.00%	4.00	DU40_X60
12.00	10.00	6.50	40.00%	4.00	DU40_X60
19.30	9.73	6.50	40.00%	3.89	DU40_X60
26.60	9.22	6.05	37.00%	3.41	DU35_X60
30.25	8.87	5.53	35.00%	3.10	DU35_X60
33.90	8.51	5.00	32.00%	2.72	DU30_X60
37.55	8.17	4.66	29.50%	2.41	DU30_X60
41.20	7.84	4.48	27.50%	2.16	DU25_X60
44.85	7.53	4.21	26.25%	1.98	DU25_X60
48.50	7.23	3.76	25.00%	1.81	DU25_X60
52.15	6.94	3.09	24.00%	1.67	DU25_X60
55.80	6.63	2.31	22.50%	1.49	FFA-W3-211_107
59.45	6.32	1.72	21.25%	1.34	FFA-W3-211_107
63.10	5.96	1.46	20.00%	1.19	FFA-W3-211_107
66.75	5.62	1.36	19.00%	1.07	NACA-63618
70.40	5.15	1.10	18.00%	0.93	NACA-63618
74.05	4.69	0.63	17.50%	0.82	NACA-63618
77.70	4.19	0.11	17.00%	0.71	NACA-63618
79.16	3.96	0.00	16.80%	0.67	NACA-63618
80.62	3.73	0.20	16.60%	0.62	NACA-63618
82.08	3.32	0.60	16.40%	0.55	NACA-63618
83.54	2.75	1.50	16.20%	0.44	NACA-63618
84.27	2.44	2.50	16.10%	0.39	NACA-63618
85.00	1.38	4.00	16.00%	0.22	NACA-63618

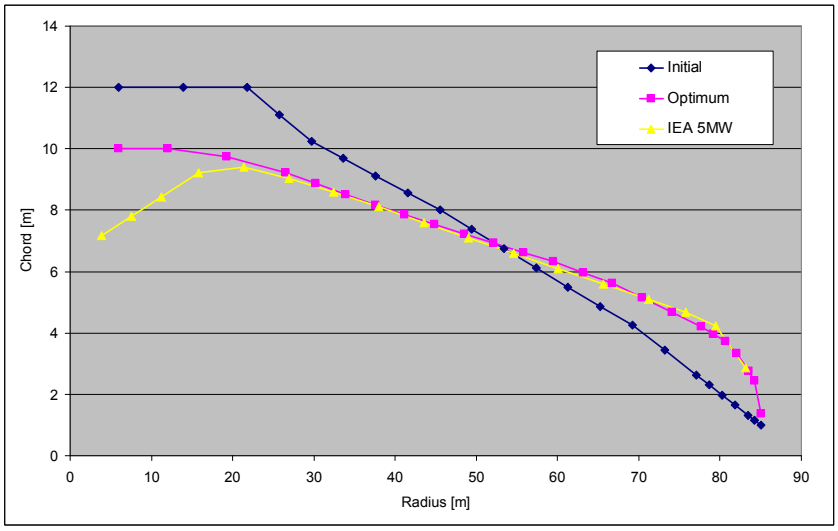

Figure 3.2: *Chord distributions.*

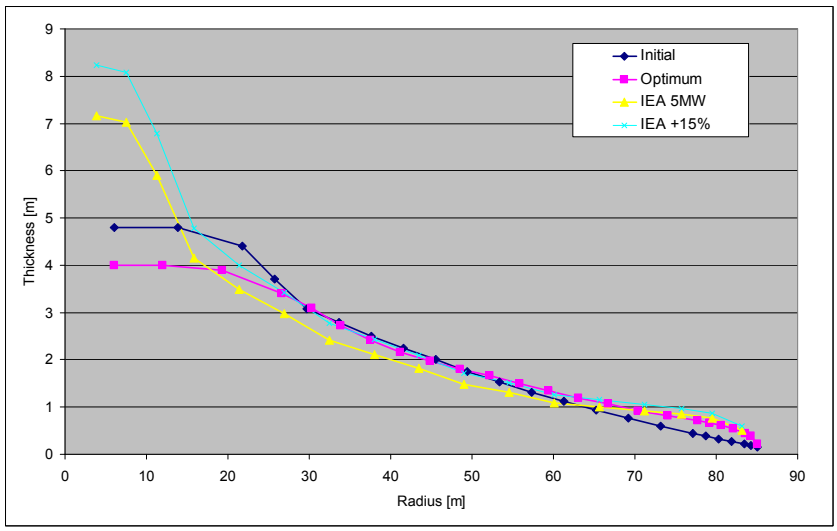

Figure 3.3: *Thickness distributions.*

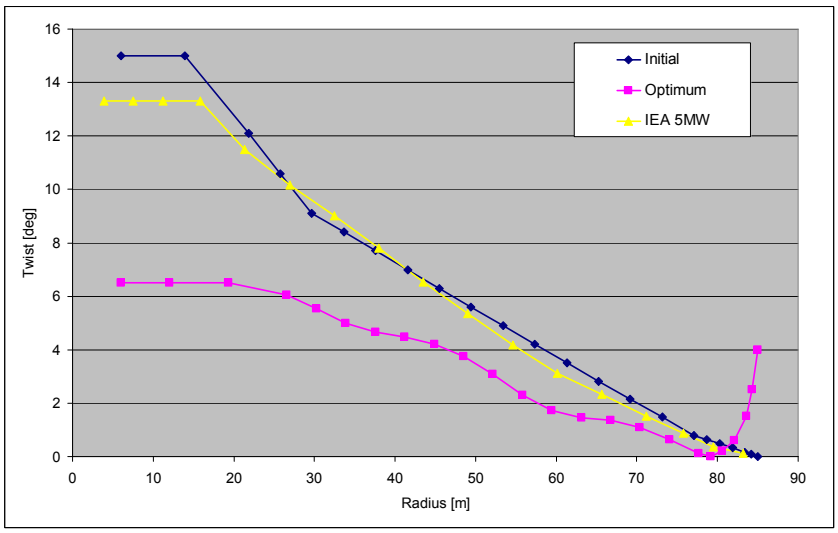

Figure 3.4: *Twist distributions.*

3.2.4.1 Performance curves

The performance for the active stall design is shown in Table 3.2. As can be seen, the tip twist angle is 0.85º (fixed for stall regulated blade). The bold values for the electrical power, the tip-speed ratio and the rotor rotational speed show the active speed stall control regulation.

Table 3.2: *Power curve for the "optimum" blade.*

U	P	θ	λ	$C_{P,aero}$	C_T	F_{ax}	$M_{bl.root}$	Ω	Q
[m/s]	[kWe]	[º]	[-]	[-]	[-]	[kN]	[kNm]	[rpm]	[kNm]
4.00	106.0	0.85	9.000	0.4907	0.9128	203.05	3795.76	4.044	250
4.50	278.1	0.85	9.000	0.4907	0.9128	256.98	4804.01	4.550	584
5.00	493.0	0.85	9.000	0.4907	0.9128	317.26	5930.87	5.056	931
5.50	755.5	0.85	9.000	0.4907	0.9128	383.89	7176.36	5.561	1297
6.00	1070.3	0.85	9.000	0.4907	0.9128	456.86	8540.46	6.067	1685
6.50	1442.2	0.85	9.000	0.4907	0.9128	536.17	10023.18	6.572	2096
7.00	1876.0	0.85	9.000	0.4907	0.9128	621.84	11624.51	7.078	2531
7.50	2376.4	0.85	9.000	0.4907	0.9128	713.84	13344.47	7.583	2992
8.00	2961.1	0.85	8.901	0.4926	0.9082	808.05	15093.94	8.000	3535
8.50	3675.0	0.85	8.378	0.5006	0.8820	885.88	16478.21	8.000	4387
9.00	4448.0	0.85	7.912	0.5037	0.8559	963.86	17855.69	8.000	5309
9.50	5277.0	0.85	7.496	0.5031	0.8295	1040.73	19203.72	8.000	6299
10.00	6155.7	0.85	7.121	0.4993	0.8023	1115.34	20505.81	8.000	7348
10.50	7076.2	0.85	6.782	0.4928	0.7752	1188.14	21772.18	8.000	8447
11.00	8037.9	0.85	6.474	0.4845	0.7487	1259.45	23013.07	8.000	9595
11.50	9036.9	0.85	6.192	0.4748	0.7228	1329.00	24229.69	8.000	10787
12.00	**10000.0**	0.85	**5.920**	0.4630	0.6957	1392.69	25360.93	**7.981**	12019
12.50	**10000.0**	0.85	**5.310**	0.4082	0.6144	1334.61	24411.38	**7.457**	12817
13.00	**10000.0**	0.85	**4.960**	0.3628	0.5583	1311.79	24044.93	**7.244**	13191
13.50	**10000.0**	0.85	**4.600**	0.3249	0.5090	1289.66	23575.37	**6.977**	13738
14.00	**10000.0**	0.85	**4.270**	0.2921	0.4680	1275.32	23191.66	**6.716**	14311
14.50	**10000.0**	0.85	**4.020**	0.2616	0.4318	1262.15	22813.45	**6.549**	14598
15.00	**10000.0**	0.85	**3.830**	0.2370	0.4021	1257.82	22594.25	**6.454**	14855
15.50	**10000.0**	0.85	**3.640**	0.2137	0.3737	1248.34	22279.48	**6.338**	15046
16.00	**10000.0**	0.85	**3.480**	0.1944	0.3498	1245.01	22097.15	**6.255**	15257
16.50	**10000.0**	0.85	**3.345**	0.1768	0.3262	1234.60	21979.92	**6.201**	15353
17.00	**10000.0**	0.85	**3.225**	0.1617	0.3064	1231.07	21935.92	**6.159**	15461
17.50	**10000.0**	0.85	**3.130**	0.1490	0.2900	1234.89	22067.49	**6.154**	15560
18.00	**10000.0**	0.85	**3.025**	0.1364	0.2742	1235.18	22046.87	**6.117**	15582
18.50	**10000.0**	0.85	**2.935**	0.1263	0.2615	1244.45	22149.89	**6.100**	15712
19.00	**10000.0**	0.85	**2.845**	0.1158	0.2483	1246.27	22115.40	**6.073**	15674
19.50	**10000.0**	0.85	**2.770**	0.1070	0.2372	1254.05	22180.76	**6.068**	15674
20.00	**10000.0**	0.85	**2.710**	0.0999	0.2282	1268.78	22369.64	**6.089**	15738
20.50	**10000.0**	0.85	**2.650**	0.0928	0.2191	1280.14	22483.85	**6.103**	15711
21.00	**10000.0**	0.85	**2.590**	0.0858	0.2101	1287.89	22522.24	**6.110**	15589
21.50	**10000.0**	0.85	**2.540**	0.0801	0.2027	1302.45	22691.05	**6.135**	15555
22.00	**10000.0**	0.85	**2.490**	0.0745	0.1954	1314.50	22804.56	**6.154**	15449
22.50	**10000.0**	0.85	**2.450**	0.0702	0.1897	1335.04	23080.43	**6.193**	15472
23.00	**10000.0**	0.85	**2.405**	0.0655	0.1835	1349.89	23227.75	**6.214**	15373
23.50	**10000.0**	0.85	**2.365**	0.0613	0.1781	1367.23	23435.48	**6.244**	15279
24.00	**10000.0**	0.85	**2.330**	0.0578	0.1735	1389.35	23726.10	**6.282**	15258
24.50	**10000.0**	0.85	**2.290**	0.0542	0.1688	1409.05	23929.39	**6.303**	15159
25.00	**10000.0**	0.85	**2.255**	0.0508	0.1645	1429.37	24178.85	**6.333**	15013

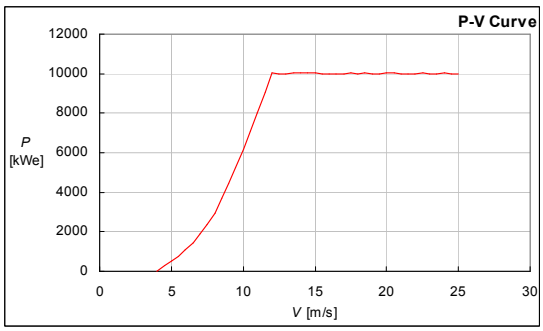

Figure 3.5: *Electric power for the optimum blade as a function of wind speed.*

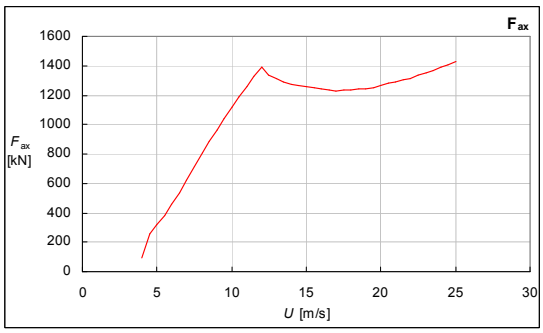

Figure 3.6: *Stationary axial force for the optimum blade as a function of wind speed.*

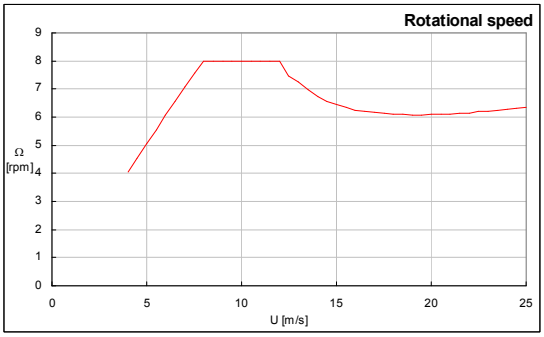

Figure 3.7: *Rotational speed for the optimum blade as a function of wind speed.*

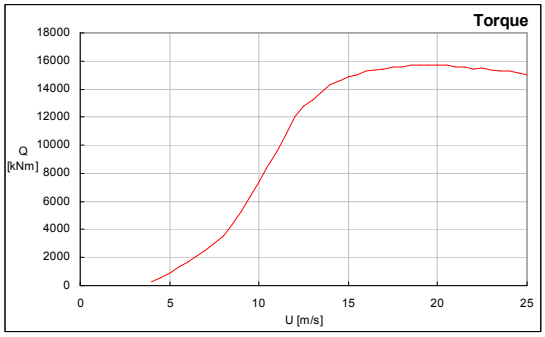

Figure 3.8: *Shaft/generator torque for the optimum blade as a function of wind speed.*

3.2.4.2 Chord, twist and profile distributions

The blade circulation distribution shown in Figure 3.9, shows a very uniform circulation distribution. Uniform circulation means little trailing vorticity. The smooth decline of circulation towards the tip shows that the trailing tip vortex is diffuse, therefore reducing the noise emissions.

The angle of attack distribution is shown in Figure 3.10 for wind speeds between 4 m/s and 25 m/s. Depending on the actual 3D lift effects stall is expected to start at the blade root. 3D Lift effects are highly dependent on the radial flow, which is not modeled in the blade element momentum method. Therefore the values for $r < 18m$ should be interpret with some care.

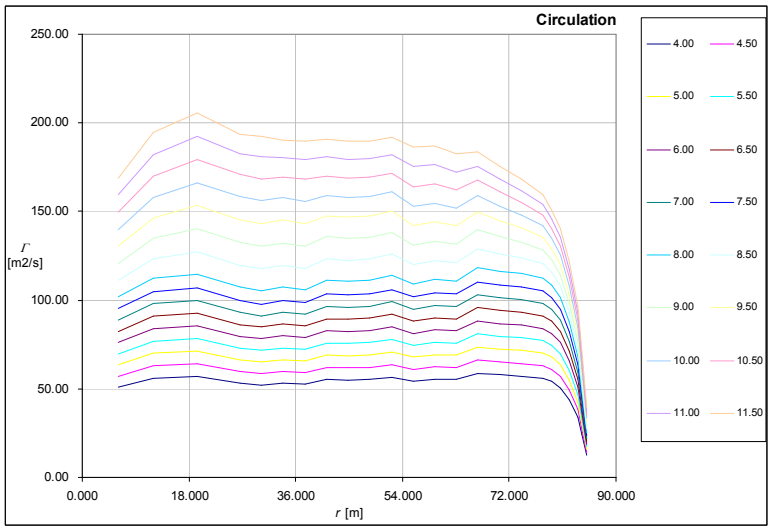

Figure 3.9: *Circulation distribution along the blade for wind speeds below rated power.*

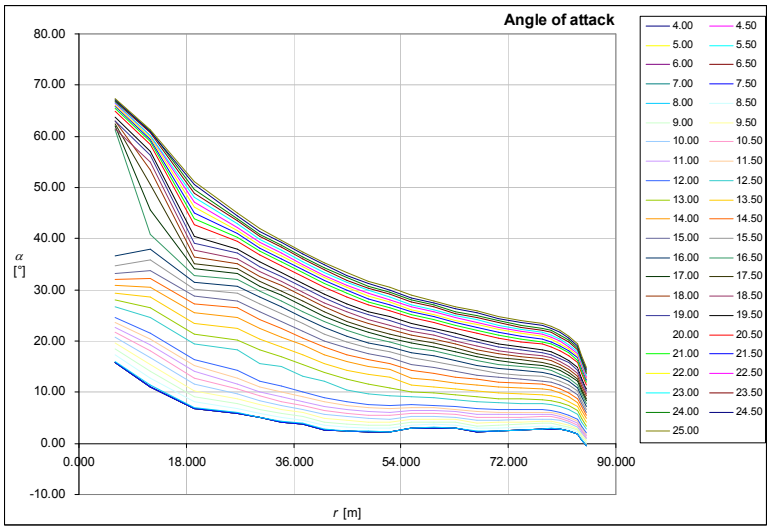

Figure 3.10: *Angle of attack distribution along the blade for all wind speeds.*

3.3 Structural design

Since the actual structural layout of the ICORASS blade is unknown, the structural properties of the UPWIND reference turbine are scaled towards the ICORASS blade dimensions. The scaled reference blade is shown in the plots for the chord, twist and thickness distribution (denoted with 'IEA 5MW' in the graphs), see Figure 3.2 - Figure 3.4.

It is assumed that each airfoil cross-section has identical structural layout. Therefore geometrical similarity and equal material properties are assumed. Then the blade properties are fully determined by the ratios of the dimensions. To be most accurate it is decided to use three independent scaling factors for the radial direction, chordwise direction and edgewise direction.

All properties are related to the relative blade position:

$$\frac{r}{R_{tip}};$$

therefore the scaling factor for the IEA 5MW blade in radial direction is simply:

$$SF_R = \frac{R_{tip,Icorass}}{R_{tip,IEA}} = \frac{85m}{63m} = 1.349.$$

The scaling factor for the chord and thickness of the IEA 5MW blade to obtain the ICORASS blade is somewhat more complicated because the IEA 5MW turbine has a three-bladed rotor. Neglecting the small discrepancy in optimum tip-speed ratio, the following scaling factor is suggested merely to obtain equal rotor solidity:

$$SF_c = SF_t = \frac{R_{tip,Icorass}}{R_{tip,IEA}} \frac{B_{Icorass}}{B_{IEA}} = \frac{85m}{63m} \cdot \frac{3}{2} = 2.024$$

Because for $r_{rel} > 0.28$ the chord distributions almost exactly match (by coincidence, therefore indicating that our blade design is quite well) this chordwise scaling factor can be applied.

The original twist and scaled profile thickness are show as well. As can be seen, except for the tip region, the IEA blade is slightly more slender (15%). Therefore the scaling factor in edge wise direction is increased to 2.024*1.15=2.328.

Table 3.3: *Scaling factors*

SF_{Radius}	= (85/63)	= 1.349
SF_{Chord}	= (85/63) * (3/2)	= 2.024
$SF_{Thickness}$	= (85/63) * (3/2) * 1.15	= 2.328

These scaling factors can be used to scale all blade properties for $r_{rel} > 0.28$. For example:
- The cross sectional area of the blade scales with: $SF_{Chord} * SF_{Thickness}$.
- The edgewise bending stiffness of the blade scale with: $(SF_{Chord})^3 * SF_{Thickness}$.

These scaling factors are used for the geometry of the blade structure as well as for the wall thickness in these directions. Note that normally the total wall thicknesses for a two-bladed rotor are smaller than those for a three-bladed rotor of equal radius to obtain equal strength. However, since both the mass and the stiffness of the blade scale with the wall thickness, this has no consequences for the value of natural frequencies and modal shapes and is therefore not taken into account.
For $r_{rel} < 0.28$, in the IEA 5MW blade a transition between actual airfoil shapes and the cylindrical blade root takes place. Therefore the blade cross sectional properties differ largely from the rest of the blade.
However, for the ICORASS blade a transition to a cylindrical root is not necessary since the ICORASS blade does not have a pitch mechanism and is manufactured in one piece. The DU40 airfoil sections extend all the way to the root. Assuming a geometrically similar structural layout, the cross sectional properties are simply scaled from the $r_{rel} = 0.28$ inwards.

In Figure 3.11-Figure 3.14 the blade properties along the span are shown graphically. A first check shows that the blade mass density is nearly linear with the radial position and that the fourth root of the stiffness is nearly linear as well.

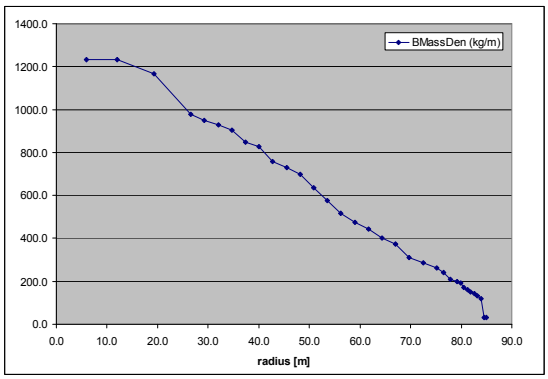

Figure 3.11: *Blade mass density.*

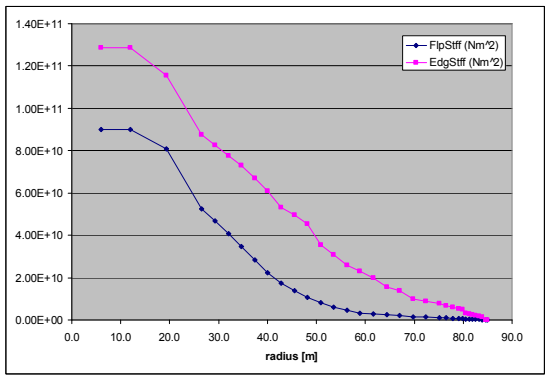

Figure 3.12: *Flat- and edgewise stiffness.*

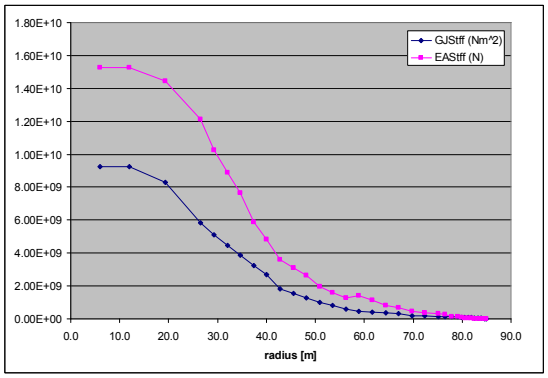

Figure 3.13: *Torsion and tension stiffness.*

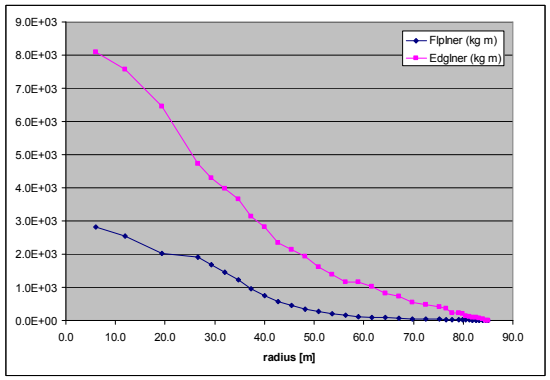

Figure 3.14: *Mass moments of inertia.*

3.4 Aeroelastic analysis

The aeroelastic stability analysis is conducted with the ECN computer code BLADMODE [3.4]. Besides the already mentioned properties, a cone angle, tilt angle and pre-bend is defined:

- Cone angle -3.0º
- Tilt angle 5.0º
- Flap pre-bend -2.5m
- Lag pre-bend 0.5m
- Pre pre-bend begin 20.0m
- Pre pre-bend end 70.0m

The quarter chord line is defined at -15% chord length from the blade axis (at the side of the LE). Logically, then the blade centre line is at +10% chord length from the blade axis. The centre of gravity, centre of elasticity and shear centre are defined as half way between the blade axis and the centre line (at +5%).

3.4.1 Analysed modes

A limited aeroelastic stability analysis is conducted. This means that only the following three modes are analysed:

- 1P gravity reaction mode.
  The reaction due to periodic gravity loading results in edgewise bending.

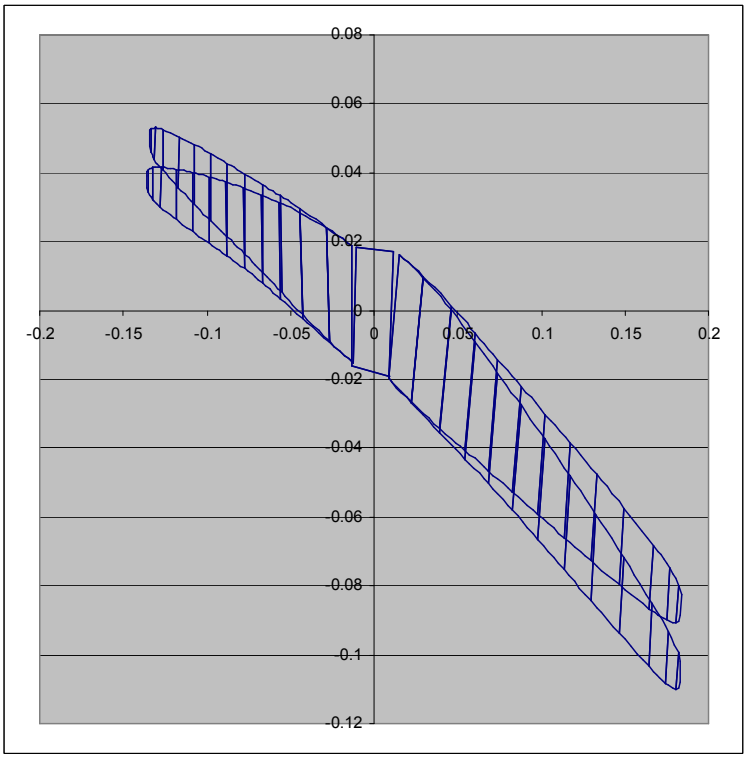

Figure 3.15: *1P Gravity loading mode.*

- Symmetric blade flatwise bending mode.
  Since no data is known, no tower top fore-aft flexibility is included in this analysis.

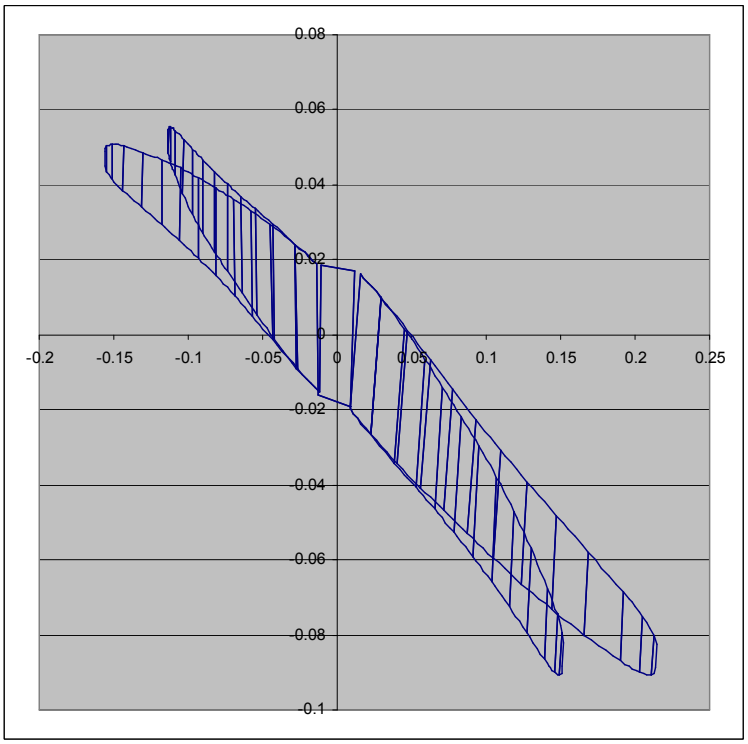

Figure 3.16: *First flatwise mode.*

- Reaction-less edgewise bending mode.
  The reaction-less edgewise has no interaction with the drive train. Because the torque control of the drive train is not known, the collective edgewise mode cannot be investigated.

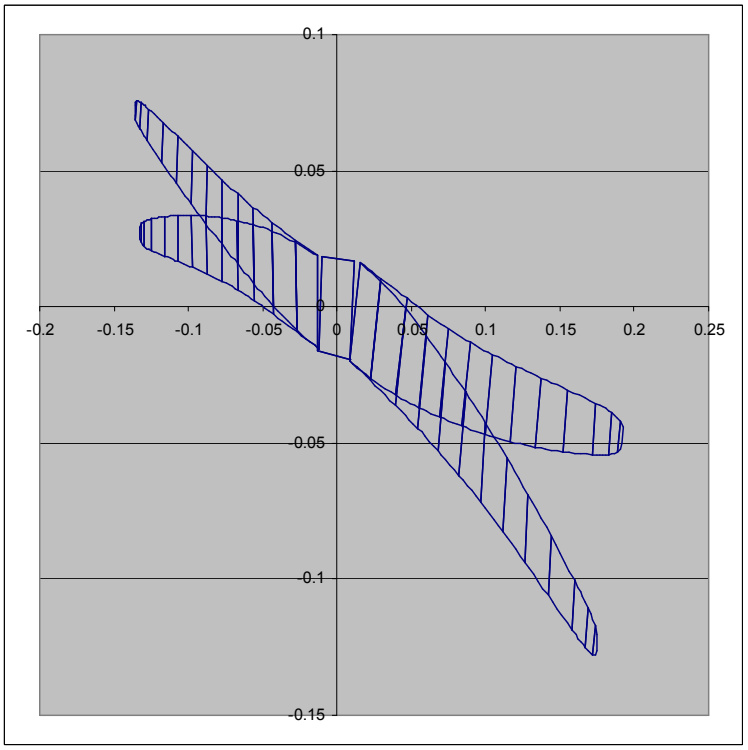

Figure 3.17: *First edgewise mode.*

3.4.2 Natural frequencies

For a uniform bar (of length L and mass per unit length m, with elasticity E and moment of inertia I) that is clamped at one side, the natural frequencies are proportional to [3.5]:

$$\omega \sim \sqrt{\frac{EI}{mL^4}}\,.$$

With a uniform scaling factor and constant density and elasticity this would imply reducing frequencies with increasing blade size:

$$\omega \sim SF^{-1}\,.$$

However, applying the directionally dependent scaling factors results in:

$$\begin{aligned} I_{flat} &\sim SF_t^3 \cdot SF_c\,, \\ I_{edge} &\sim SF_c^3 \cdot SF_t \\ m &\sim SF_c \cdot SF_t\,, \\ L &\sim SF_R\,, \end{aligned}$$

so that the natural frequencies increase slowly when scaling the IEA 5MW turbine to the ICORASS blade:

$$\begin{aligned} \omega_{flat} &\sim \sqrt{\frac{SF_t^2}{SF_R^4}} \approx 1.28, \\ \omega_{edge} &\sim \sqrt{\frac{SF_c^2}{SF_R^4}} \approx 1.11. \end{aligned}$$

Subsequently the rotational speed decreases (from a maximum of 12 rpm for the IEA 5MW to a maximum of 8 rpm for the ICORASS turbine), so that the natural frequencies correspond to a higher rotational periodicity. This can clearly be seen in Figure 3.18 where the natural frequencies of the first edgewise and flatwise modes are shown as a function of wind speed. Besides, the edgewise stiffness towards the root is very high in contrast to a conventional blade, since the blade root is not circular, but is a DU40 airfoil.

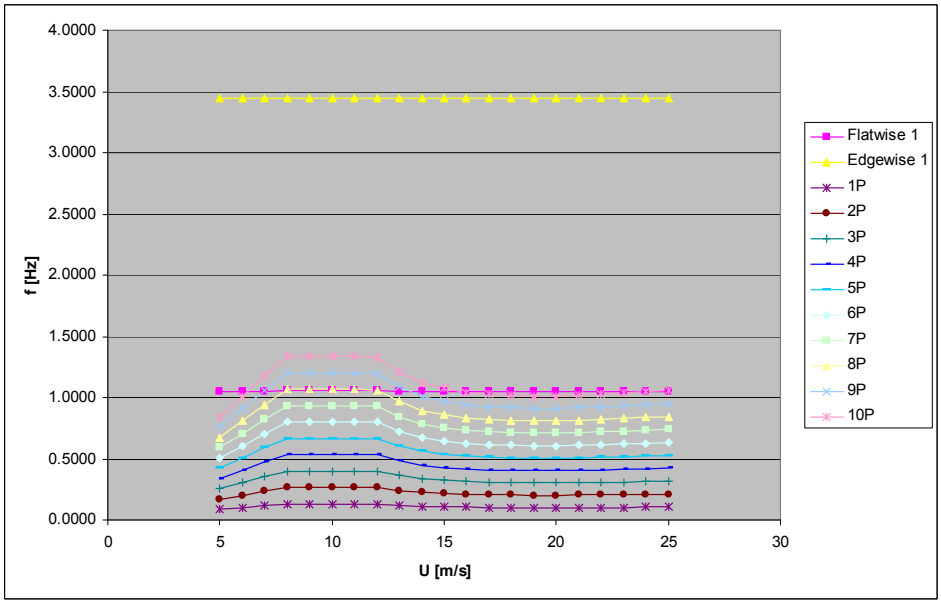

Figure 3.18: *Frequencies of the first two eigenmodes.*

3.4.3 Aerodynamic damping

BLADMODE is used to calculate the aerodynamic damping at different wind speeds. In Figure 3.19 the damping for the first flatwise mode is shown. Clearly the aerodynamic damping is highly positive. Although the tower top fore-aft bending is not included is this analysis, one might conclude that this mode will be stable.

In Figure 3.20 however, for some wind speeds around or above rated wind speed, the aerodynamic damping is found to be around zero for the first reaction-less edgewise mode and negative for the 1P gravity loading mode. For attached flow, increasing the drag coefficients to presumably more realistic values (0.01) adds some extra aerodynamic damping. E.g. at 11.0m/s the 1P gravity loading mode goes from 0.145% to 0.182%, however the reaction-less edgewise mode only goes from 0.287% to 0.294%.

The negative damping for the 1P gravity response will not lead to instability because the 1P response is not an eigenmode (resonance frequency) of the rotor. For this mode, negative damping for the 1P gravity response will result in larger amplitudes compared with those for positive damping.

Although the aerodynamic damping for the first edgewise mode is very small for some wind speeds, the structural damping (around 0.5-1.0%) will make sure that the mode is stable. Besides, structural pitch or aerodynamic tailoring can be used to increase the aerodynamic damping so that a stable aero-elastic design for the ICORASS turbine is feasible.

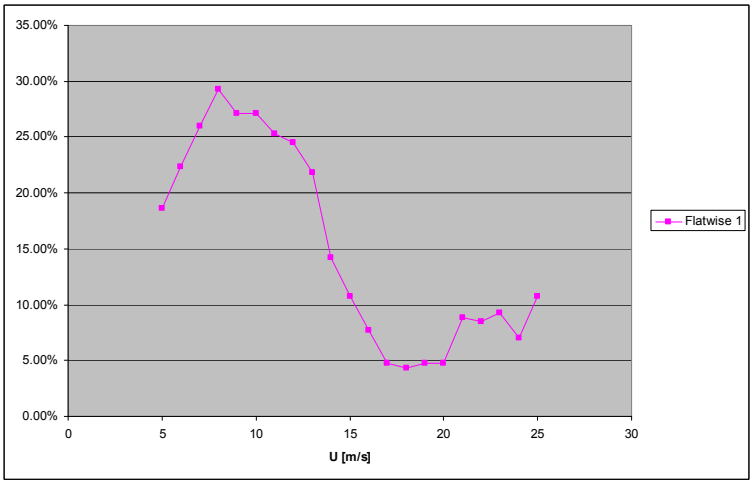

Figure 3.19: *Aerodynamic damping of the first flatwise mode.*

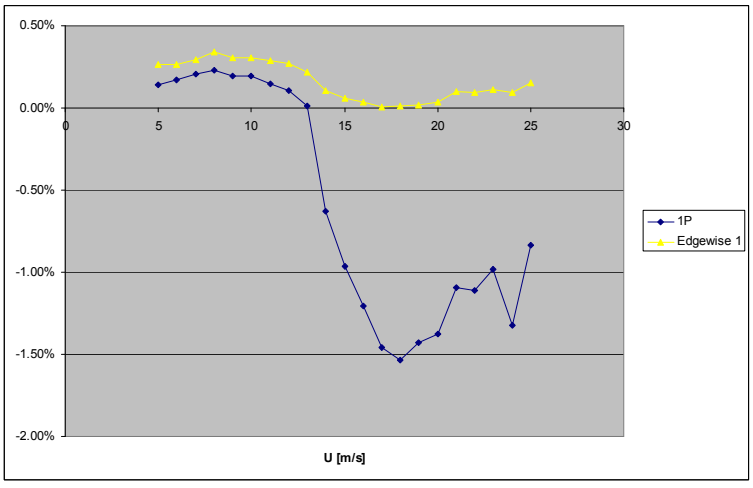

Figure 3.20: *Aerodynamic damping of the 1P gravity loading mode and first edgewise mode.*

3.5 Conclusions

An aerodynamic design is obtained with **BOT**, Blade Optimisation Tool. Its structural properties were derived by scaling of the structural properties of a three bladed rotor from the IEA 5MW turbine.

During the aero-elastic stability analysis it was noted that the power output predicted with **BOT** was a lot higher than the power output predicted with the **BLADMODE** computer code. The source of this discrepancy lies in the airfoil aerodynamics. The implementation of the correction for the rotational effect for high angles of attack within both programs differs. The higher the wind speed, the more the blade flow goes into stall and the larger the difference. This might need some extra effort, since stalled flow might be important for the critical aerodynamic damping of the first edgewise mode and the 1P gravity loading mode.

The reaction-less blade bending mode has an aerodynamic damping that is only just positive. The 1P gravity response mode has a more negative aerodynamic damping. Because the latter mode is not a resonance mode, this negative damping will not lead to instability, but will give increased response amplitude. The very low drag coefficients have an influence on the aerodynamic damping when there is attached flow.

As was mentioned, due to the applied straightforward scaling rules, the blade wall thickness is probably over-dimensioned. This results in both higher stiffnesses and higher masses so that the blade deflections and the normalised aerodynamic damping are low. Based on this data, the total integrated blade mass is 58 ton and the moment of inertia around the blade axis is 90 $Mkg \cdot m^2$.

Regarding the manufacturability of an integrated rotor, for a more detailed design it is recommended to investigate the influence of pre-bending and the cone angle at the aerodynamic performance, aero-elastic stability and tower clearance. For manufacturing purposes both should be minimized.

3.6 References

[3.1] Hoerner, S.F. & Borst, H.V. *Fluid-dynamic lift (chapter 7).* 2nd Edition. 1967.

[3.2] Hoerner, S.F. *Fluid-dynamic drag (chapter 15).*2nd Edition. 1965.

[3.3] Bot, E.T.G. & Langen, P.J. van. *Blade Optimisation Tool. User Manual.* ECN-E--06-006. Petten, August 2006.

[3.4] Lindenburg, C. *BLADMODE. Program for rotor blade mode analysis.* ECN-C--02-050. Petten, July 2003.

[3.5] Meirovitch, L. *Elements of vibration analysis (pp. 223-227).* McGraw-Hill, Singapore, 1986.

4. Consequences for the generator system and generator design

In earlier chapters of this report, the ideas behind the ICORASS concept have been discussed. The objective of this chapter is to compare the generator system of the ICORASS turbine to the generator system of a comparable wind turbine with a conventional pitch control.

Table 4.1 gives the characteristics of the turbine, and the generator materials that will be used. This chapter starts with a description of different possible control strategies. Then the results of the different control strategies are discussed. This chapter ends with a conclusion.

Table 4.1: *Wind turbine and generator material characteristics.*

Wind turbine characteristics	
Rated grid power [MW]	10
Rotor diameter [m]	170
Rated wind speed [m/s]	12
Rated speed [rpm]	10
Optimum tip speed ratio (blade tip speed divided by wind speed)	9.5
Maximum aerodynamic rotor efficiency [%]	51.5
Mass density of air [kg/m^3]	1.225
Average wind speed at location [m/s]	10
Generator material characteristics	
Slot filling factor k_{sfil}	0.65
Remanent flux density of the magnets B_{rm} [T]	1.3
Recoil permeability of the magnets μ_{rm}	1.06
Resistivity of copper at 120° ρ_{Cu} [μΩm]	0.025
Eddy-current losses in laminations at 1.5 T and 50 Hz P_{Fe0e} [W/kg]	0.5
Hysteresis losses in laminations at 1.5 T and 50 Hz P_{Fe0h} [W/kg]	2
Loss modeling	
Maximum losses in a 10 MW VSI P_{convm} [kW]	300
Maximum losses in a 14 MW VSI P_{convm} [kW]	420
Cost modeling	
Power electronics cost [€/kW]	40
Laminations cost [€/kg]	3
Copper cost [€/kg]	15
Permanent magnet cost [€/kg]	25

4.1 Control strategies

It is clear that the ICORASS wind turbine will be controlled using the rotor speed. At low wind speeds, the rotor speed will be proportional to the wind speed in order to maximize energy yield. At high wind speeds, the rotor speed will be limited or reduced in order to limit the output power. As a starting point, we use the power and torque curves of Figure 4.1 and Figure 4.2.

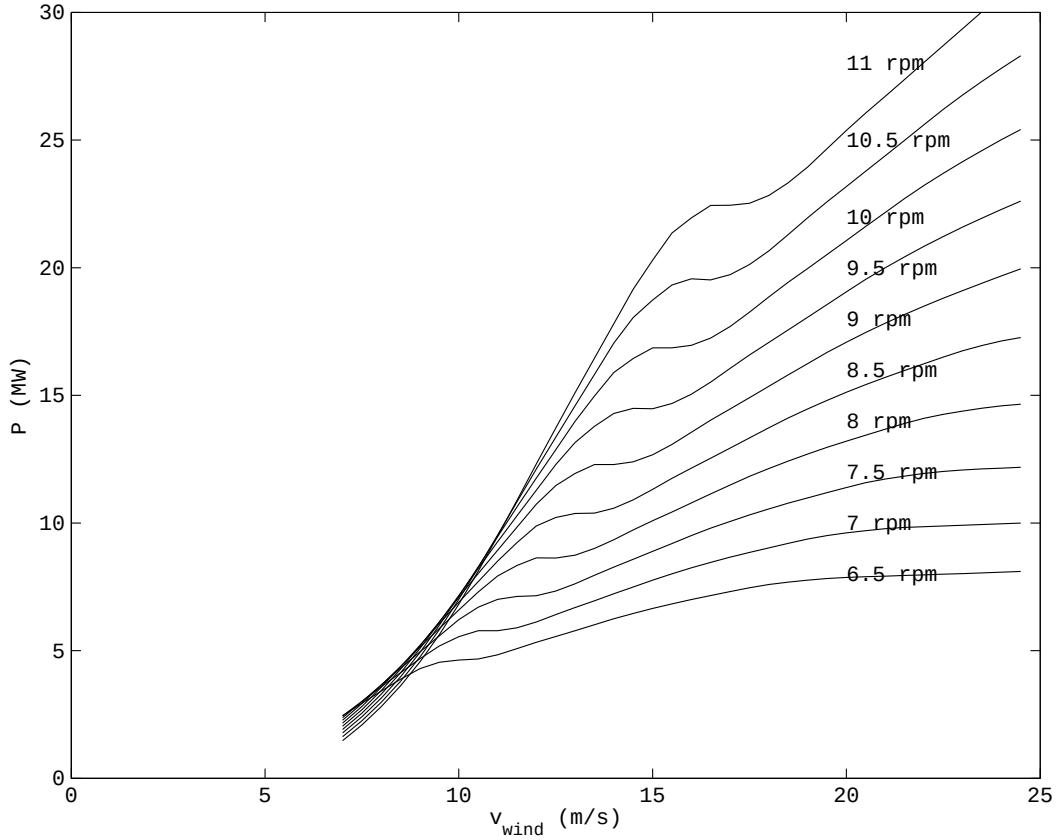

Figure 4.1: *Power curves of the ICORASS blades at constant speeds of 6.5-11 rpm.*

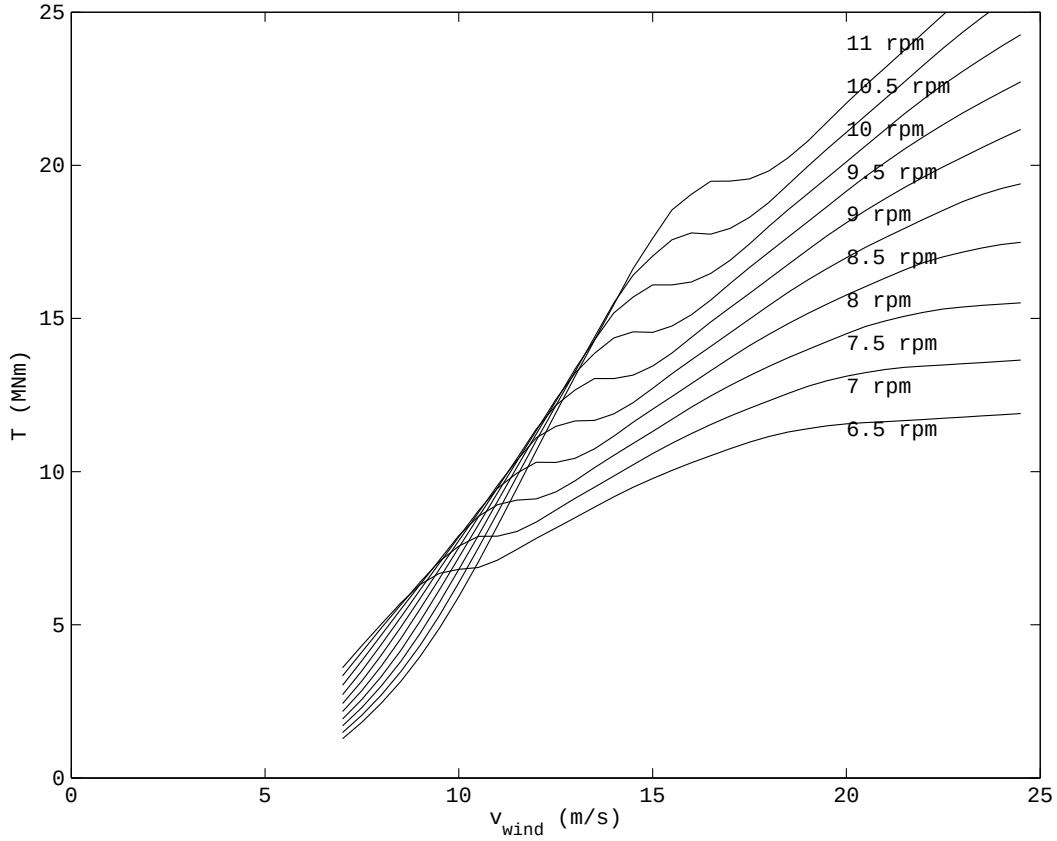

Figure 4.2: *Torque curves of the ICORASS blades at constant speeds of 6.5-11 rpm.*

The main problem is that it is not yet determined how the rotor speed of the ICORASS turbine will be controlled at these higher wind speeds. In this chapter, a few possible extremes will be discussed. To explain these extremes and why they are chosen, we use the power curves of Figure 4.1.

There are a number of ways to control the speed of the ICORASS wind turbine.

1) If the power of the generator system is not limited, we are able to control the speed. For example, if the wind speed is 12 m/s and the rotational speed is 9 rpm, the output power is about 10 MW. If the wind speed would instantaneously increase from 12 to 24 m/s, the power would instantaneously increase to 20 MW. If the generator system is able to make a power larger that 20 MW, the generator is able to reduce the speed of the rotor to 7 rpm so that the output power is 10 MW again. However, implementing a 20 MW generator system in a 10 MW wind turbine is probably too expensive.
2) A safe way of operating the wind turbine is by keeping the speed so low that the power will never exceed the 10 MW. In practise, this means that the speed has to be limited to roughly 7 rpm, because at this speed the power is limited to 10 MW for all wind speeds and all changes in wind speed. However, this will result in a rather low energy yield.
3) If we know the wind speed (averaged over the rotor surface area) in advance, we can reduce the rotor speed before the wind speed increases. In that way, we can use a 10 MW generator system. For example, if we know that in 60 seconds, the wind speed will instantaneously increase to 24 m/s, we have 60 seconds to reduce the speed to 7 rpm, which should be enough.
4) It is very unlikely that the rotor averaged wind speed will instantaneously increase from 12 to 24 m/s. If we know that the increase of the wind speed is limited, it must be possible to design a control that adapts the rotational speed based on the measured rotor speed. If the increase of the wind speed would be limited, it is possible to reduce the speed of the rotor while the wind speed increases. However, relying on this is critical, because a faster increase of the wind speed could lead to the problem that the generator system is not able to reduce the rotor speed, and then the rotor speed will increase, which results in a further increase in the power, which will destroy the turbine if the wind speed does not reduce quickly again.

An additional complication is that it is not really the power level of the generator system that is limited. The limitations are the following.

- The torque level of the generator is limited. Because of the large thermal time constant 10-20% overloading during a few minutes is mostly not a problem.
- The voltage level of the converter is limited; the converter is designed for a voltage level. Because the generator voltage is proportional to the rotor speed, the limitation of the converter voltage level also implies a limitation of the speed of the generator and thus the rotor.
- The current level of the converter is limited. Because of the small thermal time constant 10% overloading during a few seconds may already be a problem.

In the next sections, we will discuss four ways to operate an ICORASS turbine, and compare them to a pitch controlled turbine with the same rotor. The four ICORASS turbine control option characteristics are given by:

1) a generator system that is so heavily overrated that it is always able to reduce the rotor speed to values at which the power is 10 MW with a maximum rotor speed of 9 rpm,
2) a control principle in which the speed is limited to 7.2 rpm,
3) a control principle in which the power is limited to 10 MW,
4) a control principle in which the torque is limited to 14 MNm.

The consequences of these control principles will be discussed in more detail in the sections below.

4.2 Pitch control

Table 4.2 gives the characteristics of the generator system used for the pitch-controlled generator. If pitch control is used, the power is limited to 10 MW by pitching the blades. Therefore, the power ratings of generator, converter and cables are all 10 MW.
Figure 4.3 illustrates the steady-state operation characteristics of this turbine with pitch control. At low wind speeds, the turbine is operated at maximum aerodynamic efficiency up to the rated speed of 10 rpm; at high wind speeds, the pitch control keeps the speed at 10 rpm.
By integrating the area below the graph of energy as a function of wind speed, the annual energy yield can be obtained. From this graph, it can be concluded that the energy yield could be increased considerably by increasing the generator system power.

Table 4.3 gives the annual energy yield for this control principle.

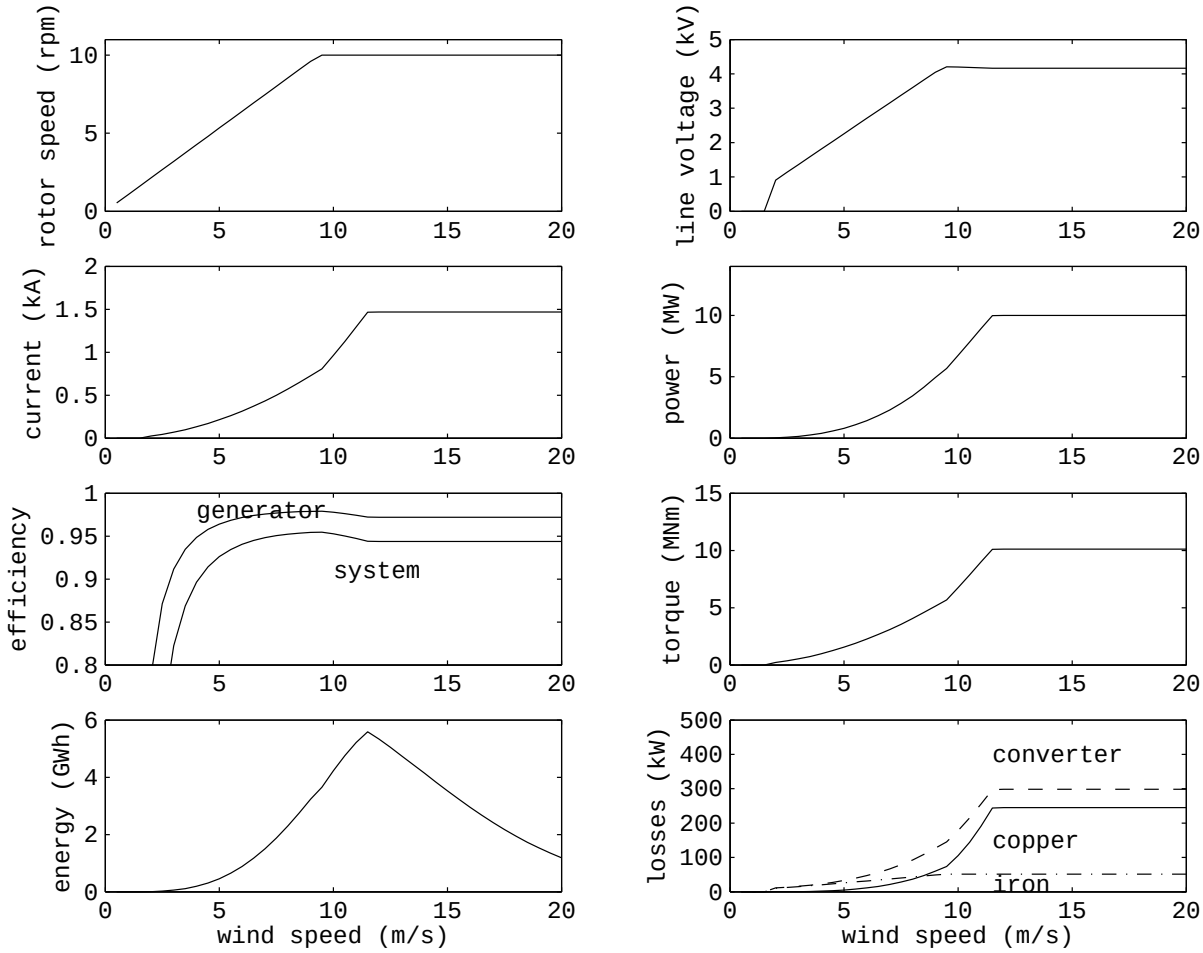

Figure 4.3: *Characteristics of a turbine with pitch control, a rated speed of 10 rpm and a rated torque of 10 MNm.*

4.3 ICORASS with heavily overrated generator system

Table 4.2 gives the characteristics of the ICORASS generator where the generator system has been overrated to such an extent that it will probably be able to operate the turbine in a safe way. This generator system can increase the torque to 20 MNm if necessary. This can be achieved by doubling the axial stack length, which has a considerable effect on weight and cost. In principle, this also implies that the offshore infrastructure has to be designed for peak power levels of 20 MW.

In this ICORASS system, the steady state power is limited to 10 MW, and the maximum rotor speed is 9 rpm. The power ratings of generator, converter and cables are all 18 MW in order to be able to cope with wind speed changes.
Figure 4.4 illustrates the steady-state operation characteristics of the turbine with this safe generator system. At very low wind speeds, the turbine is operated at maximum aerodynamic efficiency up to the rated speed of 9 rpm. At higher wind speeds, this speed is kept constant at 9 rpm, until the power level of 10 MW is reached. Then the speed is reduced to limit the power to 10 MW. In order to keep the power at 10 MW at decreasing speeds, the torque has to increase.
Table 4.3 gives the annual energy yield for this control principle. The annual energy yield is comparable to the energy yield with pitch control.
During wind speed increases, the power level of the turbine will increase to values above 10 MW. A more detailed study has to be performed to investigate what power levels will be reached

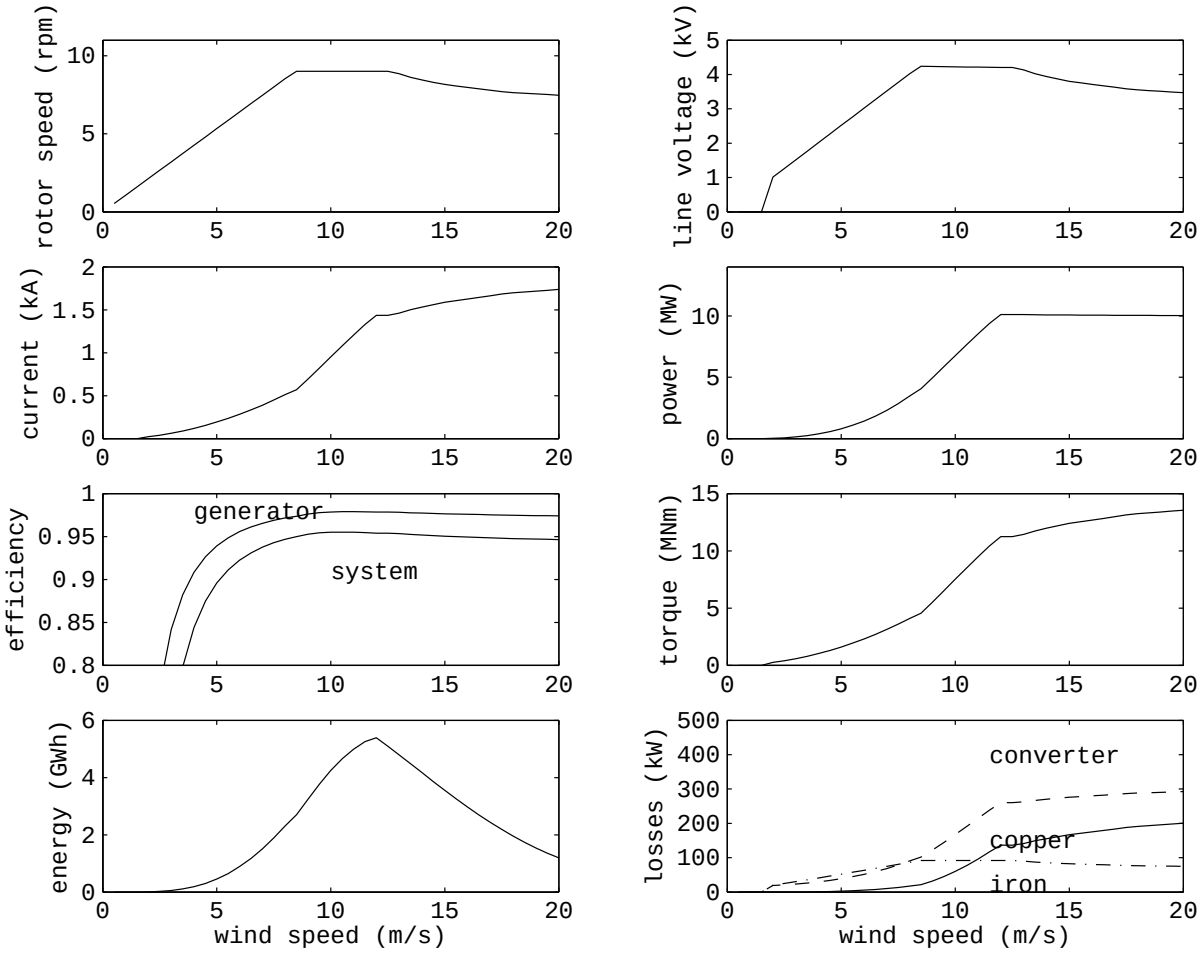

Figure 4.4: *Characteristics of an ICORASS turbine with a heavily overrated generator system that can take a power of 18 MW.*

4.4 ICORASS control with speed limit

In the previous control option, the generator system is extremely overrated and therefore relatively heavy and expensive. By limiting the speed to lower values, the power can be limited to 10 MW under all circumstances.
Table 4.2 gives the characteristics of the ICORASS generator. This generator has to be able to produce the same power at a lower speed. Therefore the torque rating has to be increased. This has been done by making the axial stack length 40% larger when compared to pitch control, which has still has a considerable effect on weight and cost.

In this ICORASS control option, the power is limited to 10 MW in a safe way, namely by limiting the speed to 7.2 rpm, so that the generator power never exceeds 10 MW. Therefore, the power ratings of generator, converter and cables are all 10 MW.
Figure 4.5 illustrates the steady-state operation characteristics of the turbine with this control concept. At very low wind speeds, the turbine is operated at maximum aerodynamic efficiency up to the rated speed of 7.2 rpm; at higher wind speeds, the torque control keeps the speed at 7.2 rpm.
Table 4.3 gives the annual energy yield for this control option. The annual energy yield reduces with 20% when compared to a conventional pitch control, which is a large reduction.

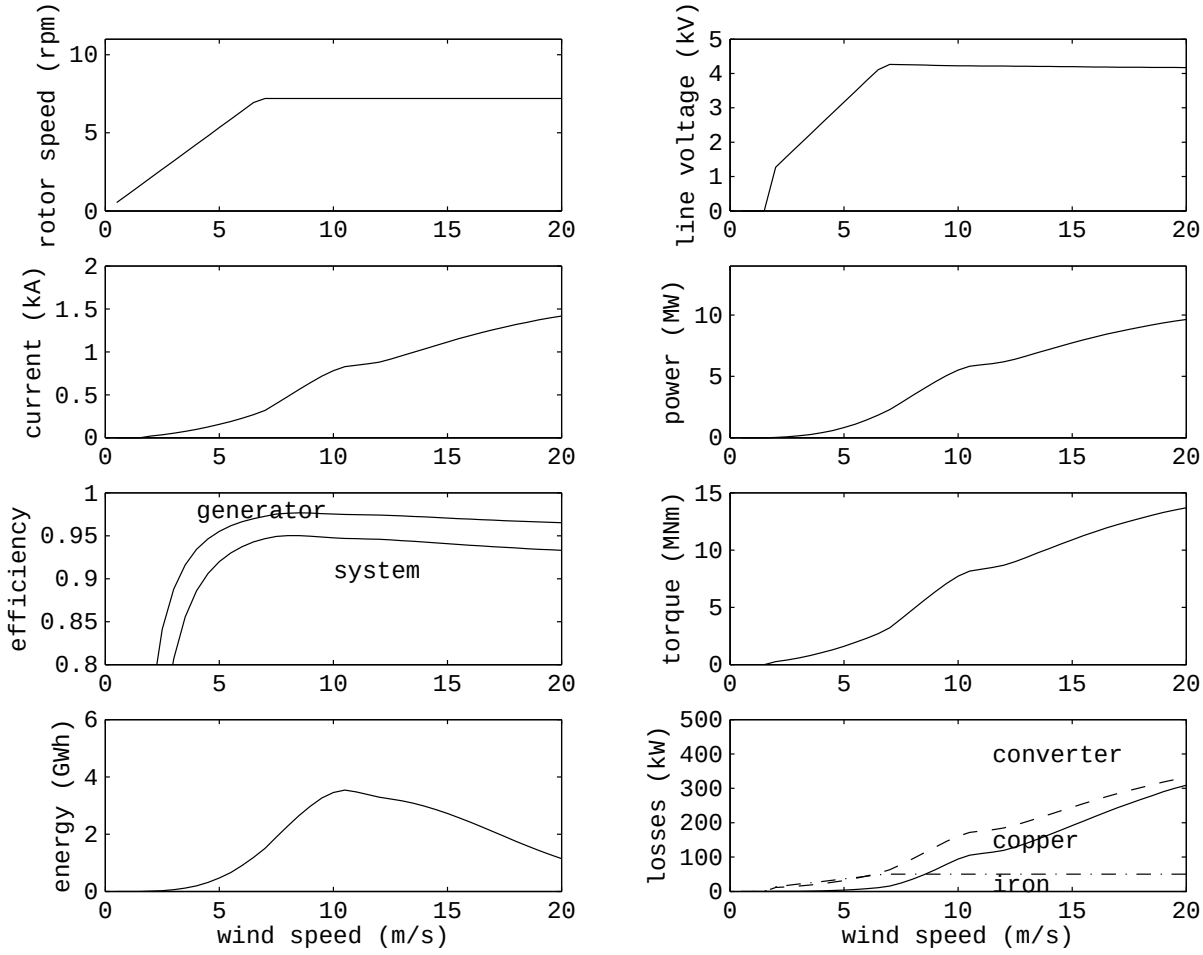

Figure 4.5: *Characteristics of an ICORASS turbine in which the speed is limited to 7.2 rpm so that the power never exceeds 10 MW. The rated torque is 14 MNm.*

4.5 ICORASS control with power limited to 10 MW.

In this control concept, the power is limited to 10 MW assuming that the wind speed changes are very low, or we know them sufficiently long before they happen.
Table 4.2 gives the characteristics of the ICORASS generator, which is the same generator as used in section 4.4, with a torque rating of 14 MNm. The converter rating and the generator rating are 12.6 MW because the machine and the converter would be able to generate 12.6 MW if the speed would be kept at 9 rpm. Because the power is limited to 10 MW, the cables can probably be dimensioned for 10 MW.
Figure 4.6 illustrates the steady-state operation characteristics of this control concept with limited power. At low wind speeds, the turbine is operated at maximum aerodynamic efficiency up to the rated speed of 9 rpm. At higher wind speeds, this speed is kept constant, until the power

level of 10 MW is reached. Then the speed is reduced to limit the power to 10 MW. In order to keep the power at 10 MW at decreasing speeds, the torque has to increase.
Table 4.3 gives the annual energy yield for this control principle. The annual energy yield is comparable to the energy yield with a conventional pitch control.
This control option can only be used if the speed of the rotor is reduced before the wind speed increases. If the turbine works at rated conditions and the wind speed increases instantaneously to twice the rated value, the power will increase to 20 MW, which is not possible for a generator system rated at 10 MW. However, at rated wind speed, the generator system is not used at its maximum torque. Therefore, if the wind speed increases sufficiently slowly, the torque can be increased to above rated to reduce the speed and in that way reduce the power. In that case, the power level will increase to above 10 MW. This will be further discussed in section 4.7.

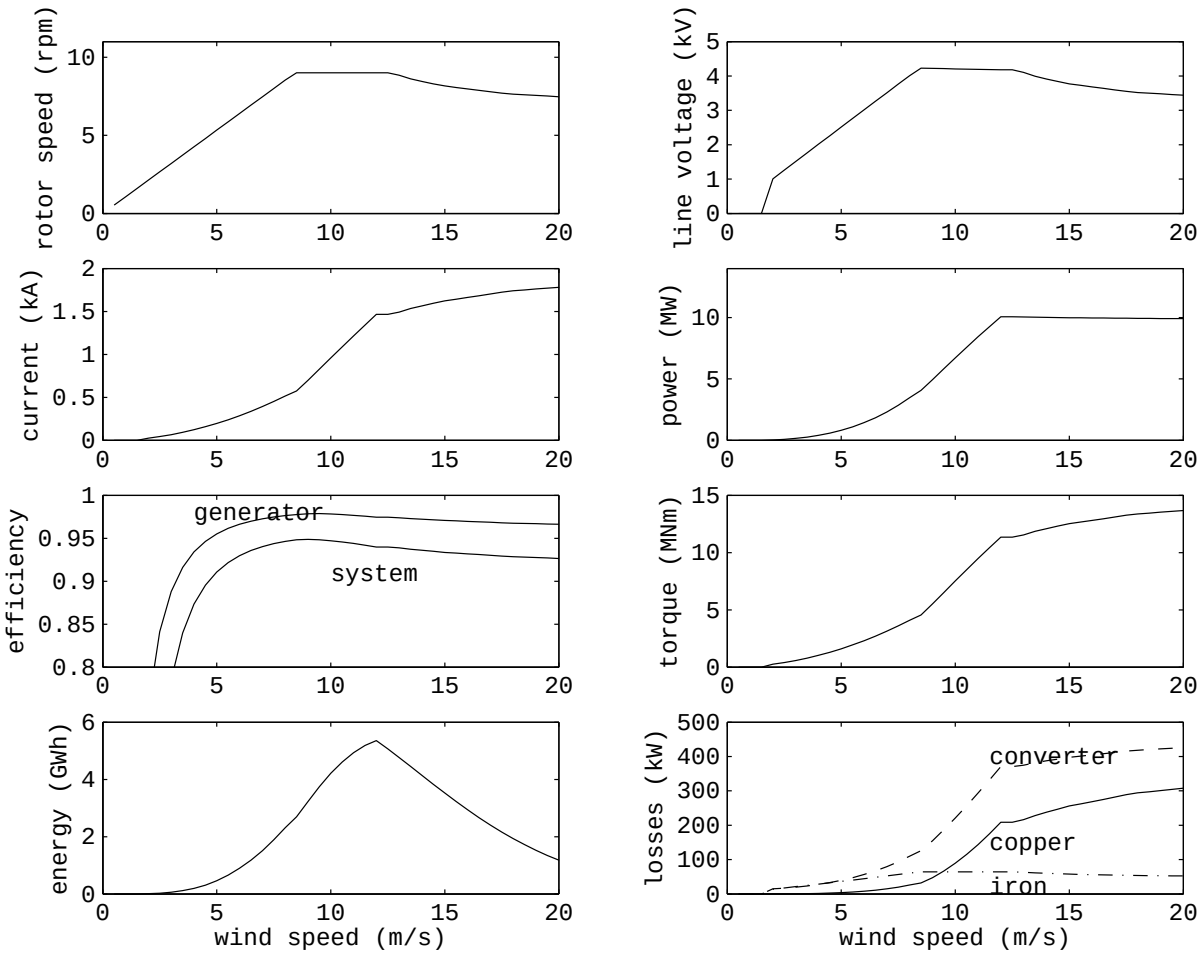

Figure 4.6: *Characteristics of an ICORASS turbine in which the power is limited to 10 MW. The rated torque is 14 MNm.*

4.6 ICORASS control with torque limited to 14 MNm.

The idea behind this control principle is that the generator and the converter are able to make 14 MNm, and therefore, it would be possible to use them up to this torque level.
Table 4.2 gives the characteristics of the ICORASS generator, which is the same generator as used in section 4.4 and 4.5, with a torque rating of 14 MNm. In this case, the generator, the converters and the cables have to be rated for 12.6 MW.
Figure 4.7 illustrates the steady-state operation characteristics of this ICORASS control concept. At low wind speeds, the turbine is operated at maximum aerodynamic efficiency up to the rated speed of 9 rpm. At higher wind speeds, this speed is kept constant, until the torque level of 14

MNm is reached. Then the speed is reduced to limit the torque to 14 MNm. In order to keep the torque at 14 MNm, the speed has to decrease, and therefore also the power decreases
Table 4.3 gives the annual energy yield for this control principle. The annual energy yield for this control concept is approximately 6% higher than for the turbine with pitch control.
This control concept can only be used if the speed of the rotor is reduced before the wind speed increases. If the turbine works at rated conditions and the wind speed increases instantaneously to twice the rated value, the torque will increase to about 20 MNm, which is not possible for a generator system rated at 14 MNm. In this case, there is also no margin, so this control concept can only be used if we know the wind speed something like 30 to 60 seconds before it occurs.

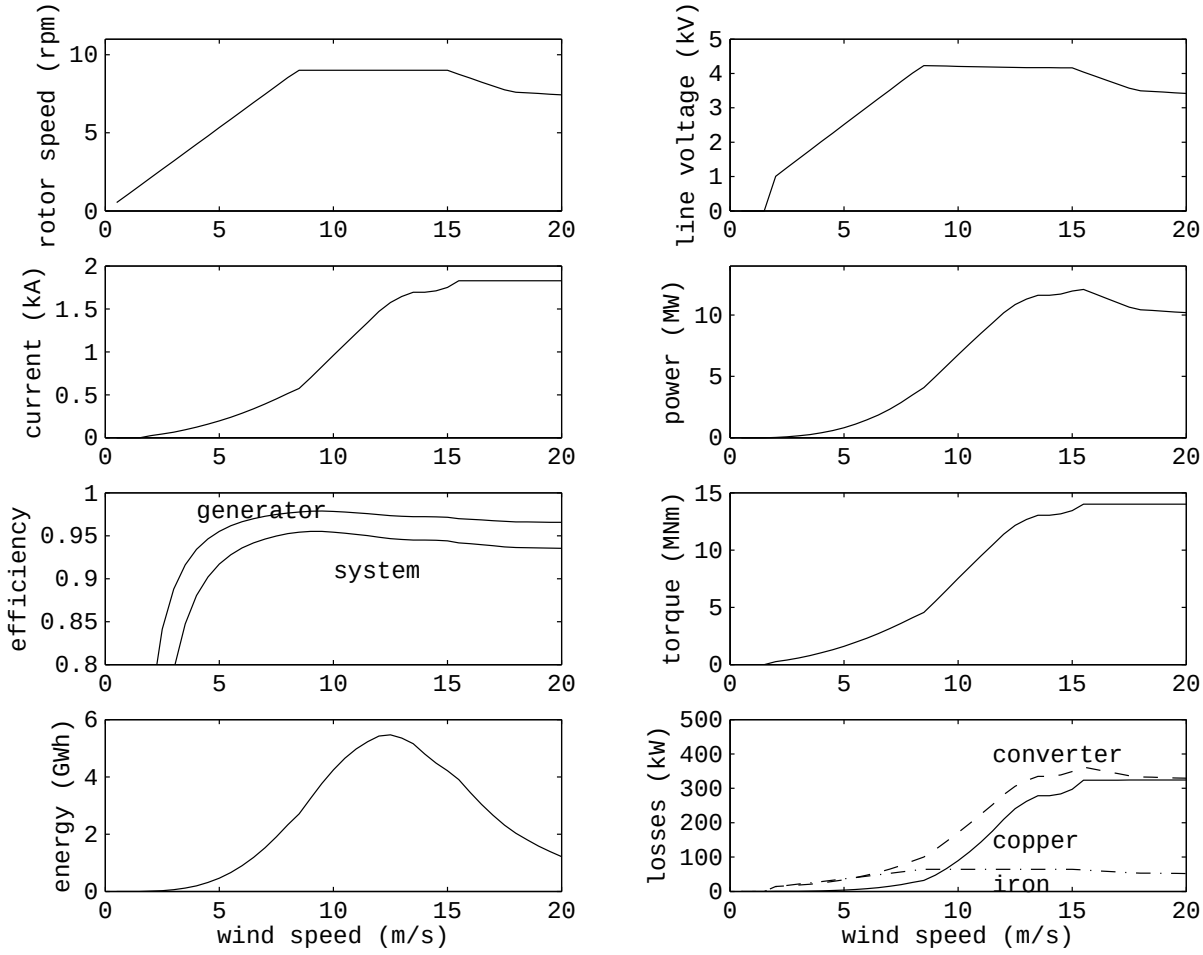

Figure 4.7: *Characteristics of an ICORASS turbine in which the torque is limited to 14 MNm. The rated power is 14 MW.*

4.7 Additional power and torque necessary for decreasing the rotor speed.

If the wind speed increases sufficiently slowly, and the generator system can be overloaded for short time intervals, this may be used to control the speed of the rotor. The additional torque necessary to decrease the rotor speed can be calculated as:

$$T_{add} = J \frac{d\omega_m}{dt}.$$

To express this additional torque as a function of the wind speed, we can rewrite this equation to:

$$T_{add} = J \frac{d\omega_m}{dv_w} \frac{dv_w}{dt}.$$

Figure 4.8 depicts the rotor speed as a function of the wind speed for the control concept where the power is limited to 10 MW. From this graph, we can derive an expression for dn/dv_w, which can be worked out to $d\omega_m / dv_w$. The largest decrease in the mechanical speed is necessary when the wind speed increases above 12.5 m/s, where

$$\frac{d\omega_m}{dv_w} \approx 0.05 \text{ rad/m}$$

The inertia J is estimated as $1.4 \cdot 10^8$ kgm^2.

If the maximum increase of the wind speed averaged over the rotor surface area $dv_w / dt = 1$ m/s^2, the additional torque is 7 MNm. This would mean that the generator system has to be overrated by 50%, which is too much.

However, if the maximum acceleration of the wind speed averaged over the rotor surface area is limited to $dv_w / dt = 0.2$ m/s^2, the additional torque is just 1.4 MNm, which means that an overrating of the generator system by 10% is sufficient. This 10% is available when the control concept where the power is limited to 10 MW is used. It can be concluded that it has to be investigated further what are realistic increases in the wind speed.

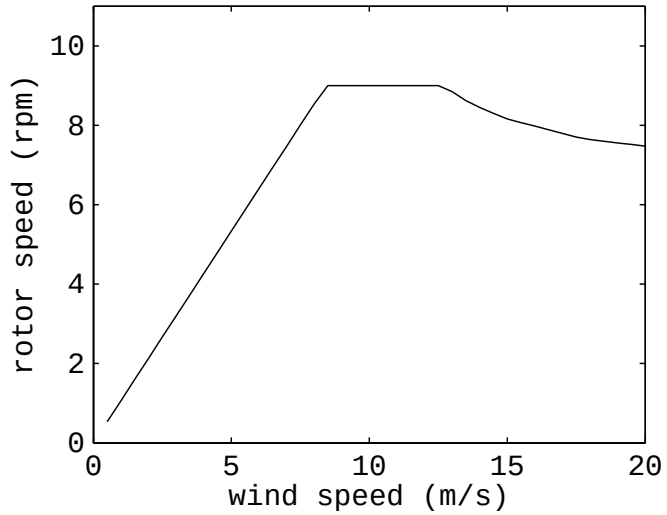

Figure 4.8: *Rotor speed as a function of wind speed for the control concept where the power is limited to 10 MW.*

4.8 Conclusions

The results of this chapter are summarized in Table 4.2 and Table 4.3. These numbers will be used in the economical evaluation of all concepts.

Table 4.2: *Generator dimensions and weights.*

	Pitch	**ICORASS overrated**	**ICORASS with speed, power or torque limit**
Generator dimensions			
Stator radius r_s (m)	5	5	5
Stack length l_s (m)	1.6	3.2	2.24
Number of pole pairs p	160	160	160
Number of slots per pole per phase q	1	1	1
Air gap g (mm)	10	10	10

Stator slot width b_{ss} (mm)	14.7	14.7	14.7
Stator tooth width b_{st} (mm)	18	18	18
Stator slot height h_{ss} (mm)	80	80	80
Stator yoke height h_{sy} (mm)	40	40	40
Rotor yoke height h_{ry} (mm)	40	40	40
Magnet height l_m (mm)	20	20	20
Rotor pole width b_p (mm)	80	80	80
Generator active material weight (ton)			
Iron (ton)	48	96	67
Copper (ton)	11	21	15
PM (ton)	6	12	9
Total (ton)	65	129	91

Table 4.3: *Generator system cost and energy yield for different control strategies.*

Generator system	**Pitch**	**ICORASS overrated**	**ICORASS speed limit**	**ICORASS power limit**	**ICORASS torque limit**
Ratings					
Generator torque (MNm)	10	20	14	14	14
Generator power (MW)	10	18	10	12.6	12.6
Converter (MW)	10	18	10	12.6	12.6
Cable power (MW)	10	18	10	10	12.6
Cost (k€)					
Generator active material	462	906	640	640	640
Converter	400	720	400	452	504
Annual energy					
Copper losses (GWh)	1.01	0.64	0.81	0.96	1.07
Iron losses (GWh)	0.36	0.64	0.39	0.45	0.45
Converter losses (GWh)	1.42	1.33	1.21	1.62	1.56
Total losses (GWh)	2.79	2.61	2.31	3.03	3.08
Energy yield (GWh)	48.4	48.3	38.8	48.2	51.1

4.8.1 Preliminary generator system choice

Since wind speed change cannot be known in advance, the option with torque limited control was assessed as not feasible. The pros and cons of the other three options are listed below:

- **Overrated generator system:**
  Increasing the power level of the generator system to such an extent that it can always reduce the speed to reduce the power to 10 MW can be done by doubling the power level of the generator and the converter. However, such a generator system is rather expensive and therefore this form of ICORASS control is not very attractive.

- **Speed limited control:**
  Decreasing the rotational speed to 7.2 rpm in order to guarantee that the power is always limited to 10 MW results in a larger and more expensive generator system and in a large decrease in energy yield of approximately 20%. Therefore, this form of ICORASS control is not very attractive.

- **Power limited control:**
  Probably the most attractive form of ICORASS control is the form of control where the power is limited to 10 MW and the speed to 9 rpm. This can be done with a generator system consisting of:
  - a generator rated for 14 MNm (40% more than with pitch control),

- a converter rated for 12.6 MW (26% more than for pitch control).
- park infrastructure and energy yield can probably remain the same w.r.t. pitch control.

Therefore, power limited control is the preferred option to control the generated power and rotational speed. When changing from pitch control to ICORASS control, a considerable increase in generator system cost is necessary because the generator system rating has to be increased substantially.

To be able to design this generator system in more detail, more research is necessary:
- it has to be investigated how well the wind speed can be predicted;
- it has to be investigated further what are realistic increases in the wind speed.

Using this information, a controller has to be designed, the variations in the output power and the power peaks have to be determined, the generator and converter have to be designed in more detail and it has to be evaluated if the park infrastructure can remain unchanged.

5. Control and safety design

5.1 Control system

The power control of the ICORASS concept is discussed in section 4. The power will be controlled on the basis of active stall by reducing the rotor speed above rated power. This option is feasible at acceptable extra cost and without any loss in energy capture.

5.2 Protection system

The protection system is defined as the system, which ensures that a wind turbine remains within the design limits. The majority of modern turbines in the last decades is equipped with an aerodynamic brake system. Either by means of full span pitching of the blades or by means of tip brakes. The ICORASS design philosophy aiming at maximum robustness has lead to a rotor in one piece. Thus, an aerodynamic braking system does not fit well with the concept.

However the protection system of the ICORASS concept has to meet the requirements in the international standards. The commonly accepted standard is the IEC 61400-1 "Wind turbine, part 1: Design requirements" [5.1]. It is likely that the edition 3 will be published in the near future [5.2]. With respect to the clauses on the protection system no drastic changes have been for seen in the revision between edition 2 and 3. The standard states that it is recommended to have at least one braking system operating on an aerodynamic principle. In the Germanisher Lloyd Rules and Regulations [5.3] this is even required. The requirements of importance for the ICORASS concept can be summarized pragmatically as follows:

- two independent braking systems are needed
- at least one braking system should be able to bring the rotor to a complete stop
- at least one braking system should act directly on the rotor or on the rotor shaft
- brakes should be designed to function even if their external power supply fails

The following options for braking systems for the ICORASS exist:

1) Mechanical brake
2) Electrical brake
3) Yawing out of the wind

ad 1. The mechanical brake consists of a braking disc with hydraulic calipers. The functioning without external power supply can be guaranteed with a hydraulic accumulator. The diameter of this brake disc will be approximately the same size as the direct drive diameter. This enables integration of the brake disc with the generator. In combination with a permanent magnet direct drive generator it needs to be avoided that the particles from the brake disc or the sheathing can enter the generator.

ad 2. Electrical brake: the electric torque of the direct drive generator can be used as braking torque. But, the specifications of the generator and the inverter need to be adapted significantly. The maximum torque needs to be increased and the system should be functional without the grid.

ad 3. Yawing out of the wind will give too high loads for this size of machine and is not recognized as a feasible option.

The most feasible option is the combination of electrical braking with a mechanical brake. Jeumont has used this concept in their 750 kW machine. That machine is equipped with a (permanent magnet) direct drive generator. Some of these machines have electric braking combined with mechanical braking. Others have a combination of mechanical braking and tip brakes. In case of a combination of two braking systems on the rotor shaft the loads will become to high

for a conventional blade design when the two braking systems act simultaneously. Therefore the torque of at least one of the two systems needs to be limited in case the other system functions normally.

5.3 Conclusion

The protection system of the ICORASS concept cannot be based on aerodynamic braking. The requirement in the standard to have two independent braking systems can be met with a mechanical brake and an electrical brake. The electrical braking torque should be controlled in order not to have too high braking torque in case both the mechanical and the electrical brake are activated at the same time. The electrical brake should remain functional in case of grid failure. This protection concept has been applied on commercial turbines and as such the development risk is very limited.

5.4 References

[5.1] International standard IEC 61400-1. *Wind Turbine Generator Systems, Part1 – Safety requirements*, 2nd edition. 1999-02.

[5.2] International standard IEC 61400-1. *Wind Turbine Generator Systems, Part1 – Safety requirements*, 3rd edition. In preparation.

[5.3] Germanischer Lloyd. *Rules and Regulations, IV Non Marine Technology, Part 2 – Regulations for the Certification of Offshore Wind Energy Conversion Systems.* Edition 1995.

[5.4] Germanischer Lloyd. *Rules and Regulations, IV Non Marine Technology, Part 1 – Regulations for the Certification of Wind Energy Conversion Systems.* Edition 1999.

6. Wind farm design

6.1 Introduction

The difference between a wind farm consisting of state of the art wind turbines of the present technology i.e. variable speed, full span pitch controlled wind turbines and a wind farm consisting of wind turbines based on the ICORASS concept is mainly the different power control and subsequently different axial force coefficient of the wind turbine. In this chapter the influence of the ICORASS concept is discussed with respect to the lay out of the wind farm and the electrical infrastructure within the wind farm and the connection to the grid.

6.2 Lay-out of wind farms with ICORASS wind turbines

The design target for the lay out of an off shore wind farm is to make the wind farm compact with low array losses and wake induced loading on the machines. Compact because the electrical cabling within the wind farm is expensive and the closer the spacing of the wind turbines in a wind farm the more wind turbines one can install in a given space. On the other hand wind turbines that operate in the wake of another wind turbine will receive lower wind speeds, a higher turbulence and a different wind profile. The energy efficiency of a wind farm can be measured in the percentage of array losses, i.e. the fraction of the average energy production of the wind turbines in the wind farm divided by the energy production of a stand alone wind turbine at the same site.

The ICORASS wind turbine power control has a relatively large axial force coefficient compared to a full span pitch controlled wind turbine near and above rated conditions. This will result in a higher average wake loss for a wind farm with ICORASS wind turbines compared to an identical wind farm with the conventional pitch regulated wind turbines. This effect is for the energy yield however only interesting for wind speeds near rated wind speed. For wind speeds far above the rated conditions, the wind speed will still be sufficiently high for the wind turbines in the wake to operate at rated power. Below rated conditions both concepts operate at λ_{opt} and will have a similar axial force coefficients and subsequently similar wake properties. The overall effect, meaning that it is integrated over the wind speed and wind direction distributions will be small in the order of a few percent. With conventional wind turbines the overall array efficiency is in the order of 95% or a little better. It is assumed that the array efficiency of a wind farm consisting of ICORASS wind turbines will be higher than 90%. The ICORASS concept will however have a more severe effect on the loading of the rotor for the turbines in wake due to the expected higher turbulence. It is quite easily possible to take this effect into account during the design process, e.g. by assuming a little higher ambient turbulence.

6.3 Electrical concepts for offshore wind farms with ICORASS wind turbines

The electrical system concerns the electrical power components between the generator shaft and the grid connection and the way these components are interconnected and operated. Its function is to convert mechanical power into electric power, to collect electric power from individual turbines, to transmit it to the shore and to convert it to the appropriate voltage and frequency. The system consists amongst other of generators, cables, transformers and power electronic converters. Systems are mainly characterized by the type of current (AC or DC) and the frequency (fixed or variable). First an inventory is made of architectures to collect the electric power from individual wind turbines in an offshore wind farm and transmit this power to an on-shore high-voltage grid node [6.1]. The inventory includes only individual variable speed

options using AC as well as mixed AC-DC-AC modes. It is clear that for the ICORASS turbine only the variable speed concept with so called individual variable speed is viable.

Two basic lay-outs are considered: one with string clustering and one with star clustering (Figure 6.1). With star clustering a turbine transformer can possibly be left out, as indicated in system IV2, if the generator voltage is sufficiently high (about 5 kV). On the other hand, the number of platforms with star clustering is higher then with string clustering, as each cluster needs its own nodal platform for switch gear and a transformer. As the figure shows, the type of clustering does not directly affect the architecture of the rest of the park; however the type of clustering is important for the voltage rating of converters in the cluster. The costs of converters is more or less linear with the apparent power of the converter, however it also rises progressively with the voltage rating because of the spacious equipment needed for insulation. This means that low power high voltage converters are relatively expensive.

6.3.1 Inventory of electrical concepts

Two options for individual variable speed are shown in Figure 6.1 and Figure 6.2. The systems of Figure 6.1 consist of traditional variable speed turbines with back-to-back low voltage (about 1 kV) converters. In system IV2 voltage converters will be required in the range of 2-10 kV when the converters are directly connected to the cable.

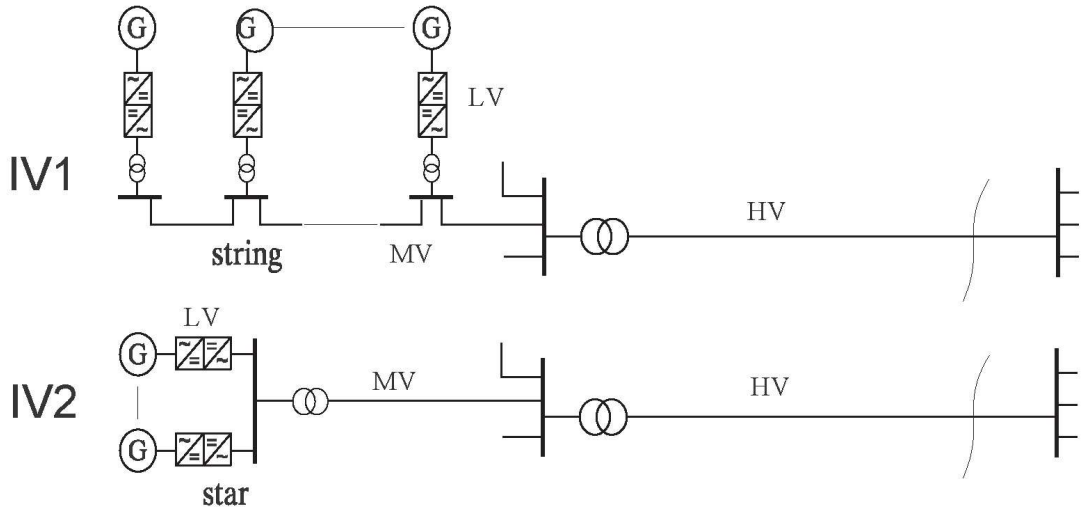

Figure 6.1: *Individual variable speed systems with back-to-back converters [6.1].*

In Figure 6.2 the back to back converter is split in separate AC/DC converters and DC/AC converters. The voltage rating of the DC-system is in the medium voltage range (10-50 kV). These medium voltage DC systems, also referred to as HVDC-Light or HVDC-Plus, are developed by several manufacturers and are based on voltage source converters. DC-systems with multiple DC-inputs (multi-terminal HVDC-Light/Plus) are not available yet and will require additional development. In configuration IV4 the DC/AC converter is placed near the cluster node whilst in configuration IV5 the DC/AC converter is placed down stream the collection point of all clusters, which results in the elimination of a cluster transformer.
On the other hand the power rating of the DC/AC converter and the DC-cable will be much higher and so is the required voltage level. Because of the high voltage level of the turbine sided converters and because of the limited power rating these converters will have relatively high costs per kVA.

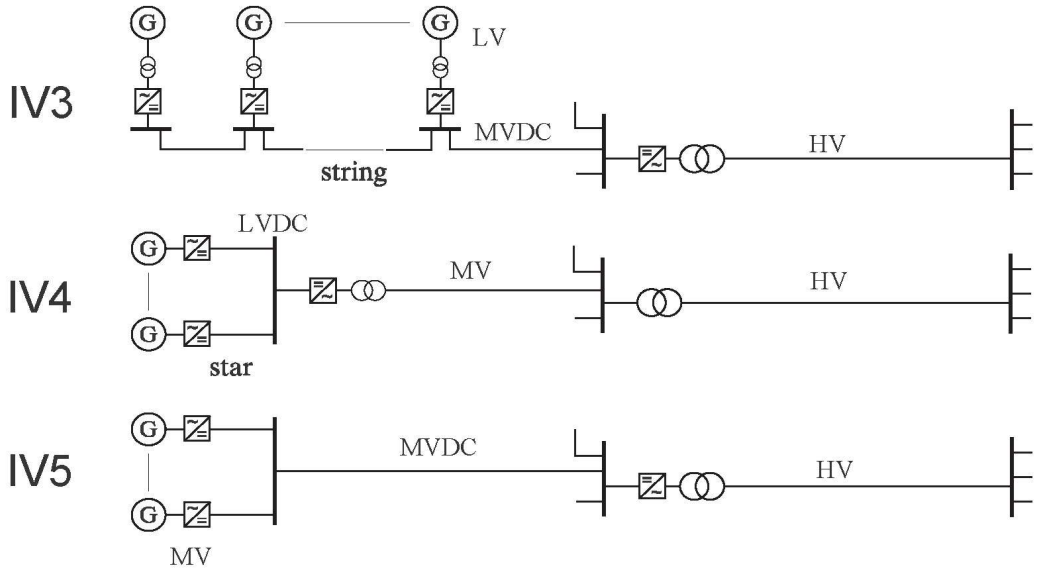

Figure 6.2: *Individual variable speed systems with multi-terminal DC [6.1].*

6.3.2 Economical evaluation: case study

The cost calculation excludes the turbines (also the turbine generators) and turbine installation costs. All major electrical equipment between turbine generator and shore is included. Small auxiliary electrical equipment, e.g. switches and safety equipment, is not taken into account.

The intermediate voltage level for the 100 MW as well as the 200 MW farm is 33 kV. The rectifiers and inverters in systems with an MVDC connection are of the PWM type (HVDC-Light/Plus). The maximum currents of the components in all configurations were checked for the rated power level. The capacitive currents in the cables are not compensated by additional inductors.

Two configurations of wind farms are calculated: IV1 and IV3. Each configuration calculates and compares three situations: 100MW, 200MW and some components have 1.5PU short time overload capability, 200MW and no overload capability.

Further, in configuration IV1, two types of turbine converters are calculated and compared: one type uses back to back VSCs, another type uses diode rectifier and VSC inverter. The calculation is based on the following assumptions:

1) The capacity of each component: $S = P/0.8$.
2) All the passive components such as cables and transformers have an overload capability of 1.5PU for a short time (several seconds).
3) VSC does not have any overload capability.
4) Thyristor bridge has 1.5PU overload capability.
5) The price of cable includes two parts: one is proportional with current rating; the other is proportional with voltage rating

Results are shown in Appendix B.

6.4 References

[6.1] Pierik, J.T.G., Pavlovsky, M., Bozelie, J., Bauer, P. & Haan, S.W.H. de. *DOWEC Electrical system baseline design.* Website: http://www.ecn.nl/en/wind/additional/special-projects/dowec/. DOWEC-045. ECN, Petten/TU-D, Delft. February 2002.

7. Support structure, installation and O&M design

In this chapter a conceptual design for the support structure is conducted. This design covers the drive train, nacelle, yaw system and tower. Besides some remarks on the installation of the ICORASS turbine and the maintenance aspects are made.

7.1 Nacelle and drive train

One of the principal starting-points for the ICORASS conceptual design is the selection of the direct drive principle. The drive train of the direct drive wind turbine consists of a (wind turbine) rotor and a generator. The turbine rotor and the generator rotor constitute the rotating part of the machine. In MW-scale wind turbines the turbine rotor and generator rotor are rigidly connected and one bearing system is used to support this assembled structure. The generator stator is connected to a compact bedplate, which has a high level of structural integration with both the generator and the yaw system.

7.1.1 Main concept

7.1.1.1 Reference concepts

As a reference for the selection of the direct drive principle, several concepts for MW-scale wind turbines are shown schematically in Figure 7.1.

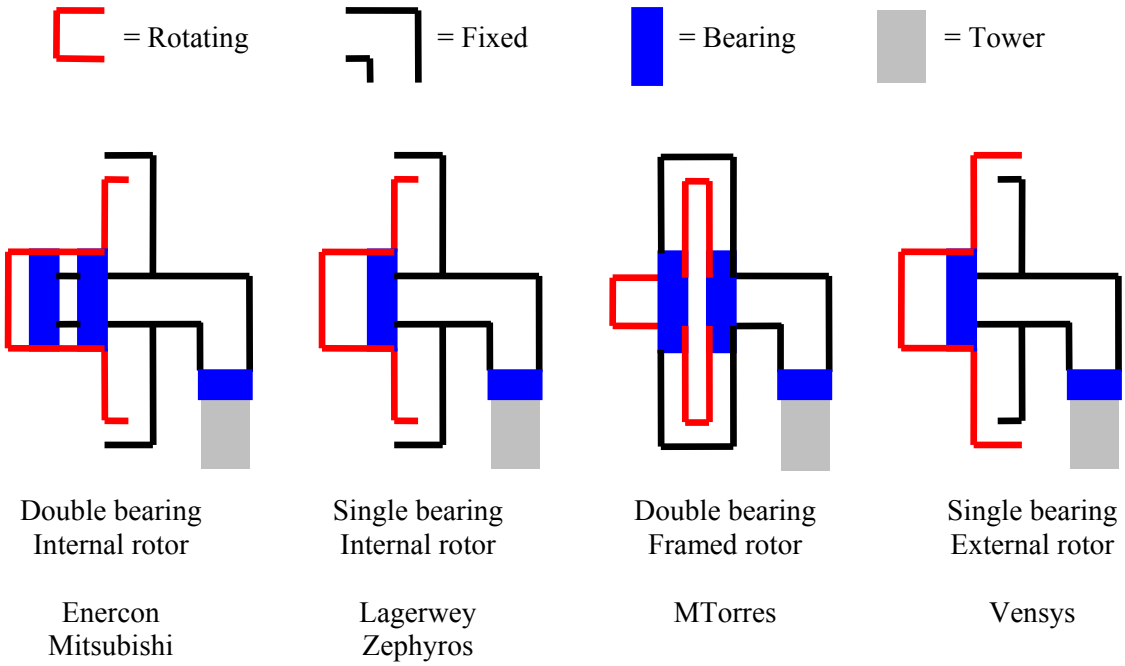

Figure 7.1: *Schematic representation of direct drive concepts with characteristics and manufacturers [7.1] – [7.7].*

Most manufactured direct drives are of the left-most concept, followed by the second concept. The third and fourth concepts only exist as prototypes. Almost all direct drive turbines use the conventional topology for the generator in which the rotor is placed on the inside of the stator. Only Vensys places the rotor on the outside. Both double bearing configurations and single bearings are used. Only MTorres places the double bearings on either side of the generator rotor. Up till now, the generator has not been integrated in the hub, but the hub is bolted to a

flange on the generator rotor. All current MW-scale direct drive wind turbines have an upwind rotor and a yaw system below the horizontal axis of the drive train.

7.1.1.2 Concept selections for ICORASS

The first step in the design of the ICORASS nacelle is the selection of a concept for each of its functions. Given the time restrictions of this investigation, the concept selections will be based on straightforward reasoning and analysis of existing technologies, without generation of an extensive design option tree and in depth assessment of advantages and disadvantages.

The rationale for an external generator rotor provided by Vensys is a reduced outer diameter of the generator [7.6]. The Vensys generator has permanent magnets in the external rotor and the windings of the three-phase coils are in the internal stator. Because the windings are not at the perimeter of the generator, this topology needs larger forced cooling to maintain the same temperature at otherwise comparable conditions for external windings. Since cooling is considered to be a more dominant design factor for the generator than a diameter reduction, the conventional internal rotor is selected.

The selection of the concept for the main bearing system is based on the simplified interpretation of robustness as a reduction of the number of components. As a consequence of this interpretation a single bearing is chosen. According to [7.8] single bearing concepts are seen more frequently for wind turbines of over 3 MW and have proven themselves also in other demanding applications. The reference concepts show a ‘shaft’ configuration, in which the inner ring of the bearing rotates, and several ‘hub’ configurations, in which the outer ring rotates. There is no preference for either configuration at this stage of the concept selection.

All reference concepts in Figure 7.1 have the generator and turbine rotor on the same (upwind) side of the tower. Apart from a compact structure, this also provides an advantageous loading situation of yaw system and tower top: The bending moment generated by the gravity force on the generator counteracts the bending moment caused by the aerodynamic thrust of the rotor. The ICORASS rotor is positioned on the downwind side of the tower. To have counteracting bending moments from the rotor thrust and gravity on the generator two configurations of generator and yaw system can be chosen, as illustrated in Figure 7.2. When the generator is positioned on the same side as the rotor, the yaw system must be above the rotating shaft of the drive train (option A). A lower yaw system can be combined with an upwind generator and a downwind rotor (option B). Combination of a downwind generator and a low yaw system is not considered as an alternative at this stage, since this will give larger maximum bending moments. A choice between the two other options will be made below.

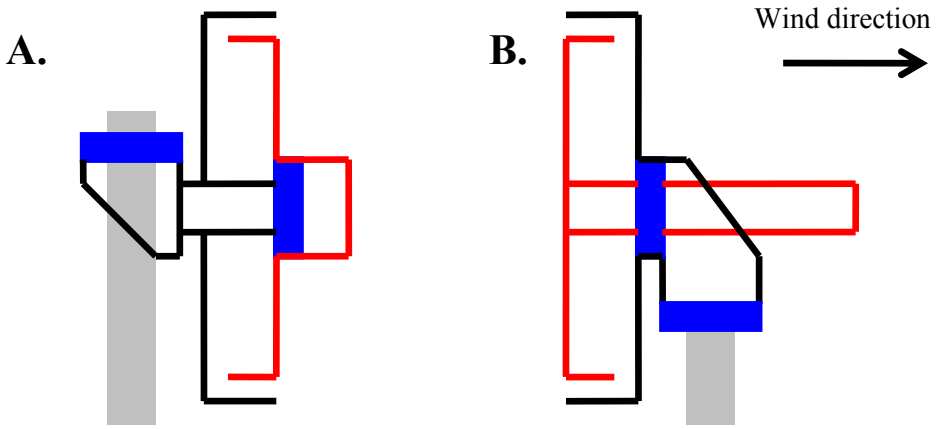

Single bearing
High yaw bearing
Downwind generator

Single bearing
Low yaw bearing
Upwind generator

Figure 7.2: *Schematic representation of two options for the nacelle concept of the ICORASS turbine.*

Some differences between option A and B are given in Table 7.1. Table 7.1 is not intended to be comprehensive or to provide a basis for a weighted comparison of the qualifications of the two options. Rather, a selection will be made based on some outstanding qualities and the consequences of that selection will be considered in the analysis of the preliminary design in Section 7.1.2.

Table 7.1: *Qualifications of nacelle concepts presented in Figure 7.2.*

	Option A	**Option B**
Structure	• Extended and adapted tower top needed • Challenge to keep bedplate compact	• Extended drive shaft needed • Challenge to limit shaft bending
Assembly	• Tower top, yaw system, bedplate, generator stator, generator rotor, hub and turbine rotor can be made modular	• Yaw system, bedplate, generator stator, generator rotor, drive shaft, hub and turbine rotor can be made modular
Installation	• Can be modular (yaw system & bedplate – generator – rotor) • Fixed installation sequence	• Can be modular (yaw system & bedplate – generator – Rotor) • Independent installation of generator and rotor
Maintenance	• Independent exchange of rotor possible, independent exchange of generator not possible	• Independent exchange of rotor and generator possible

Low maintenance cost is the main driver in the design philosophy of the ICORASS turbine. The first and most direct consequence of this approach is the targeted low failure rate. However, service and repair demand is unavoidable with current technology. Therefore, a second consequence of this approach could be easy maintainability, with low downtimes. This consequence is arguable, since the positive effect of easy maintainability gets reduced by a reduction in failure rate. Nevertheless, to adhere to the principal of maintenance cost reduction, the qualifications in Table 7.1 with respect to maintenance will be emphasised. The possibility of independent exchange of the generator in option B may provide a benefit for maintenance activities, since this may avoid lifts of the rotor, which is a sensitive process that can only be performed at low wind speeds. Lifts of the generator can be quicker and with less strict workability limits when the rotor can remain in place. Since the power output of the ICORASS turbine is controlled by variable speed operation of the rotor without adaptation of the blade pitch, the turbine rotor and hub are purely structural components. The service and repair needs of structural components are small compared with those of mechanisms, electrical and electronic equipment and hydraulics that may be present in the generator section of the nacelle [7.9],[7.10]. Thus, the need to exchange the rotor because of service or repair of itself will be much smaller than the need to exchange the generator section. Based on this consideration, option B is selected.

To minimise the number of components, the ICORASS turbine will use free yawing to align with the wind. A wind turbine rotor at a yaw angle with the wind experiences a restoring force due to the asymmetric flow through the rotor plane [7.11], [7.12]. Besides, a downwind rotor will also be restored to small yaw angles by the aerodynamic thrust. An active yawing system is needed to untwist the cables, but this system only operates when the turbine is not running.

In a free yawing system the functions of the yaw brake differ from the functions it performs in an active yawing system. In an active yaw system the brakes work at 100% pressure when the turbine is aligned with the wind and at a lower pressure when it is yawing [7.13]. During

aligned operation the brakes prevent the yawing motion of the nacelle and thus avoid cyclic loading on the yaw motors and gears. When yawing, the brakes work as a damper and as a base load for the yaw motors. Table 7.2 gives three alternatives for the yaw brakes of the free yawing ICORASS turbine, along with their main function and qualities. Based on Table 7.2 the free yawing system without brakes promises the least required maintenance, but it must be acknowledged that the dynamic response may present a development risk.

Table 7.2: *Options, functions and system qualities for yaw brakes.*

Option	Function	Advantage	Disadvantage
No yaw brakes	Allow free yawing motion	• No system components required	• Large response • Motion affects aerodynamic performance
Passive partial brakes	Dampen yawing motion	• Reliable brakes	• Wear of brakes under continuous motion • Heat production may require force cooling
Active full brakes	Prevent yawing motion when aligned – allow free yawing when misaligned	• Proven system • Most predictable dynamics	• Hydraulic compressor and controls required

7.1.2 Design and analysis of principal dimensions

7.1.2.1 Brakes

Since the blades cannot be pitched, an external braking force is needed when the blades have to be stopped. The following two options are available:

- mechanical brake, operating on the main shaft and
- electrical brake by changing the electro-mechanical torque of the generator.

Both options are needed to meet the requirement of a redundant safety system. Since there is no gearbox, an independent mechanical brake on the high speed shaft is not possible. Pitching blade tips are not considered at this stage. In this section an analysis is made of the required braking force and it is assessed whether the use of a mechanical brake is realistic. The required braking force is calculated in parallel with the aerodynamic and structural design of the rotor. Therefore, the rotor geometry, aerodynamic performance and rotor inertia were not completely available at the time. When necessary, simple scaling rules were used to assess values for the essential parameters.

The required braking force is built up by two components. First, in case of a failure that causes shut down of the generator, the braking force has to compensate for the loss of generator torque and thus dissipate the aerodynamic power of the rotor. Second, it has to decelerate the rotor which has a moment of inertia. In equation:

$$M_{Brake} = M_{Brake,Aero} + M_{Brake,Deceleration} = \frac{P_{Aero}}{\omega} + I_{rotor} \cdot \frac{d\omega}{dt}. \tag{7.1}$$

To estimate the maximum value for the first term on the right-hand side of equation (7.1), the power curves of the rotor for various rotational speeds, as shown in Figure 7.3, are used. While the turbine is operating normally, the aerodynamic power is limited to 10.8 MW, in order to limit the electrical output power to 10 MW. In full load, where the power is 10.8 MW, the set-point for rotational speed can be found for each wind speed by taking the power curve that intersects with the reference power at the selected wind speed. At the rated wind speed of around 12 m/s this yields a rotational speed of approximately 11 revolutions per minute (RPM) and at the cut-out wind speed of 25 m/s this yields about 7 RPM. Using the first term on the right-hand

side of equation (7.1), the maximum braking force to dissipate the aerodynamic power is therefore obtained at cut-out wind speed.

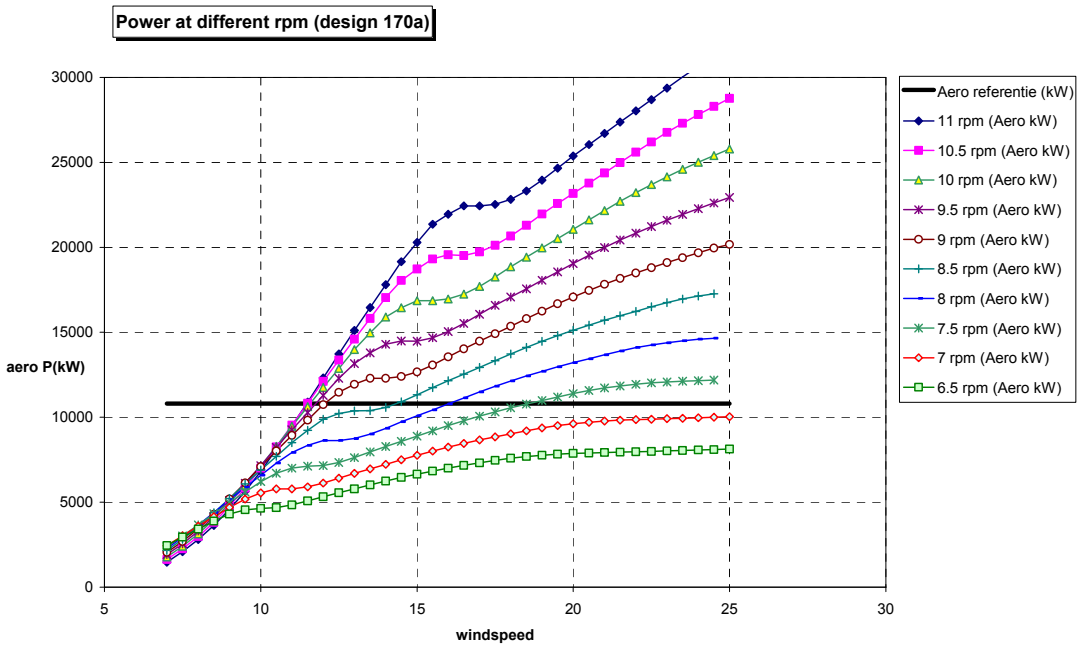

Figure 7.3: *Power curve of the ICORASS rotor for various rotational speeds.*

Both safety controller and braking system will need a reaction time to respond to the shut down of the generator. During this reaction time the rotor will speed up and as can be seen in Figure 7.3 this will result in an increase in aerodynamic power. Assuming an increase in aerodynamic power of 35% due to overspeed up to 8 RPM, the required braking force to dissipate aerodynamic power at cut-out wind speed becomes:

(7.2) $$M_{Brake,Aero} = \frac{1.35 \cdot \left(10.8 \cdot 10^6\right)}{8 \cdot \left(\frac{2\pi}{60}\right)} \approx 17\, MNm\,.$$

To estimate the deceleration of the rotor, its moment of inertia must be known. The moment of inertia is estimated from scaling rules. As a reference for scaling the DOWEC rotor with a diameter of 129 m is used, since this is the largest rotor for which the mass distribution is known to the authors [7.14]. The basis for scaling is the moment of inertia, I, of a solid disc with radius R, which equals:

(7.3) $$I = \tfrac{1}{2} m \cdot R^2\,.$$

Assuming that the dimensionless mass m/m_{Total} as a function of r/R is indifferent to scale, the same linear dependency of mass and quadratic dependency of radius can be applied to the inertia of a rotor according to:

(7.4) $$I_{Icorass} = \left(\frac{m_{Icorass}}{m_{DOWEC}}\right) \cdot \left(\frac{R_{Icorass}}{R_{DOWEC}}\right)^2 \cdot I_{DOWEC}\,.$$

To assess the change of mass of the ICORASS rotor with respect to the DOWEC rotor three aspects are taken into account:

1) The ICORASS rotor has two blades instead of three.
2) The ICORASS turbine has stall control instead of pitch control.
3) The ICORASS rotor is 160 m instead of 129 m.

Ad 1. Although the number of blades reduces by a factor 2/3, the chord increases with a factor 1.5 to get the same solidity. Due to the higher structural height the mass may be slightly reduced to get the same strength and stiffness. An overall reduction of mass to 90% has been assumed for this effect.

Ad 2. In general the loads and uncertainty therein for a stall regulated turbine are slightly higher than those of a pitch controlled turbine. An overall increase of mass to 120% has been assumed for this effect.

Ad 3. In [7.15] the scaling effects of rotor diameter have been investigated. In this report several curve fits of rotor mass as a function of rotor diameter are given, in case a power law is assumed. A more or less cubic dependency was found for various sources of data. Assuming a cubic dependency and a mass for the DOWEC rotor of 17648 kg per blade, the following power law is found:

$$m_{Blade} = 8.221 \cdot 10^{-3} \cdot D^3 . \tag{7.5}$$

Substituting the radius of the ICORASS rotor and the DOWEC rotor the increase of mass according to this scaling rule becomes a factor 1.9.

Combining the three mentioned effects leads to an estimated increase of rotor mass of approximately a factor 2. Substituting this increase in rotor mass and the increase in diameter in equation (7.4) yields an increase in rotor inertia of approximately a factor 3. With a rotor inertia of 36.5 Mkg·m^2 calculated from the mass distribution of the DOWEC rotor, the estimated moment of inertia of the ICORASS rotor becomes 0.1 Gkg·m^2.

During the braking operation the rotational speed of the rotor will decrease, which affects the aerodynamic power. Using the data in Figure 7.3, the following power law was fitted to the aerodynamic power at cut-out wind speed:

$$\frac{P_{Aero}}{\omega} \approx 23 \cdot 10^6 \cdot \omega^{1.66} . \tag{7.6}$$

Substituting equation (7.6) into equation (7.1) yields a relation between the braking torque and the rotational speed that can be integrated to obtain the time till stand still. The numerically resulting relation between braking time and braking torque is shown in Figure 7.4. As expected, the time till stand still increases rapidly as the minimum required braking torque of about 17 MNm is reached. However, small braking times are already achieved with a small extra braking torque. The kinetic energy stored in the rotor at a rotational speed of 8 RPM is approximately 38 MWs, which is comparable with the aerodynamic energy that has to be dissipated during a braking action of about 6 seconds.

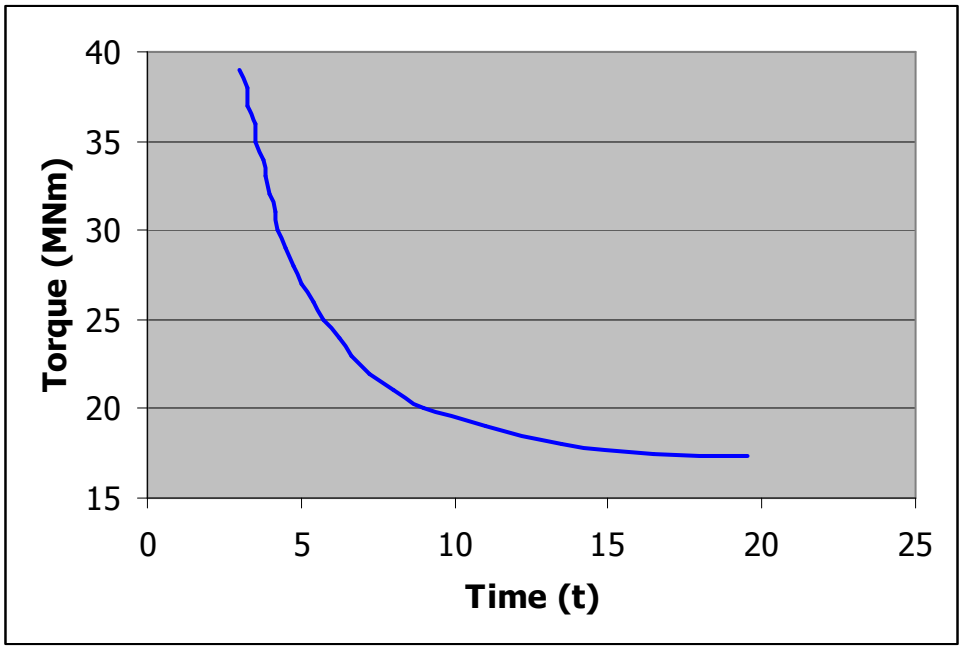

Figure 7.4: *Relation between braking torque and time till stand still after overspeed at cut-out wind speed.*

Figure 7.4 shows that the time until stand still after overspeeding at cut-out wind speed can be kept below 5.5 seconds with a braking torque of 26 MNm. When a brake disc with a diameter of 8 m is used, which is about the diameter of the generator, a total force of all brakes on the disc of 6.5 MN is needed.

As an example of a possible solution with available brakes, the number of brakes that is required is assessed from the specification of the products of 'Svendborg Brakes'. This company provides brakes for the drive train and the yaw system of wind turbines and has experience with brakes for large wind turbines [7.13]. For failsafe operation, the current approach is to use a brake with the clamping force provided by a spring. This type of brake will also operate in the absence of power. The largest available failsafe brake of 'Svendborg Brakes' is the BSFB 600, which has a maximum braking force of 500 kN [7.16]. Of these 13 would be needed. With a diameter of 8 m and a circumference of 25 m the brake disc provides nearly 2 m per brake, which would be large enough. The largest active brake of 'Svendborg Brakes', which uses hydraulic pressure to get the clamping force, is the BSAB 120 with a maximum braking force of 430 kN. Of these 16 are needed at least, which would provide a little more than 1.5 m per brake on the disc. The actual braking performance depends on various conditions, such as speed and temperature of the brake disc, and may be lower than the values used here. Friction coefficients can drop from 0.4 to as low as 0.2 for certain conditions, so without further information doubling the required number of brakes should be considered at this stage. Although this appears to be geometrically possible, a definitive conclusion about the feasibility of a mechanical brake would require a more detailed analysis of the braking action and of the structural consequences.

7.1.2.2 Main bearing

A single main bearing was selected for the ICORASS concept. This single bearing can be implemented as a four point contact ball bearing [7.17] or as a double row conical roller bearing [7.8].

Table 7.3 shows the distribution of masses in the nacelle and the aerodynamic thrust that are assumed to calculate the contributions to the loads on the main bearing. Some parameters in Table 7.3 are not used here, but will be needed to calculate the loads on the yaw system in Section 7.1.2.3.

Table 7.3: *Estimated contributions to loads on main bearing and yaw system.*

Component	**Mass (kg)**	**COG from tower centreline (m)**	**Rationale**	**Contributes to load**	
				Main bearing	Yaw bearing
Total	1,300,000	-1.37	Extrapolation from other direct drives.		
Rotor	100,000	5	Scaling rules of Section 7.1.2.1.	X	X
Hub	100,000	5	Taken equal to rotor mass.	X	X
Generator rotor	400,000	-4	Half the remaining mass.	X	X
Generator stator	400,000	-3	Half the remaining mass.	-	X
Shaft	40,000	1	Dimensions of steel structure estimated.	X	X
Main bearing	10,000	-2.5	-	-	X
Bedplate	150,000	0	Dimensions of steel structure estimated.	-	X
Yaw system	100,000	0	-	-	X
	Force (N)				
Aerodynamic thrust	1,300,000			X	X

The following simplified approach to analyse the effect of a moment and an axial force on a four point contact bearing is used from [7.17]:

$$P_r = \frac{1.2M}{\overline{PD} \cdot Sin\theta} + 0.75F_r + 0.9F_t \,, \tag{7.7}$$

where:

P_r = equivalent radial load, F_r = radial load, F_t = thrust load, M = moment load, $\overline{PD}$ = bearing pitch diameter and θ = bearing contact angle (30º for standard bearing).

Equation (7.7) shows that the equivalent radial load is a function of the bearing diameter. Using the data in Table 7.3 this function is calculated and the result is plotted in Figure 7.5. For small diameters the equivalent radial load increases rapidly, due to the effect of the moment that is exerted by the masses. This effect levels of at diameters of about 3 meter. Therefore, at diameters of the main bearing that match with the main dimensions of the nacelle and generator the moment on the single bearing is not necessarily the design driving load. As a reference, the largest main bearing currently used in a wind turbine has a diameter of 3.2m [7.8]. Further assessment of the design of the main bearing is beyond the scope of this project.

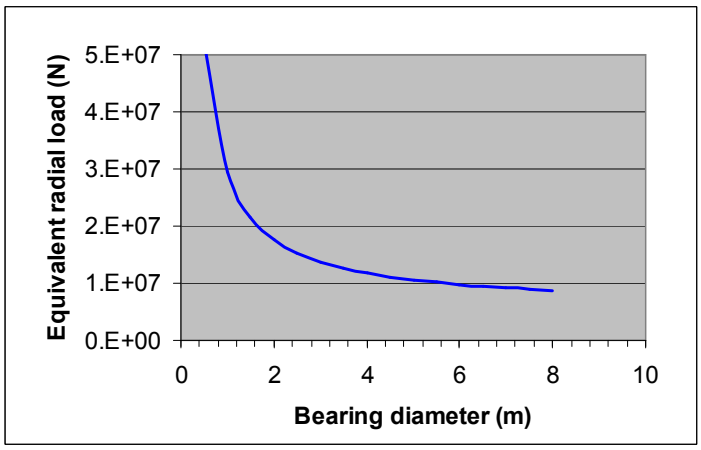

Figure 7.5: *Equivalent radial load on main bearing as a function of its diameter.*

7.1.2.3 Yaw system

The free yawing system uses the axial thrust force and the aerodynamic unbalance on the rotor to restore its aligned position. The unbalance on a rotor in yawed flow conditions is a complicated phenomenon and to explain the restoring force with blade element momentum theory a variation of the induction factor over the rotor plane has to be assumed [7.18]. Since no simulation data for the ICORASS turbine in yawed conditions is available at the time of writing, the restoring force is assessed from published small scale experiments. In [7.19] a two bladed rotor with 10m diameter is operating in a wind tunnel at 10 m/s wind velocity. At a yaw angle of 30º the average thrust equals 700 N. From the blade root moment presented in [7.19] the integrated moment of the two blades about the vertical axis through the hub's centre is calculated. The result is presented in Figure 7.6. The asymmetry in Figure 7.6 demonstrates the restoring force, as the integrated moment over a full rotation yields a positive value. This average moment of 177 Nm can be interpreted as a horizontal offset of the 700 N thrust force of approximately 0.25 m from the rotor centre. Assuming that this offset scales linearly with the rotor diameter, the 160 m ICORASS rotor will experience a restoring moment due to the aerodynamic unbalance of 5MNm at a thrust force of 1.3 MN (See Table 7.3). This restoring moment at a yaw angle of 30º can be interpreted as an aerodynamic rotational stiffness K_{rot} of 10 MNm/rad.

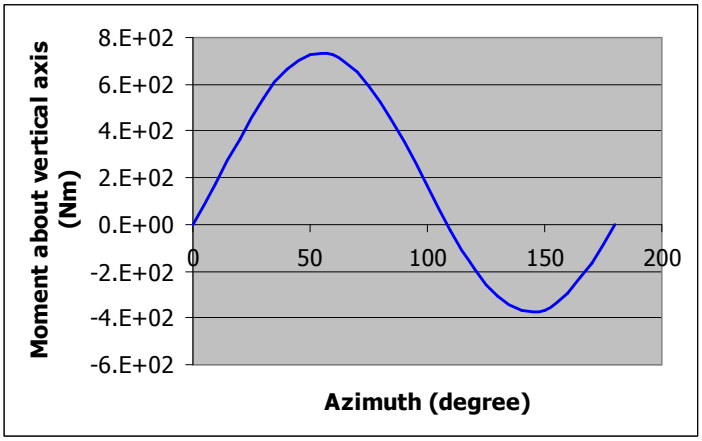

Figure 7.6: *Hub moment about vertical axis for half the rotor cycle. Azimuth equals zero for a vertical rotor.*

In addition, the thrust force on the downwind rotor can be interpreted as an aerodynamic stiffness. At a thrust force of 1.3 MN and a lever arm of 5 m (See Table 7.3 for the offset of the rotor in downwind direction), this stiffness equals 6.5 MNm/rad for small yaw angles.

The two restoring effects are similar in magnitude. At the risk of oversimplifying the physics, the cumulative stiffness of both effects and the inertia of the rotor in horizontal position (as calculated in Section 7.1.2.1) yield a natural frequency (nf) of 0.4 rad/s using the equation:

$$nf = \sqrt{\frac{k_{rot}}{I}} \text{ (rad/s).} \tag{7.8}$$

This natural frequency is well below the 1P excitation frequency of 1.15 rad/s (11 RPM) at rated wind speed and certainly well below 2P excitation. Therefore, with considerable reservation, moderate response of yaw motion can be expected.

The effect of having no yaw brakes on blade, hub and tower top loading is not obvious. Both yawing and tilting loads are affected by axial flow, blade stiffness, blade mass, misalignment, wind shear and yaw rate [7.12]. When no yaw brakes are applied, the integrated yawing loads will tend to zero, but the resultant (cyclic) yawing motion will induce additional tilting loads and the loads in the individual blades in vertical position may increase. With full brakes that prevent yaw motion the tilting moments tend to be smaller, but the torque on the tower top and the loads in the individual blades in horizontal position may increase. Even a preliminary analysis of these effects for the 10 MW ICORASS turbine is beyond the scope of this project.

Since the active yaw system to untwist the cables is working when the turbine is not running, it can be designed for substantially lower loads and power than in case of a fully active system. Therefore, no significant effects of the large scale of the ICORASS turbine on this part of the system are expected and this part is not further analysed.

The final main component of the yaw system is the yaw bearing. The main loads on the yaw bearing are the aerodynamic thrust in radial direction of the bearing, the nacelle weight in its axial direction and the moment from the thrust and the weight. The moment exerted by the thrust in configuration B of Figure 7.2 is defined to be positive. When the height of the rotor axis above the yaw system is taken equal to the generator radius of 4 m and the values in Table 7.3 are used, the maximum thrust generates a moment of 5.2 MNm and the moment due to the weight equals -17 MNm. As intended, these moments work in opposite direction, but the moment of the weight is not completely compensated by the moment of the thrust. The centre of gravity of the nacelle is 1.4 m upwind of the tower centreline. With a bearing diameter of more than 2.8 m the force on all rollers of the bearing will be downward and a single row conical roller bearing could be used. A similar analysis as used in Section 7.1.2.2 for the main bearing could be used to assess the diameter at which the influence of the moment on the yaw bearing levels of. However, the uncertainty in the position of the centre of gravity of the nacelle is too large to justify such approach. When detailing the nacelle, a shift of the centre of gravity of the nacelle to the tower centreline should be attempted. With an offset of as little as 0.2 m from the tower centreline, the total moment would vary between -2.6 MNm at zero thrust to +2.6 MNm at maximum thrust.

7.2 Support structure

7.2.1 Three or four legs

Without further analysis, it is assumed that monopiles and braced monotowers are technically or economically infeasible to support a 10 MW turbine in water depths of 30 to 40 meters. Therefore, a truss tower is chosen as the appropriate concept for the support structure. The first question that is addressed is whether there is a clear load carrying advantage of either 3 or 4 vertical main members. The top view of the cross section of these two configurations is given in Figure 7.7. Both configurations have the same radius R between the centre of the legs and the centre of the construction to keep blade clearance the same for both configurations. Due to blade clear-

ance the radius is a geometrical constraint for the support structure and it is assumed that under typical design conditions the largest possible radius is beneficial for both configurations.

The load carrying capacity of these two configurations is assessed by applying an overturning moment *M* as indicated in Figure 7.7 and addressing the following two issues:

- What are the maximum tensile and compressive forces in the legs, as an indication for material use for the legs?
- What is the circumference of the triangle respectively square in Figure 7.7, as indication for material use of the brace members?

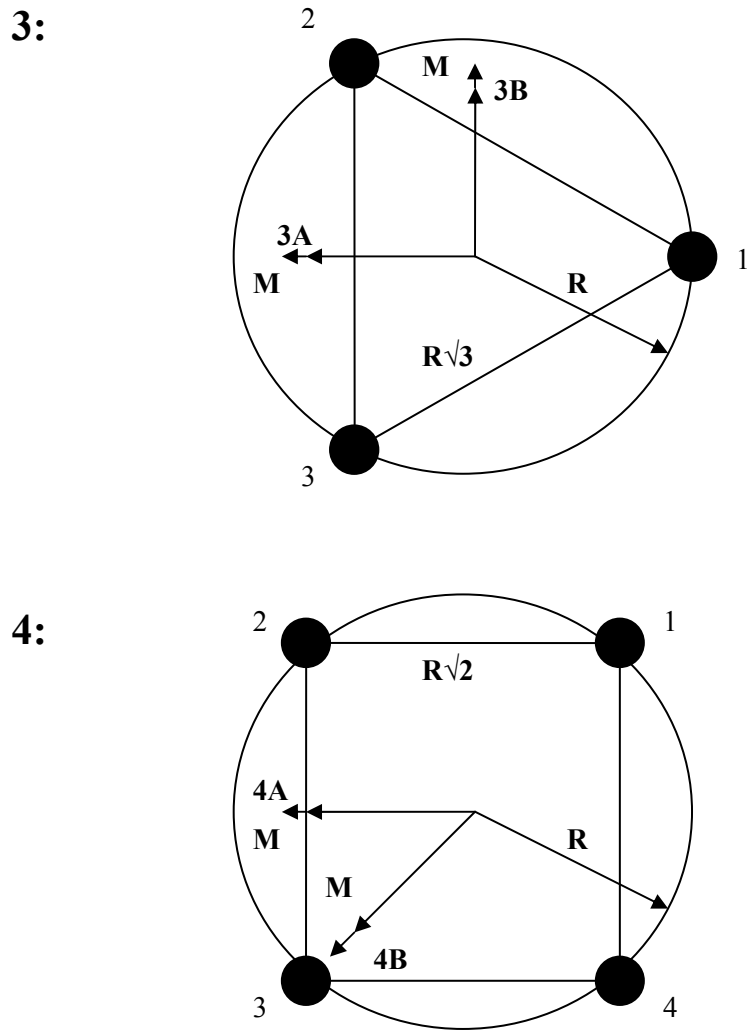

Figure 7.7: *Cross sections of truss tower configurations with 3 and 4 legs with two load cases A and B each.*

The maximum force for the triangular configuration occurs in leg 1 under load case 3B and equals (2/3)**M/R* ≈ 0.67*M/R*. When the required cross-sectional area of the member and thus material use is taken proportional to the force, the material use for three legs is proportional to 2*M/R*. The maximum force for the square configuration occurs in legs 2 and 4 under load case 4B and equals ½*M/R* = 0.5*M/R*. The material use for four legs is therefore also proportional to 2*M/R*. From this perspective there is no evident preference for either 3 or 4 legs.

The circumference of the triangular configuration equals $3*R\sqrt{3} \approx 5.2*R$. For the square configuration the circumference equals $4*R\sqrt{2} \approx 5.7*R$. This difference is fairly small. Although the total circumference of the triangular configuration is smaller, the distance between the legs of this configuration is larger and some additional material may be required for the brace members to avoid buckling.

The previous analysis shows that load carrying capacity and material use of both configurations are nearly equal. Without further comparison, e.g. of differences for manufacturing, a truss tower with four legs is selected in this investigation.

7.2.2 Pile design and stiffness

The foundation piles are designed using a tool written in Excel and described for instance in [7.20]. Given the necessary inputs, the piles are designed automatically according to the process outlined below:

Step 1: Take $D/t = 50$, with D equal to the pile diameter and t equal to wall thickness.
Rationale: the used software requires this type of input. This relatively small ratio is a rule of thumb to avoid buckling of the pile during hammering. The used value is slightly more conservative at the expected pile dimensions than the required wall thickness according to [7.21] which equals $0.00635 + D/100$ (in meters).

Step 2: Design the cross section of the pile to withstand a bending moment equal to $(T/4) \cdot l_{neutral}$, with T equal to the thrust force of 1,300,000 N and $l_{neutral}$ the pile penetration depth of 4 m at which the moment in the pile is assumed to be zero in the simplified pile model shown in Figure 7.8. A clamping depth of 8 m is assumed since a pile diameter around 1 m is expected and for dynamic analysis a deepest clamping depth of 8 times the pile diameter is suggested in [7.22].

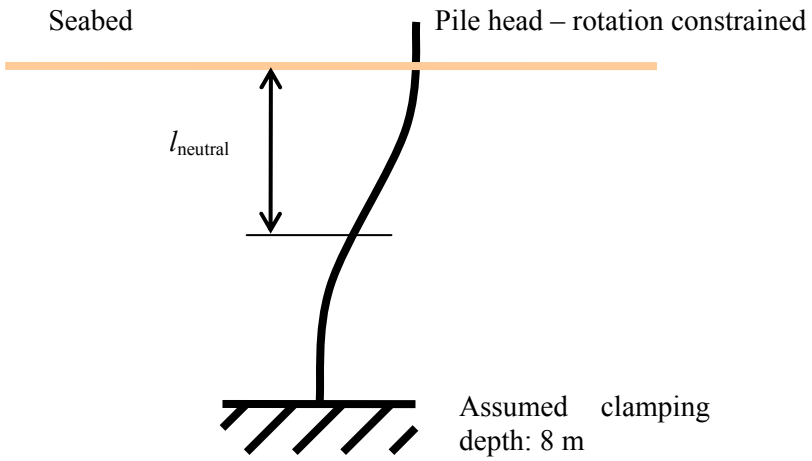

Figure 7.8: *Simplified model of pile deformation by a cantilever beam.*

Step 3: Design pile penetration depth to withstand an axial (= vertical) load of $F_{gravity}/4 \pm 0.5 \cdot T \cdot H_{hub}/R_{truss\ base}$ at the seabed, in accordance with Section 7.2.1, but by adding the weight of nacelle and tower. A homogeneous sandy soil is modelled in this step and the resulting required pile length is a function of soil friction angle.

The results of the pile design process are given in Table 7.4 for three soil types.

Once the pile is designed, the lateral and rotational stiffness of the foundations are determined using a finite element model of the pile. The used approach is recommended in [7.23] and is illustrated in Figure 7.9. The axial foundation stiffness is determined from a vertical load analysis

of the finite element model. The resulting stiffness is also shown in Table 7.4 and is used in the analysis and simulation of the support structure.

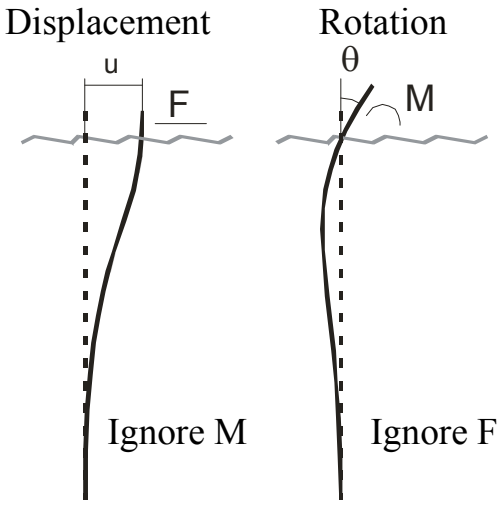

Figure 7.9: *Displacement method in a finite element analysis to get stiffness.*

Table 7.4: *Pile dimensions and elements of the pile stiffness matrix.*

Pile properties	**Friction angle 30º**	**Friction angle 35º**	**Friction angle 40º**
Penetration (m)	35.3	30.6	26.5
Diameter (m)	1.07	1.07	1.07
Wall thickness (m)	0.021	0.021	0.021
Mass [1 pile] (kg)	19,400	16,800	14,500
Stiffness:			
Lateral ($\cdot 10^6$ N/m)	64.6	132.6	180.3
Rotation ($\cdot 10^9$ Nm/rad)	0.98	1.19	1.30
Axial ($\cdot 10^6$ N/m)	88.2	99.3	96.4

7.2.3 Truss design

For truss design the total tower top mass and the aerodynamic thrust force are major design drivers. This data is summarized in Table 7.3.

Based on available data for the Lagerwey LW-750 (750kW) and the Zephyros Z72 (2MW; rotor mass 33 ton; nacelle mass 19 ton; generator mass 46 ton) one can see that typically for a direct-drive system the generator takes up half the tower top mass, defined as the combined total nacelle and rotor mass. Using the known total tower top mass for both turbines as well as for the 4.5MW Enercon E112 (500 ton; Wind Direction, 01-2003), the total tower top mass of a 10MW direct-drive system can be extrapolated towards approximately 1,300 ton.
Please note that the relative rotor plus hub mass (200 ton) is a lot lower than for the Z72 (extrapolation would give around 400-500 ton for the rotor and 550-650 for the generator). One might therefore argue that the generator mass (and therefore the total tower top mass) in Table 7.3 is quite high.

The maximal stationary and rated aerodynamic thrust is around 1.3 - 1.4 MN (see Table 3.2 and Figure 3.6). Conservative extrapolation of the extreme gust aerodynamic thrust of the DOWEC machine towards the ICORASS machine leads to a thrust of 4.19 MN.

The starting truss tower geometry is a so-called KEMA tower for a 3MW offshore wind turbine (full truss, four legs, steel piled). Used data: height = 150 m; base width = 30 m; water depth = 35m; tilt angle = 8º; maximum blade tip deflection = 13m, see Figure 7.10. Based on this geometry a finite element model is created in ANSYS. Using the extreme tower top loads (including the bending moment due to the tower top mass centre of gravity offset) the elements are dimensioned quite conservatively so that the total mass can be estimated. A total truss tower mass of 975 ton was obtained. Maximum tower top displacement of 1.2m is found and a first natural frequency of 0.919 Hz, which is higher than the 6P for the maximum rotational frequency of either 8 or 9 rpm.

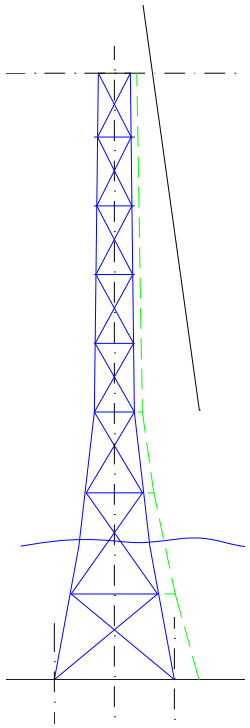

Figure 7.10: *Conceptual truss design.*

In the DOWEC project a combined material and manufacturing price of 3.5 €/kg was used for the tower, using this value results in a cost of 3.41 M€. Typically one tenth of this price is used for the foundation piles (341 k€). Using the worst soil conditions for the foundation mass calculation (see Table 7.4) results in a foundation price of 272 k€. This price is used in the economical evaluation, although one might argue that specific foundation pile material and manufacturing cost may be a lot lower (2.25 €/kg for DOWEC).

7.3 Installation

7.3.1 Focal point

The installation procedures for the ICORASS turbine deviates from most existing offshore structures by its combined high weight and height. The installation of the sub-sea structure is similar to that of platforms for the oil and gas industry and a similar structure for an offshore wind turbine has been installed in the Downvind project [7.24]. All offshore wind turbines in farms of more than two turbines installed until now have a hub height of less than 80 meter [7.25]. There are a few technology demonstration wind turbines installed in water with hub heights higher than 80 m. One of the two turbines currently installed near the Beatrice platform had a hub height of 88 m above sea level [7.26] (Note: The originally planned hub height was 107 m [7.27]). The heavy lift vessel RAMBIZ was used for this, although the lifting height of this vessel is only 80 m above the deck (which is less than 85 m above sea level) [7.28]. The rotor, nacelle and tower were assembled in the harbour and the entire structure with a lower centre of gravity was transported in the two cranes of the vessel. Another turbine with a hub height of 100 m is installed within 50 m from the shoreline in the Ems near Emden. In water depth of only 2 m, the installation was done with two mobile cranes on stabilised pontoons, using more or less that same sequence of operations as for an onshore installation [7.29].

Based on the previous observations the lifting of the (upper part of) the tower and the rotor-nacelle assembly are considered to be procedures with most opportunities for innovation. An integral lift-transport-install procedure for rotor, nacelle and tower, as used for the Beatrice turbines, is probably a technically feasible option. The principle has been demonstrated and semi-submersible heavy lift vessels that can lift over 5000 tonnes up to more than 120 m exist (See Table 7.5). However, these multipurpose vessels are very expensive [7.30] and the one-by-one installation may prove lengthy for a remote location. The special-purpose vessel M/V Sea Installer given in Table 7.5 is expected to cost less, but the maximum weight that can be lifted is less than the weight of the rotor and nacelle. The focus of the development of an installation concept in this project is therefore set on reduction of lifting vessel requirements (e.g. lower hoist height or weight). First, lifting of the tower is discussed and after that installation of rotor and nacelle.

Table 7.5: *Some heavy lift vessels with high hoisting heights.*

Name	Category	Max lift main hoist (t)	Max lift height main hoist (m)	Max lift height aux. Hoist (m)
DB 101	Semi Submersible Crane Vessel	6000	90	120
Balder	Semi Submersible Crane Vessel	7500	110	130
Hermod	Semi Submersible Crane Vessel	7200	110	130
Thialf	Semi Submersible Crane Vessel	6800	118	145
M/V Sea Installer (Proposed) [7.31]	Special type off-shore unit	1250 / 480	60 / 102	83 / 125

7.3.2 Lifting of the tower

This section describes procedures to lift and turn the tower. The consequences or requirements that the various procedures have with respect to transportation are not addressed. However, it is assumed that the tower or tower segments are transported in horizontal position on a pontoon, unless specified otherwise. Self installing towers, such as telescopic or harmonica structures are not considered here, because their technical complexity does not enable quick assessment of their potential.

Figure 7.11 shows four basic modes of operation to lift and turn the tower. The crucial point in this operation is the centre of gravity of the tower, rather than the highest point of the tower. However, the geometry of the structure will have its constraints on manoeuvrability, as will be discussed.

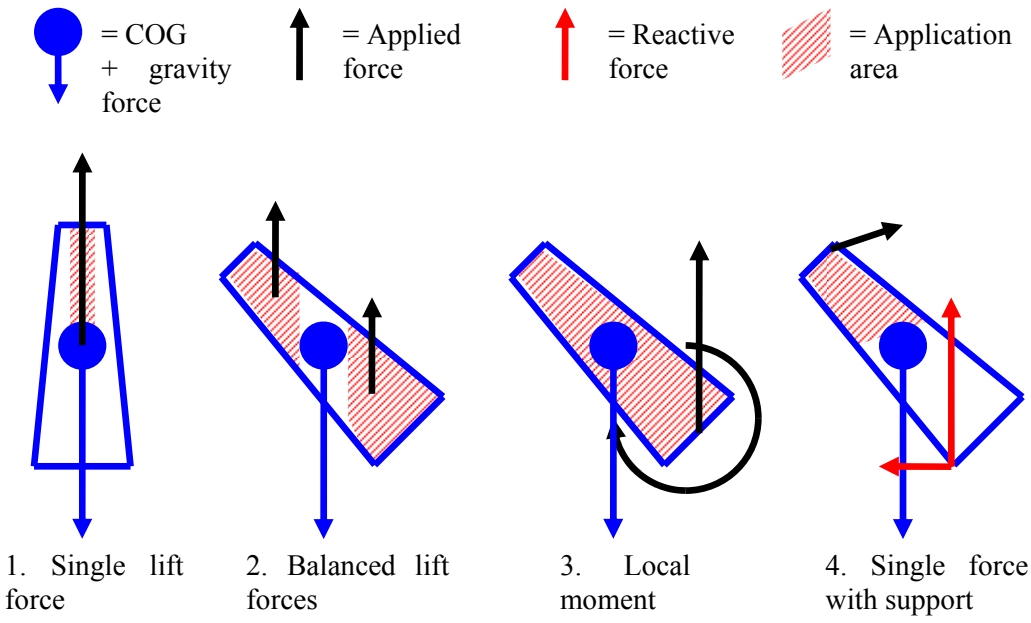

Figure 7.11: *Modes of rotation and lifting of the tower.*

In the first mode, the tower is already in the upright position and the hoisting hook can be attached anywhere vertically above the centre of gravity. With a boom above the top of the structure, the vertical movement is only limited by the boom height. When the boom is not high enough, it can stick through the structure between the centre of gravity and the tower top, to hook up in the centreline of the tower. In this case manoeuvrability of the tower is limited. This operation requires vertical transportation of the tower or a preparatory turning procedure. Vertical transport will be more sensitive to weather conditions and likely more costly than horizontal transport.
In the second mode, two forces are used to carry the tower on both sides of the centre of gravity. Highest manoeuvrability is achieved when an upper cable is operated from a boom that exceeds the final structural height and when the cable is attached to the tower top or to the outside of the structure. With a lower boom, manoeuvrability is severely restricted by structural elements. For controlled lifting and turning, both cables have to be operated from the same vessel or from two jack-up vessels.
In the third mode height and angle are controlled independently. The farther away from the centre of gravity the lifting force applies the larger the required moment on the structure. When the lifting force applies to the outside of the structure the manoeuvrability is largest. The conditions for controlled operation are the same as for mode 2.
In the fourth mode only one side of the tower is lifted and the other side is supported by the deck or a part of the structure already installed on the seabed. The direction of the lifting force may be anywhere between vertically up and horizontally in the direction of the centre of gravity. The magnitude of the lifting force and the reactive forces depend on this direction and on the point of application and they are smallest for vertical lifting at the tower top. When the lifting force applies to the outside of the structure the manoeuvrability is largest. The conditions for controlled operation are the same as for mode 2 and 3.

The most straightforward approach would be a combination of mode two for turning and mode one for lifting, using a boom which exceeds the structural height. This type of operation is used to install the space frame base structure of the Beatrice turbine. When the tower is divided in two or three segments, the lifting capacity of the M/V Sea Installer is sufficient. The lowest segment can be installed with the high capacity crane with a low boom and the upper segment(s) can be installed with the higher boom. Although this vessel only exists on the drawing board, it is an indication that high-hoisting cranes can be expected to become available in the future in a lower price category than the semi-submersible vessels. Alternatively, a boom extension of existing heavy lift vessels, such as the RAMBIZ, can be considered.

When a crane vessel is used that cannot reach above the highest point of the installed structure, the following difficulties need to be considered:

- The tower members inhibit hooking up along the centreline of the structure.
- When only one cable is connected to a side of the structure, the structure will not reach a vertical position and it will be difficult to turn the structure fully upright.
- When the support structure is divided into segments, a large upper segment has the advantage of a low centre-of-gravity, but it has the disadvantage of a high weight.

Solving these problems requires good insight in the capabilities of offshore equipment and is not attempted here.

7.3.3 Installation of rotor and nacelle

This section outlines a procedure to install the rotor and nacelle. The procedure is based on the following considerations:

- Not many heavy lift vessels that can hoist up to hub height are available and they are expensive.

- The nacelle as described in Section 0 consists of three parts: an upwind direct drive generator, a downwind rotor and hub and a bedplate, main shaft, yaw system and main bearing in the middle.
- The direct drive generator and rotor are sensitive, cumbersome and/or heavy components.
- The middle section of the nacelle doesn't contain sensitive components.

The suggested installation procedure of rotor and nacelle consists of the following steps:

1) Assemble the middle section of the nacelle with the top segment of the tower in the harbour and transport the assembly horizontally.
2) Install the assembly of the middle section of the nacelle and top segment of the tower in one lift. Because the middle section of the nacelle contains no sensitive components, this operation is no more precarious than the installation of the tower itself.
3) Transport the direct drive generator and the rotor as two separate components. Since the main bearing is assembled with the middle section of the nacelle, the rotor of the generator will be locked in a fixed position, securing the air gap between rotor and stator.
4) Hoist the rotor with a fixed crane on top of the middle section of the nacelle along a guide track at the side of the tower. A heavy lift vessel with a low hoisting height can be used to get the rotor on the guide track. Connect the flange of the hub to the main shaft.
5) Yaw the nacelle to align its other side with the guide track and hoist the generator in the same way as the rotor. Connect the flanges of the generator rotor and stator to the main shaft and middle section of the nacelle.
6) Remove the locking mechanism of the generator rotor.

Step 4 and 5 are illustrated in Figure 7.12.

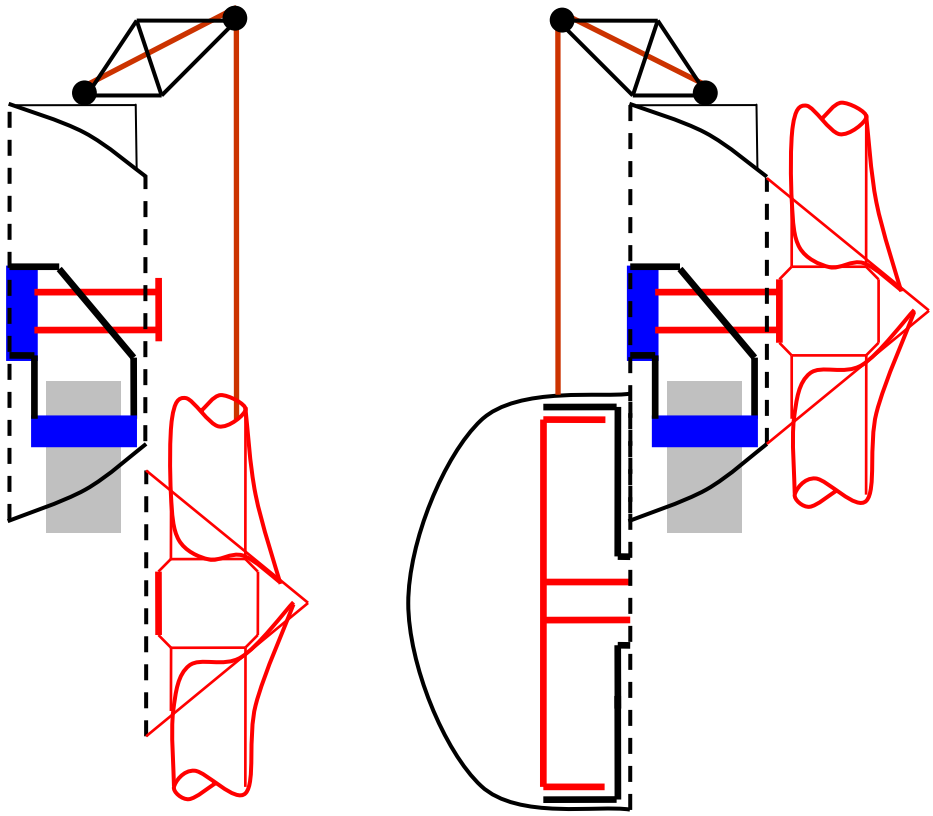

Figure 7.12: *Hoisting the rotor and generator with the same internal crane.*

Installation and assembly of the three parts of the rotor-nacelle is expected to take about 10 hours. Lifting and connecting the hub of a 4.5 MW Enercon E112 with 250 bolts was performed between 6:30 and 11:00 of one morning [7.32]. During the last phase of this procedure the heavy lift vessel is not required.

7.4 Maintenance

The basic philosophy for the ICORASS design is a reduction of maintenance costs, mainly by selecting robust concepts that potentially have low failure rates. Due to the limited scope of this project, an in depth assessment of failure behaviour, maintenance requirements and availability is not performed. However, the reliability of the selected concept is compared with the concepts presented in [7.30], using a similar approach to estimate failure rates: A typical failure rate per component is used and adaptations to this typical failure rate are based on conceptual deviations. A description of the DOWEC concepts is provided in Table 7.6. Table 7.7 presents the failure rates of these concepts, as well as those of ICORASS. In many respects, the ICORASS turbine resembles the robust turbine of the DOWEC concept study. In places where it deviates, a rationale is given for the estimated effect on failure rate.

Table 7.6: *Definition of concepts for comparison of reliability.*

Name	Number of blades	Rotor speed	Control	Brakes
Danish	3	Dual	Passive stall	Tip brakes + HSS brake
Advanced	3	Variable	Positive pitch	Pitch + HSS brake
Robust	2	Single	Passive stall	LSS brake + HSS brake
Nedwind	3	Dual	Active stall	Pitch + HSS brake

Table 7.7: *Positioning the ICORASS concept in the DOWEC Concept reliability study (Data of other concepts from [7.30]).*

Component	Danish	Advanced	Robust	Nedwind	ICORASS
Shaft & Bearings	0.02	0.02	0.02	0.02	0.02
Brake	0.05	0.05	0.10	0.05	0.05 [1]
Generator	0.05	0.08	0.04	0.05	0.06 [2]
Parking Brake	0.05	0.05	0.00	0.05	0.00
Electric	0.14	0.14	0.14	0.14	0.14
Blade	0.16	0.16	0.10	0.16	0.10
Yaw System	0.23	0.23	0.23	0.23	0.05 [3]
blade tips	0.28	0.00	0.00	0.00	0.00
Pitch Mechanism	0.00	0.28	0.00	0.25	0.00
Gearbox	0.30	0.25	0.30	0.27	0.00 [4]
Inverter	0.00	0.32	0.00	0.00	0.32 [5]
Control	0.34	0.38	0.30	0.36	0.34 [6]
Total	1.62	1.96	1.23	1.58	1.08

[1] Only one mechanical brake is applied, while the Robust concept has one mechanical brake on the high speed shaft and one on the low speed shaft. The second brake for the ICORASS turbine is from an increased generator torque.

[2] As for the squirrel cage induction generator of the Robust concept the permanent magnet generator needs no windings on the generator rotor. The failure rate is slightly increased because of the permanent magnets and the mechanical complexity of the big generator.

[3] The yaw system is only used to untwist the cable and is not used to align the turbine with the wind during operation.

[4] There is no gearbox (and no couplings).

[5] A full power inverter is applied to connect the synchronous generator to the electricity grid. Although more inverter units may be required than for the Advanced concept, it will be easier to create a system that can continue operation during failure of one unit.

[6] The control effort and required sensors are similar to that of the dual speed passive stall controlled Danish concept, since variable speed and no pitch are applied.

According to this evaluation the failure rate of the ICORASS concept is about 10% less than that of the Robust concept of the DOWEC concept study and the reduction compared to the Advanced concept is nearly 45% (in both cases the percentage is taken relative to the concept with the highest failure rate). Although the absolute values of this evaluation are imprecise, the relative performance is a good indication of the potential of the concept. Below, a rough assessment is made of the possible reductions of downtime and maintenance costs, based on the assumptions given in Table 7.8:

Table 7.8: *Assumptions relating to the potential maintenance costs and downtime reductions of ICORASS.*

Turbine comparison	**Ratio ICORASS turbine / State-of-the-art turbine**	
Rated power	3	
Hub height	1.5	
Number of visits (~ Failure rate) [1]	0.55	

Costs	**Proportional to**	**Percentage of state-of-the-art costs [7.33]**
Logistic and fixed costs	Number of visits	35
Spare parts	Rated power	40
Crane vessels and lifting equipment	Hub height	25

Downtime	**Proportional to**	**Percentage of state-of-the-art downtime [7.33]**
Storm	Number of visits	33
Logistics	Number of visits	57 [2]
Repair activity	Rated power	10

[1] State-of-the-art is characterised by the Advanced concept
[2] Includes 41% for 'No shift' during night time.

Using the assumptions in Table 7.8, the operation and maintenance costs of ICORASS per turbine equals approximately 180% of the O&M costs for a state-of-the-art turbine. The higher costs are mainly caused by the increased costs of spare parts. The maintenance costs per installed MW, which is an indicator of the cost per kWh, is only 60% of a state-of-the-art turbine. The large benefit achieved by scaling of the turbine is caused by less than proportional increase of logistic and lifting costs. The downtime for ICORASS would be approximately 80% of that of a state-of-the-art turbine. Some benefits of the reduced number of visits are cancelled out by the assumed longer repair activity. However, the proportionality of the repair time to rated power has the least support from reason or experience of all assumptions in Table 7.8. When the repair time is independent of turbine size the downtime of ICORASS would be 55% of that of a state-of-the-art turbine.

Figure 7.13 shows the layout of the nacelle and the separation lines of the generator, middle section and rotor. As stated in Section 0 the selected nacelle layout enables disassembly of the generator side, while leaving the middle section and rotor in position. Based on this, the installation described in Section 7.3.3 uses an approach in which the generator is hoisted separately. The exchange of a complete generator for service or repair is also facilitated by the guide track system used for installation. Since hoisting of the generator is less susceptible to wind than hoisting of the rotor, the working conditions can be worse for this operation. The inside of the generator

provides space for all the equipment, leaving the middle section and rotor with a low maintenance demand. The yaw motors can also be located in the generator, using a transmission. There has been bad experience with the use of a transmission chain for yawing of a Windmaster turbine, but in that case the transmission was used during operation of the turbine [7.34]. The potential of generator exchange in terms of downtime or maintenance cost reductions cannot be assessed with sufficient accuracy at this stage.

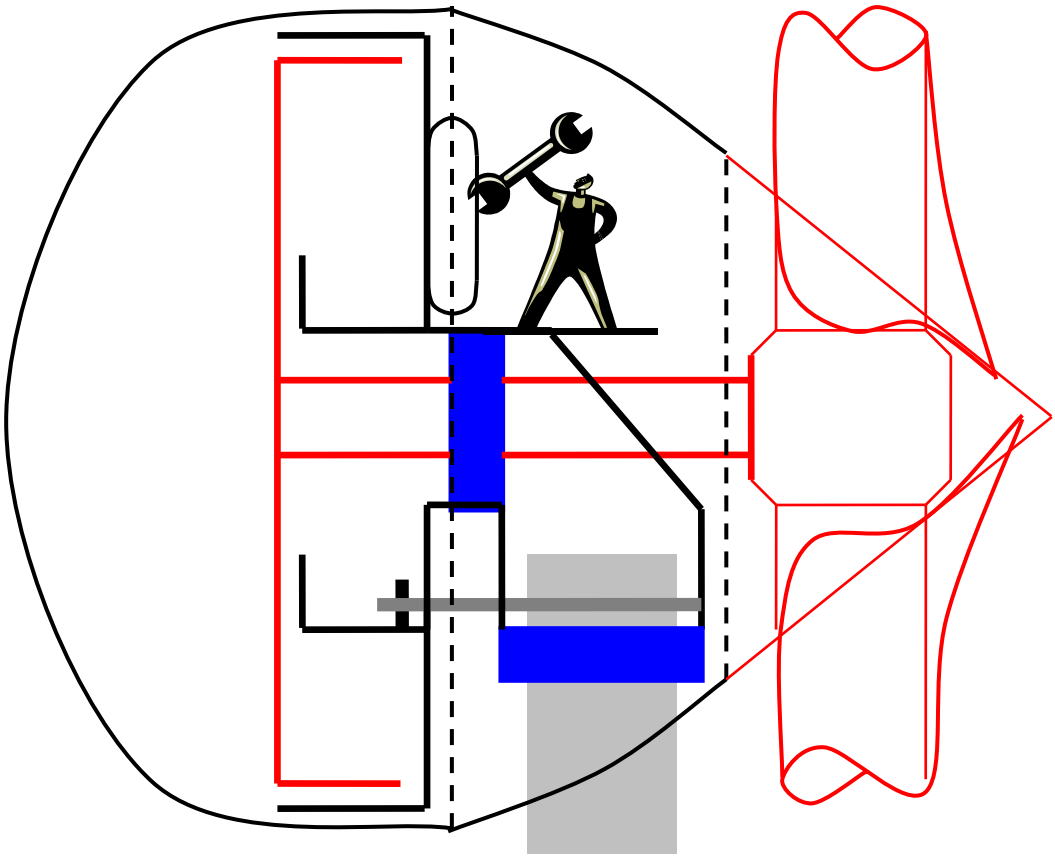

Figure 7.13: *Schematic overview of the nacelle layout, showing accessibility and the yaw system.*

7.5 References

[7.1] ENERCON GmbH. *Direct drive*. Website: www.enercon.de >Technology >Direct drive. Accessed August 2006.

[7.2] Mitsubishi Heavy Industries Ltd. Website: www.mhi.co.jp/nsmw/en/gearless.htm. Accessed August 2006.

[7.3] Lagerwey windturbine BV. *Lagerwey LW 50/750.* Product leaflet, no date.

[7.4] Harakosan Europe BV. *Products.* Website: www.harakosan.nl/products. Accessed August 2006.

[7.5] MTorres Group. Website: www.mtorres.com >English >Wind Energy. Accessed August 2006.

[7.6] Vensys GmbH. Website: www.vensys.de. Accessed August 2006.

[7.7] Jeumont. Website: www.jeumont-framatome.com/english/html/Eolienne/eoliennes_j48.asp. Accessed August 2006.

[7.8] Rettinger, M. *Lager und WEA müssen aufeinander abgestimmt sein* (In German). Erneuerbare Energien, July, 2006.

[7.9] Wisselink, H. & Winnemuller, A.H.J. *Estimation of turbine reliability figures within the DOWEC project*, Doc. no. 48, ver. 3, Bunnik, 22 Januari 2002.

[7.10] Vallinga, R. *Estimation of turbine maintenance figures within the DOWEC project - Task 17*. Doc. no. 86, ver. 0, Bunnik, 22 May 2002.
[7.11] Schepers, J.G. *An engineering model for yawed conditions, developed on basis of wind tunnel measurements.* AIAA-1999-39, 18th ASME Wind Energy Symposium, 37th Aerospace Sciences Meeting and Exhibit, Reno, NV, January 11-14, 1999.
[7.12] Manwell, J.F., Mcgowan, J.G. & Rogers, A.L., *Wind Energy Explained*, ISBN 0-471-49972-2, John Wiley & Sons Ltd., Chichester, England, 2002.
[7.13] Buddensiek, V. *Bremsen für den Wind aus der Zigarrenstadt.* Erneuerbare Energien 6, 2006.
[7.14] Kooijman, H.J.T., Lindenburg, C., Winkelaar, D. & Hooft, E.L. van der. *Aero-elastic modelling of the DOWEC 6 MW pre-design in PHATAS.* Doc. no. 46, ver. 8, ECN, Petten, April 2002.
[7.15] Nijssen, R.P.L. *Scaling rules relevant to the Lagerwey 50/750 wind turbine* (Literature study, Master thesis study). Delft, 2000.
[7.16] Svenborg Brakes A/S. Website: www.svendborg-brakes.dk. Accessed 28 September 2006.
[7.17] Engineers Edge. Website: www.engineersedge.com/bearing_menu.shtml. Accessed 9 August 2006.
[7.18] Schepers, J.G. *Annexlyse: Validation of yaw models, on basis of detailed aerodynamic measurements on wind turbine blades.* ECN-C--04-097. ECN, Petten, September 2004.
[7.19] Eggers, A.J. Jr. & Chaney, K. *Approximate modeling of deep stall effects on yawed rotor loads*. AIAA-2004-664, 42nd AIAA Aerospace Sciences Meeting and Exhibit, January 5-8, Reno, 2004.
[7.20] Zaaijer, M.B., Broek, W. van den & Bussel, G.J.W. van. *Toward Selection of Concepts for Offshore Support Structures for Large Scale Wind Turbines*. In: Proceedings of MAREC 2001, Newcastle, UK, March 2001.
[7.21] API, RP 2A-LRFD: *API Recommended Practices for Planning, Designing and Constructing Fixed Offshore Platforms – Load and Resistance Factor Design*, First Edition, July 1, 1993.
[7.22] Barltrop, N.D.P., Adams, A.J. *Dynamics of Fixed Marine Structures*, Butterworth Heinemann Ltd, Oxford, 1991.
[7.23] Zaaijer, M.B. *Foundation modeling to assess dynamic behaviour of offshore wind turbines*. Applied Ocean Research, Vol. 28, pp 45-57, Elsevier, 2006.
[7.24] Talisman Energy. *Beatrice Wind Farm Demonstrator Project*, Website: www.beatricewind.co.uk. Accessed September 2006.
[7.25] Douglas-Westwood Ltd. *The world offshore wind database*, November 2004.
[7.26] Talisman Energy. *Beatrice Wind Farm Demonstrator Project – Frequently asked questions* (www.beatricewind.co.uk/Uploads/Downloads/Beatrice%20FAQ%20Updated% 2014.02.06.pdf; Updated 14-02-2006). Accessed October 2006.
[7.27] Talisman Energy. *Beatrice Wind Farm Demonstrator Project Scoping Report.* Website: www.beatricewind.co.uk/Uploads/Downloads/Scoping_doc.pdf). Accessed October 2006.
[7.28] Scaldis – Salvage and marine contractors NV. Website: www.scaldis-smc.com/rambiz.htm >Capacity layout. Accessed September 2006.
[7.29] Enova Energysysteme GmbH. *Enova semi-offshore Ems Emden*, Website: www.enova.de/ccms/index.php3?hid=048186&spid=2. Accessed September 2006
[7.30] Zaaijer, M.B., e.a. *Starting point and Methodology of Cost Optimisation for the Conceptual Design of DOWEC.* Section Wind Energy, Delft, March 2000.
[7.31] A2SEA A/S. Website: www.a2sea.com >Fleet. Accessed 1 August 2006.
[7.32] Enercon GmbH. *Majesties in the wind*. Windblatt Issue 1, February 2006.
[7.33] Zaaijer, M.B. *O&M aspects of the wind farm*. Doc. no. 82, ver. 2, TU-D, Delft, 19 March 2003.
[7.34] Jan van der Tempel. Personal communication. August 2006.

8. Economical evaluation

This chapter is used for the preliminary economical evaluation of the ICORASS concept in comparison with the reference situation as sketched in chapter 2.

8.1 Calculation of levelized production cost

Economical assessment of offshore wind energy could be in terms of the internal rate of return (cost-benefit analysis) or in terms of the levelized production costs (cost analysis). For comparing different sites, concepts or designs the *LPC* are recommended as assessment criterion by the IEA [8.1].

As stated in chapter 2, the *LPC* can be calculated with:

$$LPC = \frac{I/a}{AUE} + \frac{TOM}{AUE} \tag{8.1}$$

in which I is the actualized initial investment, a the annuity factor, AUE the annual utilised energy and TOM the total levelized annual "downline cost" (i.e. O&M, insurance, retrofit and salvage costs). Of course, the downline costs are actually higher, since a lower AUE is obtained when the downline time increases [8.2].
Note that all investment costs (turbine hardware, electrical infrastructure hardware, transport and installation) are actualized to costs at year 0 (the year of commissioning the wind farm).

The real interest rate is needed for the determination of the annuity and can be calculated from the interest rate [8.3]:

$$r = \frac{1 + r_{\text{int}}}{1 + v_{\text{int}}} - 1 = \frac{1 + 0.07}{1 + 0.02} - 1 = 0.049 = 4.9\%\,. \tag{8.2}$$

So that the annuity is [8.3]:

$$a = \frac{1 - (1 + r)^{-T}}{r} = \frac{1 - (1 + 0.049)^{-12}}{0.049} = 8.912\,. \tag{8.3}$$

8.2 Cost breakdown

Herman [8.4] supplied a four-level overview of all costs related to the operation of a wind farm in the Dutch DOWEC project. At this state of the conceptual design process it is virtually impossible to determine all costs of the wind farm with high accuracy. Fortunately it is also not necessary to estimate all of the components in this overview to be able to evaluate the economic perspective.
Based on the experience from this project [8.5], a first top-level break down of the levelized production costs of energy (and thus on the total wind farm costs) is listed in Table 8.1.

Table 8.1: *Preliminary breakdown of the levelized production costs based on DOWEC.*

Component	**Percentage of LPC**
Design/Preparation/Other	≈ 1-5%
Hardware	≈ 50-51% (resp. 24% turbine, 9% foundation pile, 9% monopile tower, 8% electrical infrastructure)
Transport and installation	≈ 11%
Operation and maintenance	≈ 33-36% (incl. retrofit/overhaul)
Decommissioning	≈ 1% (about 10% of installation costs)

Because of high uncertainty levels, the influence of the ICORASS concept on the items design/preparation/other as well as decommissioning will not be considered here. However, one might argue that because of the ignorance of the concept the preparation costs might increase. The design/preparation/other costs are set to a fixed percentage of the *LPC* (1.2% for DOWEC) and the decommissioning cost contribution to a fixed percentage of the installation cost contribution to the LPC (11.7% for DOWEC).

The DOWEC baseline wind farm lies at the NL7 site (water depth=22m, distance to shore=50km) with a total rated power of (80*6MW=) 480MW. This site [8.6] is totally comparable to the conditions for the ICORASS project as specified in chapter 2. Therefore this site is used for the ICORASS study as well.

The economic lifetime was 20 years. Because of the large wind farm size, actually a somewhat complicated model was used in which the farm was built in stages (therefore the lifetime was more or less 20.5 years). Using the *LPC* (5.54 €ct/kWh), the expected net energy yield over the whole lifetime (34,816 GWh) and the percentage for the different costs [8.5], we obtain the total effective costs (94.1 M€/yr). Finally the investment costs can be checked with the given values [8.5], note that the yearly O&M costs are lower (17M€ in stead of 26M€) since an improved O&M baseline model was derived during DOWEC [8.2],[8.7].

Table 8.2: *DOWEC wind farm costs.*

	Percentage LPC	**Lev./Eff. Costs**	**Ann. Eff. Costs**	**Actualised Costs Yr 0**	**Investment Costs**
	%	**M€**	**M€/yr**	**M€**	**M€**
WF Design	***1.2%***	23.1	1.1	14.3	***13***
Hardware	***50.8%***	979.6	47.8	604.3	***576***
T&I	***11.1%***	214.1	10.4	132.0	***132***
Yearly O&M (20.5x)	***28.1%***	541.9	26.4	334.3	***17***
Overhaul (3x)	***7.5%***	144.6	7.1	89.2	***30***
Decommissioning	***1.3%***	25.1	1.2	15.5	***41***
Total		1928.4	94.1	1189.6	

Since determining all costs for the ICORASS concept in high detail is an impossible mission at this state of the design process, let us evaluate the economic benefit or disadvantage with respect to the DOWEC LPC. Using the cost data from the DOWEC project, educated guesses are made on the variation of the hardware, T&I and O&M costs for the various concepts. Note that the total LPC for the DOWEC project is a lot lower than assumed for current commissioned offshore wind farms; this is partly due to the used economic model. For this study however we will just look at the relative difference between both concepts.

8.3 Concept variation effects on *LPC*

Five different conceptual rotor and drive train designs were presented in chapter 4: pitch regulated, overrated generator, speed limited generator, power limited generator and torque limited generator. These concepts differ in rotor and drive train hardware costs, but also largely in annual energy yield. Because it was stated that the ICORASS power regulated concept is probably the most feasible option, this one is compared to the DOWEC project. To separate both up scaling effects and integrated rotor effects, also the direct-drive pitch regulated machine is evaluated.

1) DOWEC, 6MW,
2) Pitch regulated DD, 10MW,
3) ICORASS power limit, 10MW (cable power, 12.6MW generator power).

8.3.1 Energy yield

For the energy yield from the DOWEC project the following values are used [8.5]:

- Expected wind farm yield for 20.5 year = 34,618 GWh (1698.3 GWh/yr),
- Turbine availability = 0.970,
- Farm availability = 0.985,
- Aerodynamic farm efficiency = 0.917,
- Electric infrastructure efficiency =0.980,
- Electric transmission efficiency = 0.961.

Therefore the total combined efficiency and availability is 0.825. Then the capacity factor of a solitaire (always available) DOWEC wind turbine is:

$$c = \frac{1698.3\mathrm{E}+9/0.8251}{480.\mathrm{E}+6\cdot 24\cdot 365} = 0.490, \tag{8.4}$$

which is a very common number. The capacity factor including availability and efficiency losses is:

$$c = \frac{1698E9}{480E6\cdot 24\cdot 365} = 0.490\cdot 0.825 = 0.404. \tag{8.5}$$

For the new designs, the optimum annual energy yield per turbine is given in chapter 4.8. Using a ratio of the rated power (10/6), the ratio of the hub heights (110/90), the DOWEC annual failure rate (1.55) and the ICORASS annual failure rate (1.08, 1.36 for the pitch controlled turbine) we can determine the turbine down time reduction with the data in section 7.4. Using the energy yield as stated in section 4.8, Table 8.3 is obtained. We can see that a 13% increase of energy is obtained with both new concepts. This is mainly due to the relatively larger rotor diameter [$(170\mathrm{m}/129\mathrm{m})^3$=2.29 and $(10\mathrm{MW}/6\mathrm{MW})^{3/2}$=2.15] and also due to the higher hub height (higher wind speeds), higher aerodynamic efficiency (little root losses) and lower down time (higher availability). Reduced aerodynamic farm efficiency is not taken into account.

Table 8.3: *Energy yield per wind turbine.*

	DOWEC	ICORASS Pitch	ICORASS power limited	
Opt. energy yield	25.7	48.4	48.2	*GWh/yr*
Failure rate	1.55	1.36	1.08	*/yr*
Turbine availability	0.970	0.971	0.976	
Total eff./avail.	0.825	0.826	0.830	
Energy yield	21.23	39.99	40.03	*GWh/yr*
Energy yield / farm	1698.3	1919.5	1921.2	*GWh/yr*
Farm yield increase	-	13.0	13.1	%

8.3.2 Costs

Because this economical evaluation is used merely for concept variation analysis, only a high as possible accuracy in the relative cost variation is needed [8.1]. In this section the relative change in costs between the DOWEC wind farm and the ICORASS wind farm is assessed.

8.3.2.1 Operation &Maintenance costs

The ratio of O&M costs between the DOWEC project and the ICORASS concept can be calculated from section 7.4 as well. Using the ratios between hub heights, rated power and failure rate the O&M costs increase 27.9% for the pitch regulated turbine and 21.6% for the ICORASS turbine. However, since the number of turbines in the farm decreases with a factor (48 / 80 =) 0.6, the total O&M costs for the pitch regulated turbine decrease with 23.2% and for the ICORASS turbine with 27.0%.

8.3.2.2 Hardware costs

For the DOWEC project the total hardware investment costs are split into five components, see Table 8.4. A best guess on the change in hardware cost is made.

- *Electrical system*
  Since the wind farm size remains the same, the investment cost for the electrical transmission system remain unchanged. Although due to the decreasing number of wind turbine the cost may go down, for simplicity the electrical collection system remains unchanged as well because it has no significant impact on the total costs. Of course the electrical system cost per wind turbine increases with a factor 80/48.
- *Support structure*
  For the support structure a price of 3.5€/kg material is used, similar to the DOWEC project. Based on the mass of the support structure, the material cost can be calculated.
  Tower: 975 ton - 3,412 M€.
  Foundation: 4 x 19.4 ton - 271.6 k€.
- *Rotor and hub*
  For the rotor and hub it is again assumed that the costs are merely mass determined. Starting off with the DOWEC rotor, the rotor cost therefore increases with a factor 2 (from 50 ton unto 100 ton) and the hub cost with a factor 3.3 (from 30 ton up to 100 ton). This means that the mass specific rotor cost is 13.3 €/kg and the hub cost is 11.7 €/kg. Added are costs for the pitch system, which are scaled with the rated power according to: $P^{3/2}$.
- *Nacelle*
  The nacelle costs are by far the most difficult to examine. First of all, the nacelle concept is completely different from the DOWEC concept, the gearbox is removed, the main shaft is elongated, the yaw system is passive, and the generator is a direct drive system. For current available direct drive turbines (e.g. Enercon) no hardware cost data is available. Therefore again the coarsest method is used, namely the fixed price per mass.
  For the DOWEC turbine 1965.1 k€ / 188 ton = 10.5 €/kg. Therefore the price for the 10MW nacelle is 1100 ton 10.5 €/kg = 11,550 k€.

Table 8.4: *Hardware investment costs.*

	DOWEC per farm	DOWEC per WT	Pitch per farm	Pitch per WT	ICORASS per farm	ICORASS per WT	
Foundation	103608	1295.1	13056	272	13056	272	*k€*
Tower	103608	1295.1	163776	3412	163776	3412	*k€*
Rotor + hub	119080	1488.5	168854	3517.8	119938	2498.7	*k€*
Nacelle	157208	1965.1	554400	11550.0	554400	11550.0	*k€*
Elec. Coll.	23024	287.8	23024	479.7	23024	479.7	*k€*
Elec. Trans	69072	863.4	69072	1439	69072	1439	*k€*
Total	575600	7195.0	992161	20670.0	943246	19651.0	*k€*
Cost increase	-	-	72.4	187.3	63.9	173.1	%

As can be seen, the total wind farm hardware costs increase with approximately 70%. This increase is almost entirely due to increased nacelle costs.

8.3.2.3 Overhaul costs

This study pays no attention to the periodically major overhaul or retrofit costs, nor does the DOWEC study.

Some factors that play a role when going from the DOWEC design to the 10MW design:

- Overhaul is planned in advance. Therefore costs associated with down time because of travelling are equal because the location and weather regime are similar.
- The number of turbines goes down (from 80 to 48).
- The cost of spare parts increases with increasing turbine power.

- Both gearbox and pitch mechanism are not present any more (overhaul cost reduction).
- Generator (expensive) and rotor (no possibility of replacement of one blade) replacement costs increase.

Since it is impossible to incorporate all these effects at this stage, for this study it is stated that the overhaul costs are proportional to the wind turbine hardware costs.

8.3.2.4 Transport & Installation costs

For simplicity, the T&I costs remain unchanged for the total wind farm. Although the number of turbines decreases from 80 to 48, the installation itself will take longer and will therefore be more expensive per turbine. A number of small piles in stead of one big one must be driven, and the installation is at higher (hub) heights. However, using a guide track at the side of the tower for hoisting the rotor and the generator may speed up the process and enlarge the working weather window.

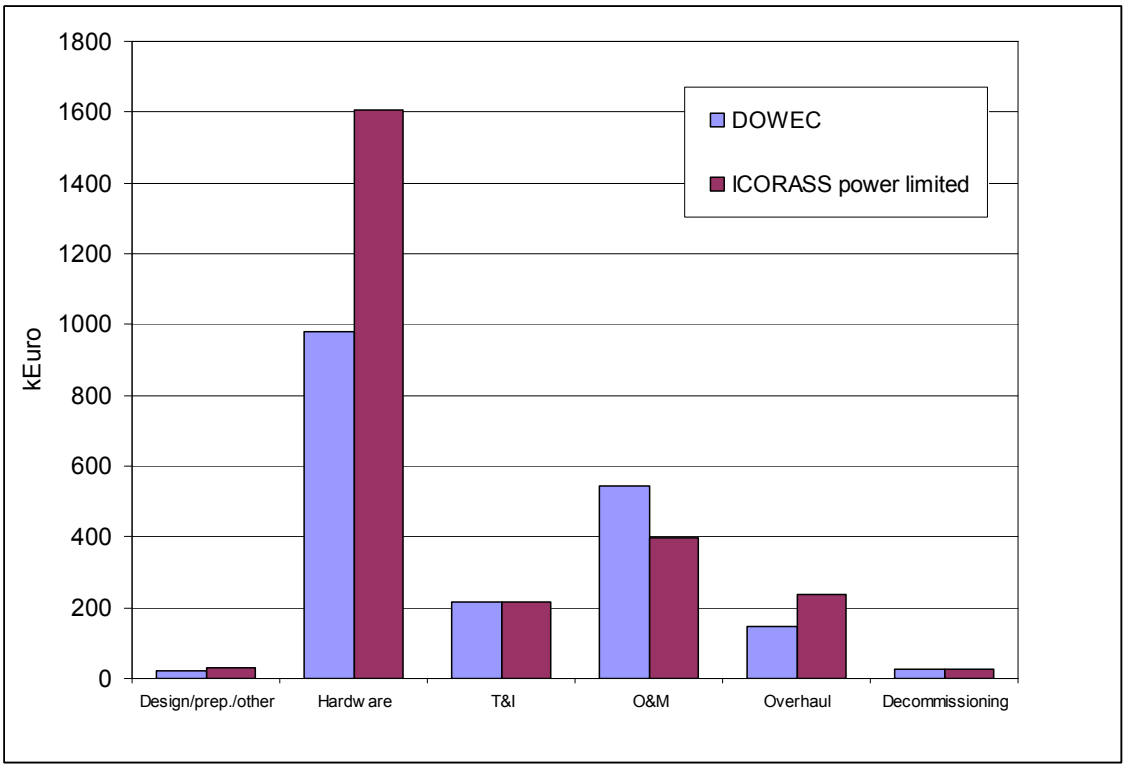

Figure 8.1: *Total levelized wind farm costs.*

8.4 Conclusions

The previous study showed the *LPC* trends that can be observed with the various ICORASS concepts compared to the DOWEC study. It is again explicitly stated that this chapter is not meant to give a very accurate value of the *LPC*. In Table 8.5 one can see that the estimated LPC increase is roughly 15% with respect to the DOWEC study.

Table 8.5: *Energy yield and cost of the ICORASS concept compared tot the DOWEC Concept.*

	Pitch	ICORASS power limited	
Yield increase	13.0	13.1	%
Cost increase	36.1	30.0	%
LPC increase	20.4	**14.9**	%

Zaaijer et al. [8.1] stated that possible errors in assessing manufacturing costs for totally different concepts are highly uncorrelated (e.g. monopile-truss tower or gearbox-direct drive) and therefore the uncertainty in this comparison is quite high. Because of this high uncertainty at this moment the moderate *LPC* increase indicates that refinement of the economical evaluation should take place before the ICORASS concept is either rejected/modified as inferior to the current concepts or accepted as superior.
Another conclusion that can be drawn from both increasing *LPCs* is that this increase is merely due to the currently used cost calculation regarding both the up scaling and the direct drive concept. The integrated rotor concept seems to prove an important improvement with respect to the equivalent pitch regulated turbine due to the lower hardware costs and the lower O&M costs. This emphasizes the viability of the concept and shows that more research on this concept might be needed to accurately assess the hardware and O&M costs.

Some recommendations can be made to improve this economical evaluation:

- A more detailed aerodynamic analysis needs to be conducted to ensure that the expected annual energy yield can be met.
- Nacelle cost needs to be determined with a higher reliability, because they are a major factor in the *LPC*. Since hardware investment costs form half the total cost, an uncertainty of 20% results in an uncertainty of 10% in the *LPC* calculation!
- For the accurate determination of the O&M, T&I and overhaul costs very specific data of repair times and rates and availability of lifting vessels are needed.

8.5 References

[8.1] Zaaijer, M.B., Kooijman, H.J.T., Herman, S.A. & Hendriks, H.B. *How to benefit from cost modelling of ofshore wind farms?* In: Proceedings of the European wind energy conference & exhibition, Madrid 16-19 June 2003.

[8.2] Zaaijer, M.B. *O&M aspects of the wind farm.* Website: http://www.ecn.nl/en/ wind/additional/special-projects/dowec/. DOWEC-082. TU-D, Delft, October 2003.

[8.3] Kooijman, H.J.T. & Hagg, F. *OWECOP-I: Modellering van kosten en potentieel van offshore windenergie in de Nederlandse Exclusieve Economische Zone van de Noordzee (NEEZ).* ECN-Wind Memo-01-035. Petten, May 2001.

[8.4] Herman, S.A. *DOWEC cost model. Implementation.* Website: http://www.ecn.nl/en/ wind/additional/special-projects/dowec/. DOWEC-068. ECN, Petten, April 2003.

[8.5] Hendriks, H.B. & Zaaijer, M.B. *DOWEC. Executive summary of the public research activities.* Website: http://www.ecn.nl/en/wind/additional/special-projects/dowec/. ECN, Petten /TU-D, Delft. January 2004.

[8.6] Goezinne, F. *Terms of reference DOWEC.* NEG-Micon. Bunnik, September 2001.

[8.7] Rademakers, L.W.M.M. & Braam, H. *O&M ASPECTS OF THE 500 MW OFFSHORE WIND FARM AT NL7. (80 * 6 MW Turbines). Baseline Configuration.* Website: http://www.ecn.nl/en/ wind/additional/special-projects/dowec/. DOWEC-080. ECN, Petten, July 2002.

Conclusions and recommendations

At this moment it can be concluded that the ICORASS concept is most likely technological viable and in potential economical competitive. It is still too early to judge this concept on its future ability to decrease offshore wind energy costs and because of that to form a substantial part of offshore wind energy.

From this feasibility study one might question the usefulness of further wind turbine up scaling. Because of the square-cube law, for equal energy yield the number of turbine reduces with R^{2+}, while the turbine hardware cost increase with R^3. Therefore a large reduction in hardware costs is needed before we should make this step. Hopefully, within the European UPWIND project a provisional statement will be elaborated on the ideal turbine size. Possibly a fully elaborated ICORASS concept can provide a hardware and O&M cost reduction needed for larger turbines.

Aerodynamics for a stall regulated Multi MegaWatt size wind turbine needs more investigation. With current knowledge on stall behavior on rotating wind turbine blades, the uncertainty in power and load prediction is simply too high. High performance CFD calculations will probably be needed to remove this uncertainty. Besides, dedicated airfoils and flow control devices might be necessary to increase the confidence in the aerodynamic controllability of an active speed stall regulated turbine.

Using this new aerodynamic knowledge, it is recommended to elaborate a detailed structural blade design in corporation with a manufacturer, as was originally an objective within this project. High detail is required to be able to predict accurately the aero-elastic response of the turbine. Besides aero-elastic tailoring can be applied to increase the stability. An accurate assessment of fatigue strength and loads needs to be made to evaluate the added value of this concept with respect to a wind turbine with individual pitch control.

The main conclusions of the ICORASS feasibility project are:

- The ICORASS wind turbine is a feasible concept for which it will be necessary to perform additional research in a number of areas to reduce the development risk, these areas are:
  - two bladed rotor has an effects on a number of subjects like different loading on the drive train and support structure, like power quality.
  - down wind rotor has a higher dynamic loading due to tower shadow, although a rotor in front of the tower is also submitted to a tower effect it is assumed that the tower effect is more sever when the rotor is behind the tower and it is also assumed that the effect is increased due to the fact that the chosen concept of the tower a truss tower.
- The aerodynamic blade design showed no fundamental obstacles;
- To predict the power output at high wind speeds a more accurate tool with a sophisticated aerodynamic model is needed;
- The aeroelastic stability analysis showed no fundamental obstacles, although some of the investigated modes showed small positive damping;
- It has not been investigated whether the rotor can be manufactured in one piece.
- It is recommended to investigate pre-bending and the cone angle together with the aeroelastic stability and tower clearance;
- A direct drive generator can be used to control the power of the rotor using a low lambda approach. It will be necessary that:
  - The generator power and maximum torque will need to be substantially higher, up to 40%, compared to a pitch controlled machine;
  - The converter power needs to be substantially higher, up to 26%, compared to a pitch controlled wind turbine;

- The electrical infrastructure of the wind farm can probably be equal compared with standard pitch controlled wind turbines;
- A controller needs to be designed using wind predictions;
- Based on recommended research it can be determined whether the park electrical infrastructure can remain unchanged;
- It is recommended to investigate, for. the chosen power control concept :
  - how well can the rotor averaged wind speed be predicted;
  - what are realistic accelerations in the rotor averaged wind speed.

Appendix A Airfoil characteristics

The airfoil distribution is shown in Table A.1.

From this data a few observations can be made:

- The DU25 and NACA-63618 have relatively high maximum camber (around 3%), which introduces a shift in the lift towards lower angles of attack and stall (reduction of lift and a sharp increase in drag) for lower angles of attack. This shift in angle of attack introduces undesired jumps in circulation along the blade span.

- Very low values for the drag coefficient in the region of the laminar drag bucket are found (below 0.01). One might argue the height of these wind tunnel measured drag coefficients since laminar flow is not likely to occur in a non-uniform ambient velocity (the wind).

- The smoothly increasing $(Cl/Cd)_{MAX}$ ratio with decreasing airfoil thickness shows the normal and preferred trend.

Finally for an accurate final design it is worth noting that the Reynolds numbers for the data below are twice as low as they will be on a full scale ICORASS turbine (for the low-lambda control option). For wind speeds around rated wind speed the Reynolds number for the larger part of the blade is around 20M. This might lead to a slight delay of stall, which is of great importance for the speed control above rated. Obviously, for a high-lambda controlled turbine compressibility effects should be taken into account as well.

Table A.1: *Spanwise airfoil distribution.*

Airfoil	**Re**	$\alpha_{CL=0}$	$C_{L,\alpha=0}$	$\alpha_{CL,MAX}$	$C_{L,MAX}$
DU40_X60	7M	-1.5	0.121	10.5	1.210
DU35_X60	7M	-1.5	0.190	13.0	1.602
DU30_X60	7M	-2.0	0.286	12.0	1.486
DU25_X60	7M	-3.5	0.442	10.0	1.422
FFA-W3-211_107	10M	-2.5	0.325	13.0	1.738
NACA-63618	10M	-4.0	0.473	14.0	1.550

Airfoil	$\alpha_{L/D,MAX}$	L/D_{MAX}	$C_{D,MIN}$
DU40_X60	6.5	68.4	0.0118
DU35_X60	8.5	105.8	0.0100
DU30_X60	7.5	112.4	0.0088
DU25_X60	5.0	135.2	0.0067
FFA-W3-211_107	6.0	143.8	0.0052
NACA-63618	4.5	173.6	0.0049

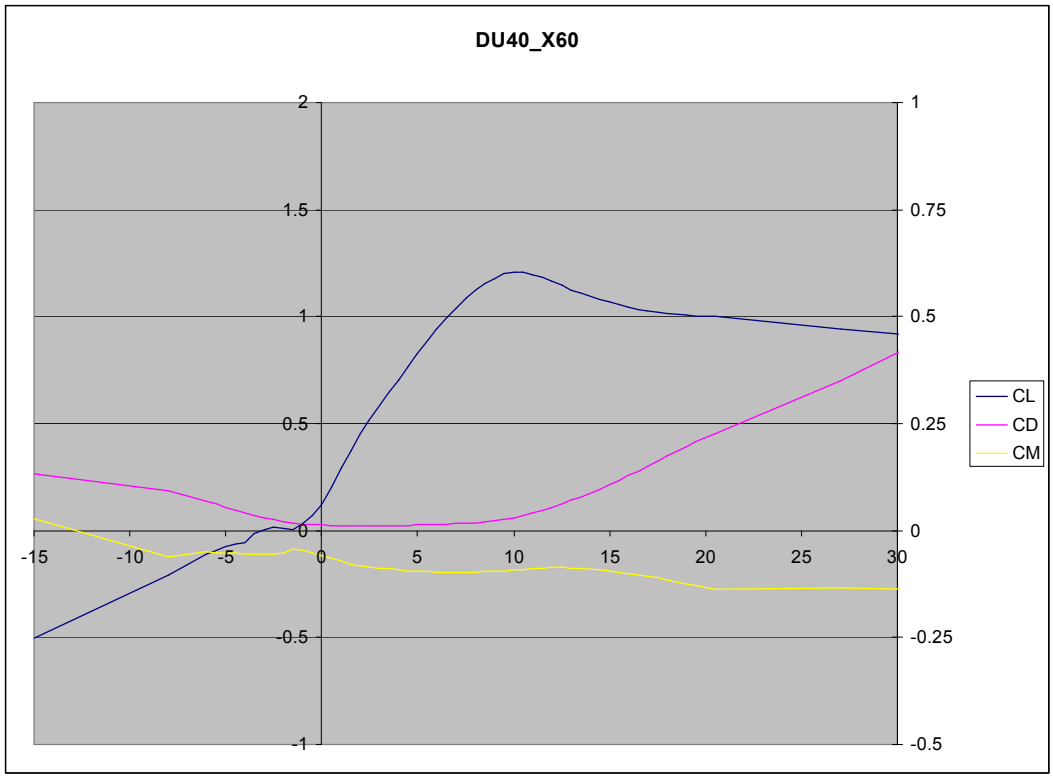

Figure A.1: *Airfoil characteristics DU40_X60.*

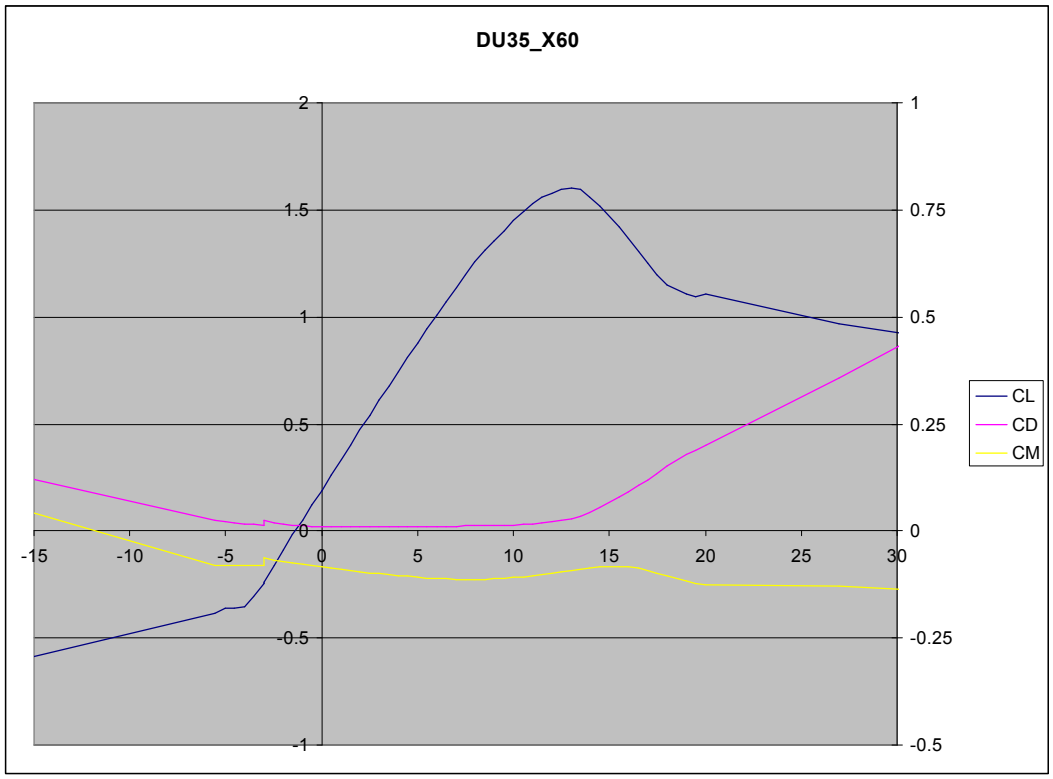

Figure A.2: *Airfoil characteristics DU35_X60.*

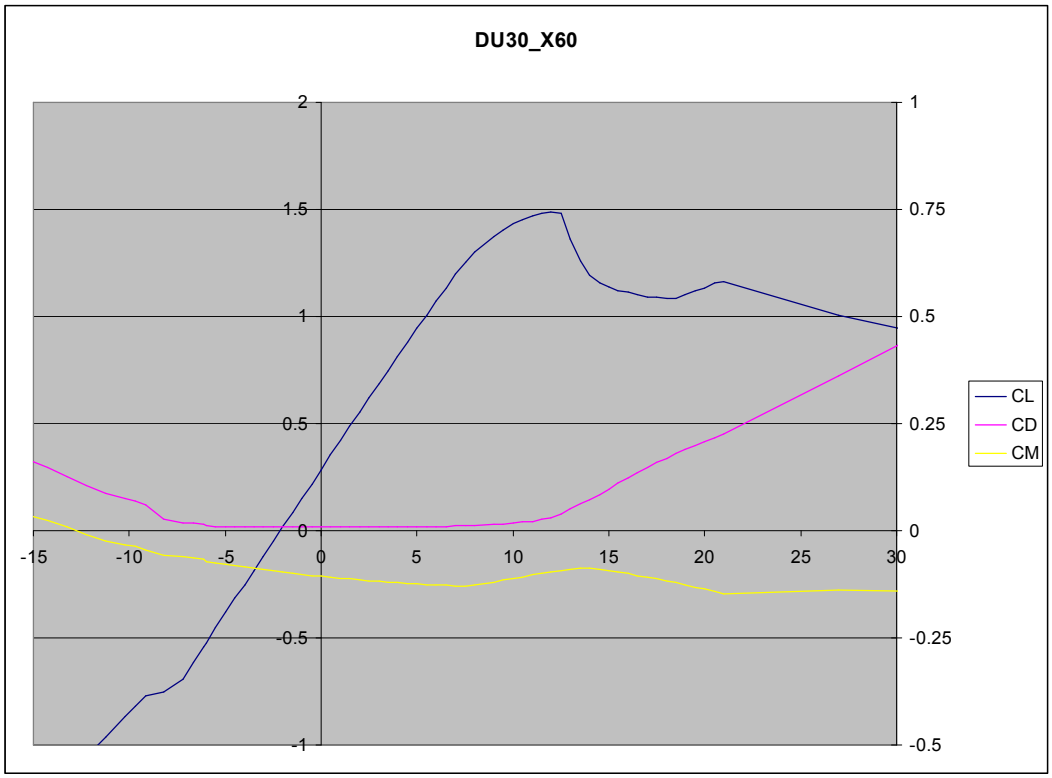

Figure A.3: *Airfoil characteristics DU30_X60.*

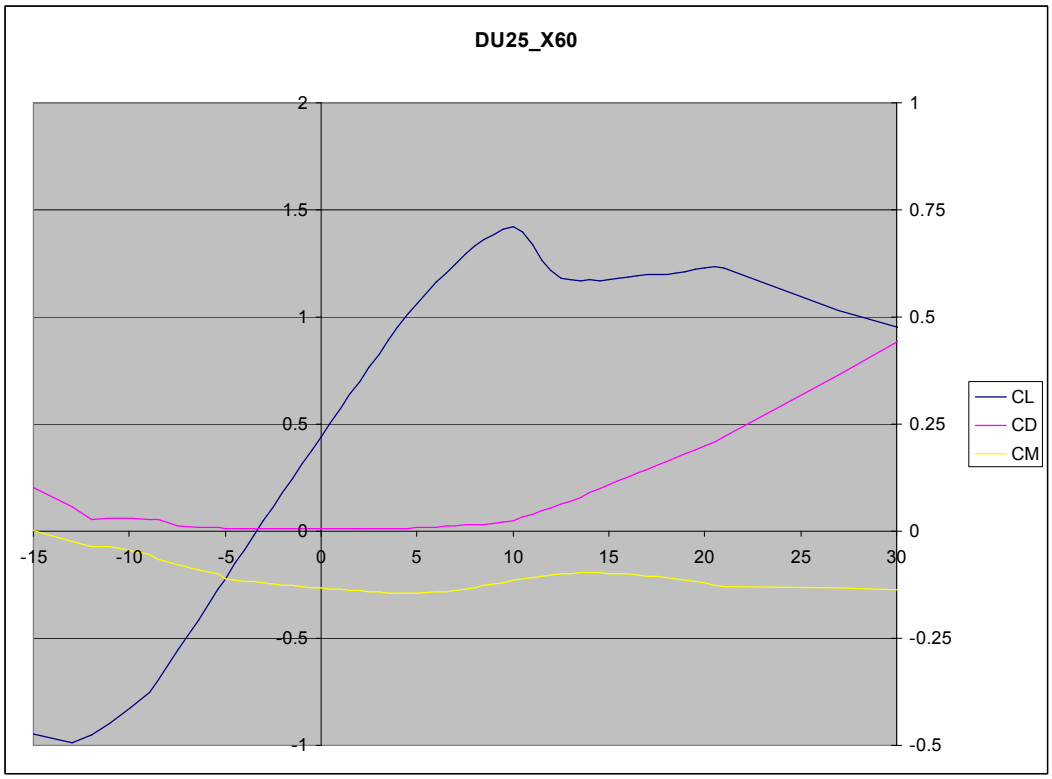

Figure A.4: *Airfoil characteristics DU25_X60.*

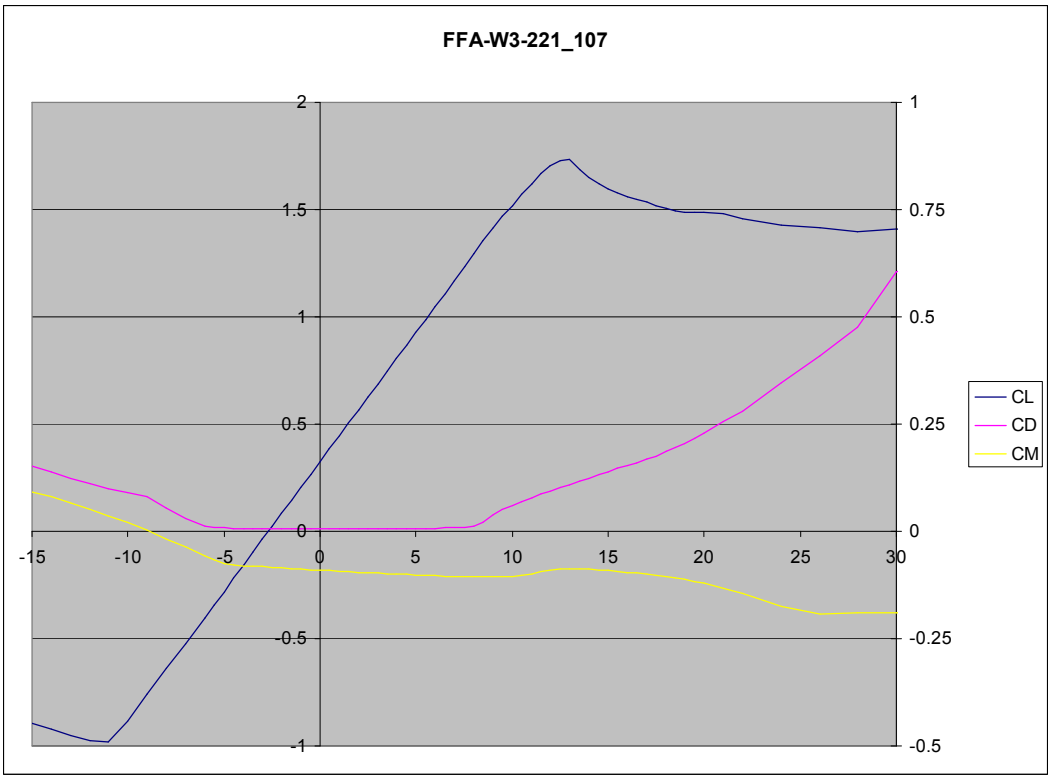

Figure A.5: *Airfoil characteristics FFA-W3-221_107.*

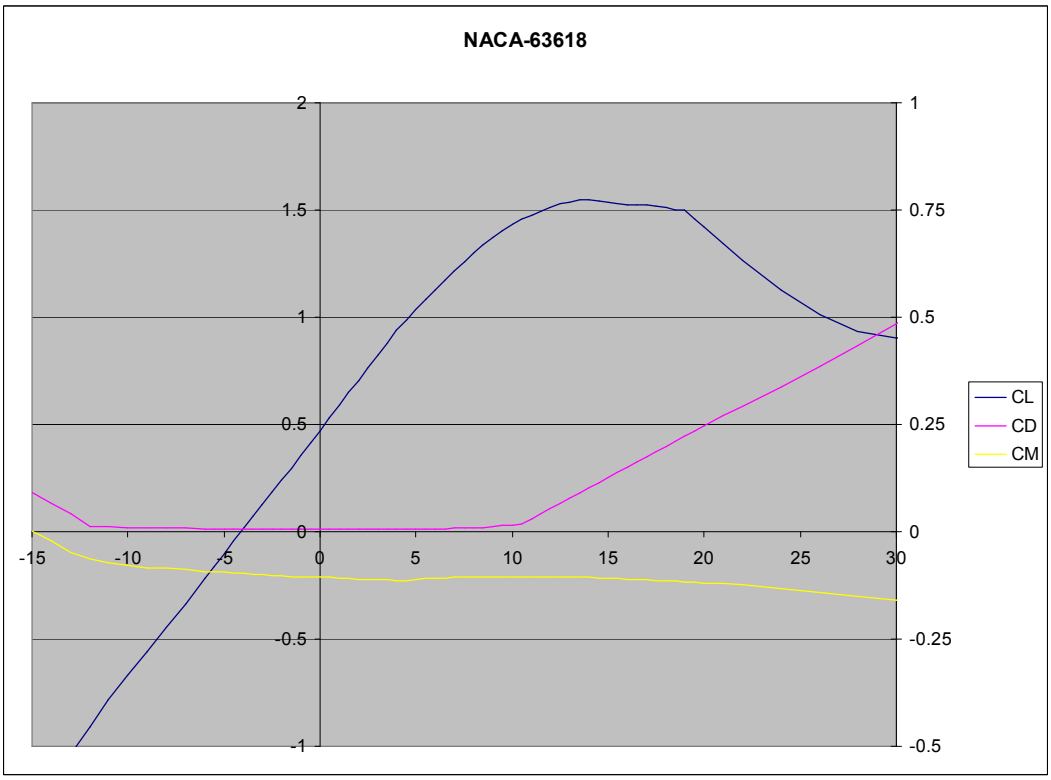

Figure A.6: *Airfoil characteristics NACA-63618.*

Appendix B Economical evaluation of the offshore wind farm layout

For the case study discussed in section 6.3.2 this appendix contains four elaborated economical assessments of different wind farm layout options:

1) IV1 wind farm
   P_{farm} = 200MW
   Turbine converters are back to back voltage source converters
   No overload capability

2) IV1 wind farm
   P_{farm} = 200MW
   Turbine converters are diode rectifiers plus voltage source converters
   No overload capability

3) IV3 wind farm
   P_{farm} = 200MW
   Transformers and cables have 1.5PU overload capability for several seconds

4) IV3 wind farm
   P_{farm} = 200MW
   No overload capability

B.1 Electrical wind farm layout 1

Table A.2: *Hardware cost calculation for electrical wind farm layout 1.*

IV1 wind farm;
200MW;
Turbine converters are back to back voltage source converters;
no overload capability.

Component	Type	Reference	Vnom (kV)	Snom (MVA)	Price (k€)	Number	Length	Total Price (k€)
Turbine			4,2	10				
Tur Rectifier and Inverter	Tur B2B VSCs	Based on the cost trends of Siemens 6,7	5	25	4667	10	1	46670
Tur Trafo		Based on the cost trends of Siemens 27,60	5/33	25	284	10	1	2840
MV Cable		Based on the cost trends of Pirelli 18,19	33	25	324,704	2	1,05	681,8784
				50	469,408	2	1,05	985,7568
				75	614,112	2	1,05	1289,6352
				100	758,816	2	1,05	1593,5136
				125	903,52	2	1,05	1897,392
HV Trafo		Siemens 21	33/150	250	2840	1	1	2840
HV Cable		Pirelli 16	150	250	572	1	20	11440
						Total Price (k€)		70238,176

B.2 Electrical wind farm layout 2

Table A.3: *Hardware cost calculation for electrical wind farm layout 2.*

IV1 wind farm;
200MW;
Turbine converters are diode rectifiers plus voltage source converters;
No overload capability.

Component	Type	Reference	Vnom (kV)	Snom (MVA)	Price (k€)	Number	Length	Total Price (k€)
Turbine			4,2	10				
Tur Rectifier and Inverter	Tur Diode Rectifier + VSC Inverter	B2B VSI 2	5	25	2190	10	1	21900
Tur Trafo		Based on the cost trends of Siemens 27,60	5/33	25	284	10	1	2840
MV Cable		Based on the cost trends of Pirelli 18,19	33	25	324,704	2	1,05	681,8784
				50	469,408	2	1,05	985,7568
				75	614,112	2	1,05	1289,6352
				100	758,816	2	1,05	1593,5136
				125	903,52	2	1,05	1897,392
HV Trafo		Siemens 21	33/150	250	2840	1	1	2840
HV Cable		Pirelli 16	150	250	572	1	20	11440
						Total Price (k€)		45468,176

B.3 Electrical wind farm layout 3

Table A.4: *Hardware cost calculation for electrical wind farm layout 3.*

IV3 wind farm;
200MW;
Transformers and cables have 1.5PU overload capability for several seconds.

Component	Type	Reference	Vnom (kV)	Snom (MVA)	Price (k€)	Number	Length	Total Price (k€)
Turbine			4,2	10				
TurTrafo			4.2/25	16,7	189,7	10	1	1897
Tur Rectifier	VSC	Based on cost trends of Siemens Rec 13, 15	25/50	25	6401	10	1	64010
MV DC Cable		Based on cost trends of 84kV DC cable 13, 15	84	16,7	193,42	2	1,05	406,182
				33,4	236,84	2	1,05	497,364
				50,1	280,26	2	1,05	588,546
				66,8	323,68	2	1,05	679,728
				83,5	367,1	2	1,05	770,91
MV Inverter	VSC	Based on cost trends of Siemens Inv 25,26,27,29	50/33	250	40000	1	1	40000
HV Trafo		Siemens 21	33/150	167	1894	1	1	1894
HV Cable		Pirelli 16	150	167	430	1	20	8600
						Total Price (k€)		119343,73

B.4 Electrical wind farm layout 4

Table A.5: *Hardware cost calculation for electrical wind farm layout 4.*

IV3 wind farm;
200MW;
No overload capability.

Component	Type	Reference	Vnom (kV)	Snom (MVA)	Price (k€)	Number	Length	Total Price (k€)
Turbine			4,2	10				
TurTrafo			4.2/25	25	189,7	10	1	1897
Tur Rectifier	VSC	Based on cost trends of Siemens Rec 13, 15	25/50	25	6401	10	1	64010
MV DC Cable		Based on cost trends of 84kV DC cable 13, 15	84	25	215	2	1,05	451,5
				50	280	2	1,05	588
				75	345	2	1,05	724,5
				100	410	2	1,05	861
				125	475	2	1,05	997,5
MV Inverter	VSC	Based on cost trends of Siemens Inv 25,26,27,29	50/33	250	40000	1	1	40000
HV Trafo		Siemens 21	33/150	250	2840	1	1	2840
HV Cable		Pirelli 16	150	250	572	1	20	11440
						Total Price (k€)		123809,5